# Design, evaluation and future projections of the ~~NARCliM2.0~~NARCliM 2.0 CORDEX-CMIP6 Australasia regional climate ensemble

**Giovanni Di Virgilio[1,2], Jason P. Evans[2,3], Fei Ji[1,3], Eugene Tam[1], Jatin Kala[4], Julia Andrys[4], Christopher Thomas[2], Dipayan Choudhury[1], Carlos Rocha[1], Stephen White[1], Yue Li[1], Moutassem El Rafei[1], Rishav Goyal[1], Matthew L. Riley[1] and Jyothi Lingala[4]**

[1]Climate & Atmospheric Science, NSW Department of Climate Change, Energy, the Environment and Water, Sydney, Australia

[2]Climate Change Research Centre, University of New South Wales, Sydney, Australia

[3]Australian Research Council Centre of Excellence for Climate Extremes, University of New South Wales, Sydney, Australia

[4]Environmental and Conservation Sciences, and Centre for Climate Impacted Terrestrial Ecosystems, Harry Butler Institute, Murdoch University, Murdoch, WA 6150, Australia

*Correspondence to*: Giovanni Di Virgilio (giovanni.divirgilio@environment.nsw.gov.au; giovanni@unsw.edu.au)

**Abstract**. ~~NARCliM2.0~~NARCliM 2.0 comprises two Weather Research and Forecasting (WRF) regional climate models (RCMs) downscaling five CMIP6 global climate models contributing to the Coordinated Regional Downscaling Experiment over Australasia at 20 km resolution, and south-east Australia at 4 km convection-permitting resolution. We first describe ~~NARCliM2.0~~NARCliM 2.0's design, including selecting two, definitive RCMs via testing seventy-eight RCMs using different parameterisations for planetary boundary layer, microphysics, cumulus, radiation, and land surface model (LSM). We then assess ~~NARCliM2.0~~NARCliM 2.0's skill in simulating the historical climate versus CMIP3-forced ~~NARCliM1.0~~NARCliM 1.0 and CMIP5-forced ~~NARCliM1.5~~NARCliM 1.5 RCMs and compare differences in future climate projections. RCMs using the new Noah-MP LSM in WRF with default settings confer substantial improvements in simulating temperature variables versus RCMs using Noah-Unified. Noah-MP confers smaller improvements in simulating precipitation, except for large improvements over Australia's southeast coast. Activating Noah-MP's dynamic vegetation cover and/or runoff options primarily improve simulation of minimum temperature. ~~NARCliM2.0~~NARCliM 2.0 confers large reductions in maximum temperature bias versus ~~NARCliM1.0~~NARCliM 1.0 and 1.5 (1.x), with small absolute biases of ~0.5K over many regions versus over ~2K for NARCliM1.x. ~~NARCliM2.0~~NARCliM 2.0 reduces wet biases versus NARCliM1.x by as much as 50%, but retains dry biases over Australia's north.

~~NARCliM2.0~~NARCliM 2.0 is biased warmer for minimum temperature versus ~~NARCliM1.5~~NARCliM 1.5 which is partly inherited from stronger warm biases in CMIP6 versus CMIP5 GCMs. Under shared socioeconomic pathway (SSP)3-7.0, ~~NARCliM2.0~~NARCliM 2.0 projects ~3K warming by 2060-79 over inland regions versus ~2.5K over coastal regions. ~~NARCliM2.0~~NARCliM 2.0-SSP3-7.0 projects dry futures over most of Australia, except for wet futures over Australia’s north and parts of western Australia which are largest in summer. ~~NARCliM2.0~~NARCliM 2.0-SSP1-2.6 projects dry changes over Australia with only few exceptions. ~~NARCliM2.0~~NARCliM 2.0 is a valuable resource for assessing climate change impacts on societies and natural systems and informing resilience planning by reducing model biases versus earlier NARCliM generations and providing more up-to-date future climate projections utilising CMIP6.

**Keywords:**

Climate change; climate impact adaptation; dynamical downscaling; CORDEX-CMIP6; model design; model evaluation

# 1. Introduction

Climate projections are foundational to informing climate change mitigation and adaptation planning at various spatial scales (IPCC, 2021). Regional climate models (RCMs) dynamically downscale global climate models (GCMs) at ~100-200 km resolution to simulate higher resolution climate projections that better resolve local-scale influences on regional climate, such as mountain ranges, land-use variation, land-sea contrasts, and convective processes (Torma et al., 2015; Giorgi, 2019). As such, whilst GCMs are the best tools for investigating climate at global scales, RCMs provide improved guidance for climate policy at regional scale, which is the scale at which climate change impacts are experienced (Hsiang et al., 2017).

The NARCliM programme (New South Wales and Australian Regional Climate Modelling) is now in its third generation. Like its predecessors, NARCliM version 2.0 ('~~NARCliM2.0~~NARCliM 2.0'), aims to produce robust, detailed regional climate projections at spatial scales relevant for use in local-scale climate change analysis. A key feature of all NARCliM generations is to simulate the climate over the Coordinated Regional Downscaling Experiment (CORDEX)-Australasia domain, and a higher resolution inner domain over southeast Australia via one-way nesting (Figure 1). With one-way nesting the inner domain obtains its initial and lateral boundary conditions from the simulation over CORDEX-Australasia. ~~NARCliM1.0~~NARCliM 1.0 simulated the climate of Australasia for three periods (1990-2009, 2020-2039, 2060-2079) at 50 km resolution and southeast Australia at 10 km using three configurations of the weather research and forecasting (WRF) RCM (Skamarock et al., 2008) to downscale GCMs from Coupled Model Intercomparison Project phase three (CMIP3) under the SRES A2 greenhouse gas (GHG) scenario (Evans et al., 2014). ~~NARCliM1.5~~NARCliM 1.5 used CMIP5 GCMs under representative concentration pathways (RCP) 4.5 and 8.5 to simulate continuously for 1950-2100 on the same grids as ~~NARCliM1.0~~NARCliM 1.0 using two of its RCMs (Nishant et al., 2021).

~~NARCliM2.0~~NARCliM 2.0 aims to improve performance in simulating the Australian climate relative to previous NARCliM generations with the goal of better informing community resilience to climate change (New South Wales Government, 2022, 2023). All NARCliM projects include a bottom-up design ethos involving multi-sectoral end-user engagement in specifying model requirements to ensure model performance and outputs meet end-user needs. Key requirements from the ~~NARCliM2.0~~NARCliM 2.0 user-consultation include providing increased detail in climate simulations via higher resolution and improving the simulation of precipitation and temperature as these are fundamental inputs to climate impact studies. Whilst ~~NARCliM1.0~~NARCliM 1.0 and 1.5 (1.x) confer the expected level of performance in simulating the Australian climate (Di Virgilio et al., 2019; Evans et al., 2020b), recent technological and scientific advancements mean that aspects of their performance might now be improved. NARCliM1.x RCMs show widespread cold biases in maximum temperature exceeding −5K for some RCMs. Conversely, minimum temperature is simulated more accurately with biases in the range of ±1.5K. NARCliM1.x RCMs overestimate precipitation, particularly over Australia's socio-economically important eastern seaboard (Di Virgilio et al., 2019).

As they are expensive to run from both computational and data storage perspectives, dynamical downscaling projects like ~~NARCliM2.0~~NARCliM 2.0 use a subset of available GCMs as driving data, necessitating careful model selection. Similarly, a large combination of different physical parametrisations available for the WRF RCM enables many structurally different RCMs to be potentially used to downscale GCMs. A key component of ~~NARCliM2.0~~NARCliM 2.0's design is testing the viability of alternative RCM parameterisations via a three-phase approach, with each phase building on the preceding phase to identify the RCM parameterisations that perform well during testing to meet ~~NARCliM2.0~~NARCliM 2.0's aim of improving the simulation of Australia's climate. GCM and RCM statistical independence are also sought to avoid creating a biased sample of climate change. Hence, the aims of this paper are to:

1) describe how and why ~~NARCliM2.0~~NARCliM 2.0 differs from its predecessors in terms of its design and production processes, explaining the model test and evaluation approaches underlying its design decisions. A key focus is on the design and testing of seventy-eight structurally different WRF RCMs and their evaluation to identify a subset of RCMs for use in ~~NARCliM2.0~~NARCliM 2.0;

2) characterise the performance improvements of CMIP6-~~NARCliM2.0~~NARCliM 2.0 RCMs in simulating the Australian climate relative to previous NARCliM generations by evaluating their skill in simulating mean maximum and minimum temperature and precipitation versus observations;

~~and~~ 3) summarise the climate projections produced by CMIP6-~~NARCliM2.0~~NARCliM 2.0 and how these differ from previous CMIP3-5-NARCliM generations.

The following section summarises the basic design features of each NARCliM generation; ~~section 3. describes NARCliM2.0's design process with a focus on its RCM physics testing, as well as a brief overview of its production process; s~~Section ~~4~~3. describes evaluation methods and metrics; Section 4. describes NARCliM 2.0's design process with a focus on its RCM physics testing, as well as a brief overview of its production process; S~~s~~ection 5. summarises the RCM physics test results; ~~s~~Section 6. evaluates the performance of all NARCliM models in simulating the recent Australian climate; ~~s~~Section 7. provides an overview of their future projections; and S~~s~~ection 8. discusses key results and summarises this paper.

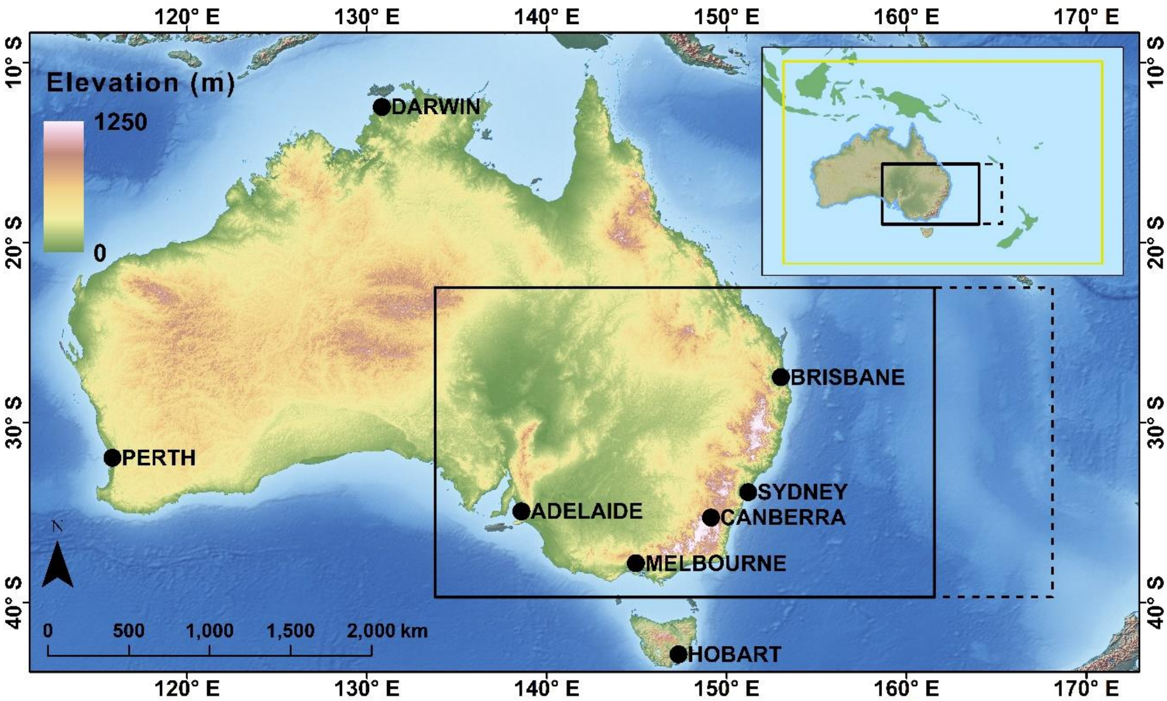


**Figure 1.** Model domains for NARCliM regional climate simulations. The southeast inner domain for ~~NARCliM2.0~~NARCliM 2.0 is delineated with a solid black rectangle; the corresponding inner domain for ~~NARCliM1.0~~NARCliM 1.0 and 1.5 is delineated with a dashed black line. The elevated terrain of the Australian Alps which form part of the Great Dividing Range is in eastern Australia. Inset shows the CORDEX-Australasia outer domain.

# 2. Three generations of NARCliM: model overviews

The design of ~~NARCliM1.0~~NARCliM 1.0 is described in Evans et al. (2014); ~~NARCliM1.5~~NARCliM 1.5 used the same design approach but used CMIP5 rather than CMIP3 GCMs. All generations of NARCliM use different versions of the WRF model ~~(Skamarock et al., 2008)~~ to perform dynamical downscaling of GCMs since the WRF model goes through regular updates. The southeast Australian inner domain captures five of Australia's eight capital cities (Figure 1) and over 75% of the Australian population (Australian Bureau Statistics, 2024). Additionally, the inner domain captures coastal regions that are characterised by topographic complexity and land-use class variation. Regions east of the Great Dividing Range mountains in southeast Australia (Figure 1) show different responses to oceanic climate modes compared to inland semi-arid regions (Murphy and Timbal, 2008) and are impacted by events such as rapidly developing storms, including east coast lows (Pepler and Dowdy, 2021). Such atmospheric processes are not adequately resolved by GCMs due to coarse resolutions (Di Virgilio et al., 2022; Grose et al., 2020).

~~NARCliM2.0~~NARCliM 2.0 encompasses several design advancements over its predecessors (Table 1). ~~NARCliM2.0~~NARCliM 2.0 RCMs have a 20 km resolution CORDEX-Australasia domain (versus 50 km) and 4 km (versus 10 km) domain over southeast Australia and use 45 (versus 30) vertical levels. The aim of increasing the resolution of this inner domain from 10 km to 4 km is to render these simulations convection-permitting (Kendon et al., 2021; Lucas-Picher et al., 2021). Hence, whilst the 20 km-resolution outer domain uses cumulus parametrisation, simulations over the 4 km domain do not use cumulus parametrisation. ~~NARCliM2.0~~NARCliM 2.0 also includes a new collaboration with the Western Australian government, with separate 4 km simulations being performed over south-west and north-west Western Australia (not shown in Figure 1) as part of the Western Australian climate science initiative (DWER, 2023). Boundary conditions derived from the 20 km ~~NARCliM2.0~~NARCliM 2.0 CORDEX Australasia domain are used to drive these simulations. Additional major differences in model setup for ~~NARCliM2.0~~NARCliM 2.0 include:

- ~~NARCliM1.0~~NARCliM 1.0 RCMs use different parameterisations for planetary boundary layer (PBL) physics, surface physics, cumulus physics, land surface model (LSM), and radiation (Evans et al., 2014). These RCM parameterisations were also used for ~~NARCliM1.5~~NARCliM 1.5. Owing to the project aims stated above, RCM parameterisations for ~~NARCliM2.0~~NARCliM 2.0 differ to those of NARCliM1.x (see ~~s~~Sect. ~~3~~4).
- ~~NARCliM2.0~~NARCliM 2.0 increases the number of driving GCMs to 5 and simulates for a wider range of plausible future climates via three shared socioeconomic pathways (SSP). SSP1-2.6 is selected as a low GHG scenario envisaging a future climate with $CO_2$ emissions cut to net zero by around 2075 and warming held to below 2˚C by 2100; SSP2-4.5 estimates projected warming under a ‘middle of the road’ scenario where temperatures increase to ~2.7˚C by 2100; and SSP3-7.0 is a high GHG scenario which assumes warming of ~4˚C by 2100 (IPCC, 2021).
- Urban physics is activated in ~~NARCliM2.0~~NARCliM 2.0 (WRF setting: sf_urban_physics=1) to represent surface energy balance in urban areas via a single layer urban canopy model (Kusaka and Kimura, 2004).
- Input of different aerosol species is activated for the RCM radiation scheme using the Tegen et al. (1997) climatology available in WRF (aer_opt=1). This aerosol forcing is the same for all GCMs, and not model-specific.
- The eastern boundary of the ~~NARCliM2.0~~NARCliM 2.0 inner domain is located further westward relative to that of NARCliM1.x (Figure 1).

**Table 1**. High-level design features of three generations of NARCliM regional climate models

| | Model Generation | | |
|---|---|---|---|
| | ~~NARCliM1.0~~NARCliM 1.0 | ~~NARCliM1.5~~NARCliM 1.5 | ~~NARCliM2.0~~NARCliM 2.0 |
| **Release date** | 2014 | 2020 | 2023-2024 |
| **Years simulated** | 1990-2009, 2020-2039, 2060-2079 | 1950-2100 | 1950-2100 |
| **Grid resolutions: CORDEX-Australasia; NARCliM inner domains** | 50 km; 10 km | 50 km; 10 km | 20 km; 4 km |
| **Vertical levels** | 30 | 30 | 45 |
| **Global Climate Models** | 4 CMIP3 GCMs | 3 CMIP5 GCMs | 5 CMIP6 GCMs |
| **Regional Climate Models** | 3 RCM configurations (WRF3.3) | 2 RCM configurations (WRF3.6.0.5) | 2 RCM configurations (WRF4.1.2) |
| **Future emission scenarios** | SRES A2 | RCP4.5, RCP8.5 | SSP1-2.6, SSP2-4.5, SSP3-7.0 |
| **Reanalysis-driven (CORDEX Evaluation)** | NCEP: 1950-2009 | ERA-Interim: 1979-2013 | ERA5: 1979-2020 |
| **Computational resources (core hours)** | 30M | 30M | 1060M |

# 3. Evaluation methods

This section largely focuses on the methods and metrics used for the NARCliM 2.0 RCM physics testing and comparisons of model biases and future climate projections against previous generations of NARCliM. Details on methods and results for the CMIP6 GCM evaluation used to select driving GCMs and the ERA5-NARCliM 2.0 RCM evaluation used to select two, definitive RCMs for the GCM-driven simulations are available in Di Virgilio et al. (2022) and Di Virgilio et al. (in review), respectively, with overviews of these components of NARCliM 2.0 design provided in Sections 4.2 and 4.4 below.

## 3.1 Observations

Australian Gridded Climate Data (AGCD version 1.0; (Evans et al., 2020a) are the observational data used to evaluate the NARCliM 2.0 RCM physics test RCMs. These daily gridded data for maximum and minimum temperature and precipitation are obtained from an interpolation of station observations across Australia. AGCD data are on a regular WGS84 grid with a grid-averaged resolution of 0.05°. For the NARCliM 2.0 RCM physics tests, the AGCD data were re-gridded to correspond with the RCM data from the inner domain on their native grids using a conservative area-weighted re-gridding scheme. All data (RCM and AGCD) were restricted to a common extent contained within the inner domain over southeast Australia, and a land mask was applied so that statistics were computed using only land pixels. Treatment of AGCD for the CMIP6 GCM evaluation and the ERA5-NARCliM 2.0 RCM evaluation is described in Di Virgilio et al. (2022) and Di Virgilio et al. (in review), respectively.

## 3.2 Methods and metrics: phase I-III NARCliM2.0 physics tests

Test RCM performances in reproducing observations for daily maximum and minimum temperature and daily precipitation were assessed by calculating the model bias, i.e., model outputs minus AGCD, and the RMSE of modelled versus observed fields. Model biases and RMSEs were calculated at annual and seasonal timescales. The model representations of the hottest and the wettest day on an annual time scale over the study region were also compared with AGCD. Probability density functions (PDFs) were calculated for each variable using daily data. The Perkins skill score (PSS) (Perkins et al., 2007) was calculated to assess the overall degree of overlap between modelled and observed distributions, with PSS = 1 indicating that distributions overlap perfectly.

There are several methods to evaluate the overall performance of RCMs. In this study, we ranked the RCMs individually based on their bias, RMSE, and PSS for maximum temperature, minimum temperature, and precipitation. Each variable was ranked separately for each metric. The ranks were then summed to determine the overall ranking for each RCM.

## 3.3 Independence assessments

We used the method of Bishop and Abramowitz (2013) as one of two methods of assessing the independence of physics test RCMs and the target CMIP6 GCMs under evaluation for use in NARCliM 2.0. This approach uses the covariance in model errors as the basis to define model dependence; specifically, independence coefficients are derived from the error covariance matrix of the RCMs or GCMs. Model independence is quantified using the correlation of model errors. For the physics test RCMs, errors are computed by comparing the climatology of maximum and minimum temperature and precipitation over the south-east Australia inner domain for 2016 with corresponding AGCD observations. The same calculation is performed for the CMIP6 GCMs, except for the Australian continent. Daily timeseries of precipitation, maximum and minimum temperature are calculated individually for each RCM and for AGCD. The simulated and observed daily timeseries of each variable are then normalised by the standard deviation of the corresponding observed variable. These normalised variables are concatenated for each RCM (GCM) and AGCD. An anomaly time series for each grid cell is then produced. These time series are used to create a model error covariance matrix containing the errors for all RCMs (GCMs). The coefficients of a linear combination of the RCMs (GCMs) that optimally minimises the mean square error depends on both model performance and model dependence (Bishop and Abramowitz, 2013). The result of this minimisation problem is written in terms of the covariance matrix. The magnitude of coefficients assigned to each RCM (GCM) reflects a combination of their performance and independence. Highly independent models have different errors when simulating the recent climate. Models with the largest coefficients have the most independent errors versus observations.

The Herger method of subset selection (Herger et al., 2018), as implemented here, uses quadratic integer programming to find the subset of models whose equally-weighted subset mean (EWSM) minimises a quadratic cost function. This cost function is chosen to measure the performance of the EWSM in comparison to a given observational product. The two cost functions used here are: the mean squared error (MSE) between the EWSM and the observational product (Herger et al. 2018, Eq. 1); and another which measures a combination of the MSE of the EWSM, the average MSE of each subset member, and the average pairwise mean squared distance between subset members (Herger et al. 2018, Eq. 2).

## 3.4 NARCliM2 CMIP6-RCMs: historical evaluation and climate change projections

Performances of NARCliM 2.0 versus NARCliM1.x RCMs in reproducing the recent Australian climate are evaluated by calculating the model biases (model outputs minus AGCD observations) for mean maximum and minimum temperature and precipitation for 1990-2009. To enable comparison of future projections between NARCliM 1.0, NARCliM 1.5 and NARCliM 2.0 (where NARCliM 1.0 modelled for 1990-2009, 2020-2039, and 2060-2079), all NARCliM ensemble projected changes are shown as far future (2060–2079) minus present day (1990–2009).

## 3.5 Statistical significance

When quantifying RCMs’ future climate change projections (compared to the historical period) and biases in maximum and minimum temperature, the statistical significance is calculated for each grid cell using t-tests assuming equal variance. The Mann–Whitney U test is used for precipitation given its non-normality. Significance thresholds were adjusted to account for multiple testing using Walker's test (Eq.2 in Wilks, 2016). For individual RCMs, grid cells showing statistically significant changes are stippled, otherwise they are shown in colour where change is statistically insignificant. Results on the statistical significance of each ensemble mean are separated into three categories following Tebaldi et al. (2011): 1) statistically insignificant areas are shown in colour, denoting that less than 50% of RCMs are significantly biased/different; 2) in areas of significant agreement (stippled), at least 50% of RCMs are significantly biased/different and at least 70% of significant models in the CMIP6-NARCliM 2.0 RCM ensemble agree on the sign of the bias/difference. In such areas, many ensemble members have the same bias sign which is an undesirable outcome; and 3) areas of significant disagreement, where at least 50% of RCMs are significantly biased/different and fewer than 70% of significant models agree on the bias sign, are shown with diagonal hatching for the CMIP6-NARCliM 2.0 historical evaluation and climate change signals.

# ~~3~~4. ~~NARCliM2.0~~NARCliM 2.0 design and production process overview

The ~~NARCliM2.0~~NARCliM 2.0 design and production processes are summarised below in reference to Figure 2. The design process is an adaptation of that introduced in Evans et al. (2014). Two companion manuscripts describe elements shown in Figure 2, ~~and~~ which are therefore only summarised briefly in this manuscript: Di Virgilio et al. (2022) describes the CMIP6 GCM selection process summarised in Box 2, and Di Virgilio et al. (in review) describes the ERA5-RCM evaluation undertaken in Boxes 5 and 6.

**I. Design Phase:**

i) **Box 1:** model design requirements are identified via consultation between ~~NARCliM2.0~~NARCliM 2.0 modelling groups and multi-sectoral end-users, as well as adherence to CORDEX-CMIP6 design requirements (WCRP~~erp~~, 2020).

ii) **Box 2:** NARCliM1.x selected driving CMIP3-5 GCMs (respectively) via literature review of existing GCM evaluations. During ~~NARCliM2.0~~NARCliM 2.0 design, there were no pre-existing comprehensive evaluations of individual CMIP6 GCMs for the Australian region, including assessments of climate change signals and GCM statistical independence. Hence, an evaluation and selection of CMIP6 GCMs was conducted (see Di Virgilio et al. 2022). This evaluation selected five GCMs to force two ~~NARCliM2.0~~NARCliM 2.0 RCMs (see S~~s~~ect 4.2 and 4.4). The relative contribution to uncertainty/variation in climate projections can be larger for GCMs than for RCMs (e.g. Lee et al., 2023).

iii) **Boxes 3-4:** a new WRF RCM multi-physics test ensemble is created for ~~NARCliM2.0~~NARCliM 2.0: RCM physics testing is conducted via a three-phase approach, with each phase building on the findings of the preceding phase to identify the RCM parameterisations that perform well during testing with the aim of improving the simulation of the Australian climate. In this way, RCMs are parameterised with different physics settings via each test phase, systematically removing poor performing options while facilitating the fine tuning and improvement of the parameterisations that perform well during testing to build a total ensemble size of seventy-eight structurally different test RCMs. The performance~~s~~ of the different test RCM configurations ~~are~~ is evaluated, ultimately leading to the selectio~~n~~g of a subset of seven RCMs for subsequent downscaling of ERA5 reanalysis ~~and comprising~~as part of the CORDEX evaluation experiment.

iv) **Boxes ~~4~~5-6:** These seven RCMs are used to downscale ERA5 reanalysis over the 20 km and 4 km domains for 1979-2020. Evaluating these ERA5-forced simulations informs selection of two definitive, ~~‘~~production~~’~~ RCMs for CMIP6-forced downscaling (see ~~s~~Sect. 4.4 and Di Virgilio et al. in review).

**II. Production Phase:**

i) **Boxes 7-8:** CMIP6 GCM data are pre-processed to create initial and boundary conditions to drive simulations for the historical (1950-2014) and SSP experiments (2015-2100). A code repository used for this GCM preprocessing is available on Zenodo at: https://doi.org/10.5281/zenodo.11184830~~https://bitbucket.org/oehcas/narclim2-0_design_and_evaluation_2024_support_materials/src/main/~~ within the WRF/repo_snapshots subdirectory. Quality assurance/quality control (QA/QC) is performed on these data before initiating the simulations (e.g. variables are checked to confirm data do not contain significant outliers across ensemble members).

ii) **Boxes 9-11:** the 151-year CMIP6-forced ~~NARCliM2.0~~NARCliM 2.0 RCM simulations are run using National Computational Infrastructure at Canberra, Australia (NCI, https://nci.org.au/). File integrity verification and QA/QC are performed on each year of raw WRF output throughout the simulation lifecycle and prior to post-processing to CORDEX-compliant format climate variables. QA/QC tests include calculating the minimum, maximum, mean and standard deviation for key variables over consecutive periods of six simulation days. Variables are categorised as either normally distributed or otherwise. Normally distributed variables (e.g. surface temperature) are deemed potentially erroneous if their minima/maxima are greater than five standard deviations away from the global mean of the relevant statistic of the rolling six-day period. Non-normally distributed variables (e.g.~~,~~ snow depth and precipitation) are checked only for global minima and maxima ~~only~~.

iii) **Boxes 12-13:** after each year of simulation raw output is generated, their post-processing is initiated to produce CORDEX CORE, Tier 1 and Tier 2 variables (WCRP, 2022). A statistical QA/QC process is automatically applied to each year of post-processed

CORDEX CORE variables as they are generated throughout the simulations. QA/QC tests include:

- Check for presence of missing values.
- Check that all values are within realistic ranges for minima and maxima.
- Check minima and maxima are not equal at any timestep with exceptions (e.g., snow depth which can be zero everywhere in the outer domain).
- Check that changes over time are within realistic ranges (~~i.e.~~i.e., assess temporal gradients).
- Check that changes between neighbouring data points are within realistic ranges (~~i.e.~~i.e., assess spatial gradients).
- Check the number of grid cells with NaN (non-numerical) values do not exceed the threshold set for the variable.

Reasonable ranges for variables are determined using a series of threshold values that are based on historical records and/or empirical analysis. QA/QC computer scripts generate 'exceedance files' which output every data point that surpasses the threshold values, and these exceedance files are then manually reviewed to determine whether an issue is a true or false positive, etc.

iv) **Box 14:** Once each year of WRF raw files ~~are~~ is post-processed, raw files are transferred to a tape facility for long-term storage.

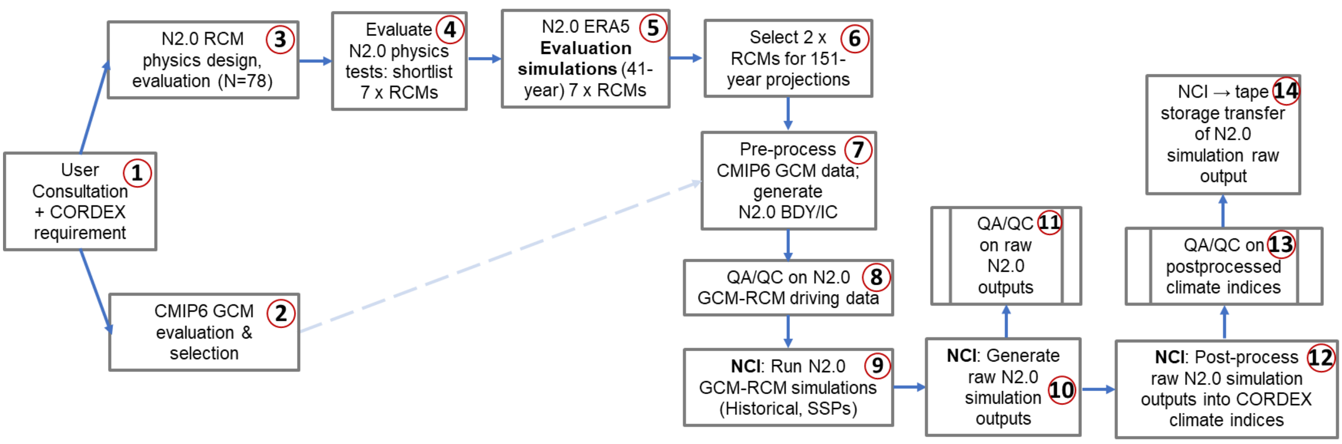


**Figure 2.** Simplified overview of ~~NARCliM2.0~~NARCliM 2.0 (N2.0) design and production processes. ERA5 = ECMWF Reanalysis v5 data; BDY = boundary conditions; IC = Initial conditions; QA/QC = Quality Assurance / Quality Control; NCI = National Comput~~ing~~ational Infrastructure (high performance computer used ~~for~~ to run N2.0 ~~production~~ simulations).

These model design and production stages are now described in more detail:

## 4~~3~~.1 Model evaluation and selection

Practical constraints such as available compute and data storage resources enforce an upper limit on GCM-RCM ensemble size. Thus, ~~NARCliM2.0~~NARCliM 2.0 uses a subset of available CMIP6 GCMs and WRF RCM configurations, necessitating careful GCM and RCM selection to create a subset of GCM-RCMs that provide robust climate simulations whilst also adequately sampling model uncertainty. In selecting a subset of GCMs and RCMs for dynamical downscaling, it is desirable to reject models that perform consistently poorly relative to their peers in simulating the current climate, as this provides lower confidence in the projected change (Evans et al., 2020b; Di Virgilio et al., 2022; Grose et al., 2023). Furthermore, the modelled climate space sampled is reduced when selecting a subset of GCMs, which can create a biased view of the climate, as well as the plausible change in climate. Care must therefore be taken to ensure that the subset of models used for downscaling are representative of the full range of possible climates, and that model errors are uncorrelated, ~~i.e.~~i.e., that models are statistically independent. The steps taken to evaluate and select GCMs and RCMs for ~~NARCliM2.0~~NARCliM 2.0 are described next.

## 4~~3~~.2 CMIP6 GCM evaluation

A three-phase process was used to evaluate individual CMIP6 GCMs (for further details see Di Virgilio et al. 2022):

### *4~~3~~.2.1 CMIP6 GCM Performance*

~~The~~ We evaluated the performances of individual CMIP6 GCMs ~~in simulating the Australian climate were assessed with respect to climate means, extremes, climate modes, and daily climate variable distributions their skill~~ in simulating the following aspects of the observed historical climate of Australia:

- annual and seasonal climatologies and daily distributions of maximum and minimum temperatures and precipitation.
- climate extremes, such as the 99th percentiles of daily maximum temperature and precipitation, and the 1st percentile of minimum temperature.
- teleconnections of oceanic climate modes and Australian regional rainfall.

Temperature and precipitation variables are chosen for evaluation because, being well-represented in high-quality gridded observational data sets for the Australian continent, they provide the most direct comparison to observations (King et al., 2013). They are also often prioritised for impact studies. Given variables such as winds (U, V), air temperature (T), water mixing ratio (Q), geopotential height (Z), sea surface temperature (SST), and sea level pressure (PSL) serve as boundary conditions for driving RCMs, these could be incorporated into future GCM evaluation studies. However, evaluating such variables would require use of re-analysis data as surrogate observations.

A set of GCMs that performed consistently poorly across the variables and statistics considered were identified. These models, as well as those with insufficient data to enable dynamical downscaling using the WRF RCM, were excluded from further evaluation leaving 27 GCMs for subsequent assessment.

### *4~~3~~.2.2 CMIP6 GCM Independence*

The retained 27 GCMs were subjected to the Bishop and Abramowitz (2013) and Herger et al. (2018) independence analyses (see ~~s~~Sect. 3.5). The GCMs were then ranked according to their relative level of statistical independence.

### *4~~3~~.2.3 Sampling CMIP6 GCM Climate Change Spread*

For climate change risk assessments, climate projections should reflect as much of the range of plausible future climate changes as possible (Whetton and Hennessy, 2010). The subset of CMIP6 GCMs selected for ~~NARCliM2.0~~NARCliM 2.0 spanned a wide range of future changes in annual mean temperature and precipitation. Climate change signals were calculated for 2080-2099 minus 1995-2014 for the Australian continent and south-east Australia under SSP3-7.0 (for the latter, see Figure 3). The GCM independence rankings were placed within this climate change space, with higher independence rankings viewed as favourable, along with consideration of the following criteria:

i) A balanced range of GCM Equilibrium Climate Sensitivities (ECS) were sampled. ECS is the long-term increase in global mean surface air temperature in response to the radiative forcing caused by a doubling of pre-industrial $CO_2$ concentrations. ECS is related to global temperature change, not just changes over Australia, however, it correlates strongly with regional warming. Around one third of CMIP6 GCMs show ECS values higher than the upper end of the likely range of 2.5°C to 4°C (IPCC, 2021). An upper range of > ~5°C cannot be ruled out (Meehl et al., 2020; Bjordal et al., 2020; Sherwood et al., 2020).

ii) Some CMIP6 GCMs that are favourable in terms of model performance and independence could not be selected as input to WRF for ~~NARCliM2.0~~NARCliM 2.0 owing to insufficient data availability for key variables~~/variable~~, where ideally, WRF requires sub-daily data for the variables shown in Supporting Information, Table S1.

As a result of the above process, the five CMIP6 GCMs listed in Table 2 are selected to force each of the two definitive ~~NARCliM2.0~~NARCliM 2.0 RCMs selected via the RCM physics testing and ERA5 evaluation processes.

**Table 2.** Basic details of the CMIP6 GCMs used to ~~-~~force the two definitive ~~NARCliM2.0 simulations~~RCMs comprising the NARCliM 2.0 CORDEX-CMIP6 ensemble.

| CMIP6 GCM | Institution | Variant/Run | Atmosphere lat/lon grid (º) |
|---|---|---|---|
| ACCESS-ESM1-5 | CSIRO | r6i1p1f1 | 1.2 × 1.8 |
| EC-Earth3-Veg | EC-EARTH consortium | r1i1p1f1 | 0.7 × 0.7 |
| MPI-ESM1-2-HR | Max Planck Institute for Meteorology (MPI) | r1i1p1f1 | ~0.9 |
| NorESM2-MM | Norwegian Climate Centre | r1i1p1f1 | 0.9 × 0.9 |
| UKESM1-0-LL | UK Met Office and NERC research centres | r1i1p1f2 | 1.3 × 1.9 |

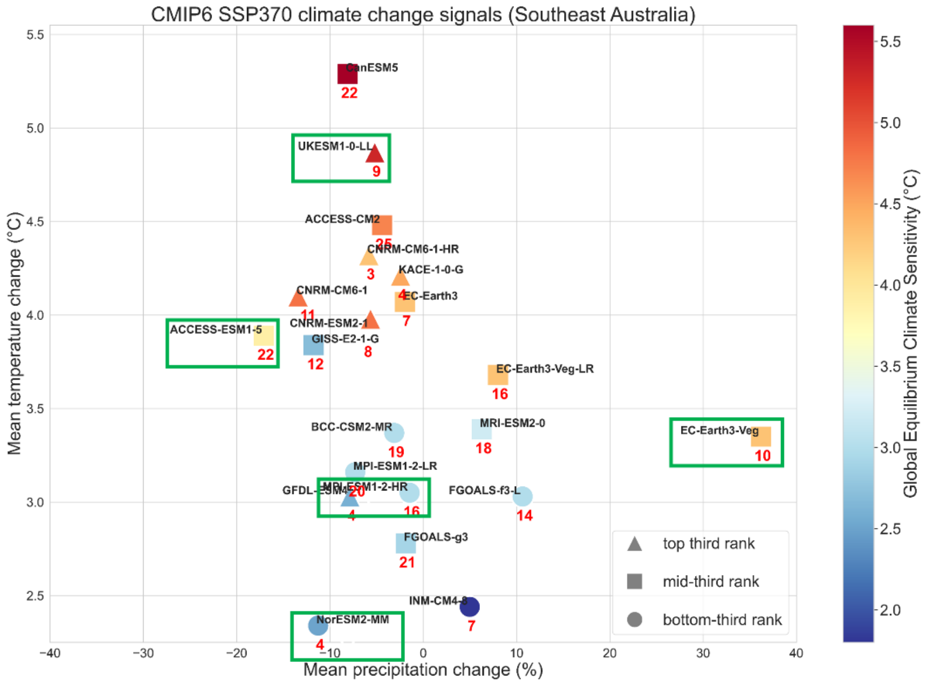


**Figure 3.** CMIP6 GCM climate change signals (2080-2099 versus 1995-2014) over south-east Australia for the subset of GCMs retained following the model performance evaluation in Di Virgilio et al. (2022), and that simulated at least monthly mean near surface air temperature and precipitation for the SSP-3.70 scenario. Boxed GCMs are selected to force ~~NARCliM2.0~~NARCliM 2.0 RCMs. Marker shapes indicate overall GCM performance; markers are coloured according to their global equilibrium climate sensitivity (ECS) values; **Red** numbers represent the smallest Herger Method 1 set for that GCM.

## 4~~3~~.3 ~~NARCliM2.0~~NARCliM 2.0 RCM physics testing

The ~~NARCliM2.0~~NARCliM 2.0 RCM physics testing aims to identify and exclude RCMs that perform consistently poorly in simulating the southeast Australian climate and to select RCMs that have high statistical independence. The selection of RCMs in ~~NARCliM2.0~~NARCliM 2.0 involves the creation of a multi-physics ensemble where each RCM uses different physical parametrisations for PBL, microphysics, cumulus, radiation, and LSM. This enables many structurally different RCMs to be constructed and tested. In ~~NARCliM1.0~~NARCliM 1.0, 36 WRF RCM configurations were designed, tested, and evaluated (Evans et al. 2014). ~~NARCliM2.0~~NARCliM 2.0 physics testing assesses 78 RCM configurations which are progressively tested via three phases, where each test phase is informed by the outcomes of the preceding phase to systematically remove poor performing RCM options while facilitating the selection of parameterisations that perform well during testing. The N=36 RCMs tested for ~~NARCliM1.0~~NARCliM 1.0 were evaluated based on eight representative storm event simulations each of two-weeks duration (Evans et al. 2014). ~~NARCliM2.0~~NARCliM 2.0 physics simulations were run over an entire annual cycle (2016) with a two-month spin-up period commencing 1 November 2015. Australia experienced a range of weather extremes during 2016 driven by a range of climatic influences making 2016 a suitable target year (Bureau of Meteorology, 2017). Whilst assessing RCMs for an entire year improves on assessing for discrete storm events as per physics testing for ~~NARCliM1.0~~NARCliM 1.0, it was not feasible to run a large RCM physics ensemble for a longer duration. Initial and boundary conditions for all phases of the ~~NARCliM2.0~~NARCliM 2.0 RCM physics test simulations were derived from the ERA-Interim reanalysis data set (Dee et al., 2011). ERA-Interim was used because ERA5 was not available at the time. The three phases of ~~NARCliM2.0~~NARCliM 2.0 physics testing are as follows:

### *4~~3~~.3.1 Phase I (N=36)*

Thirty-six RCMs we~~we~~re evaluated in Phase I. One radiation scheme (RRTMG) ~~i~~was tested for both long and short-wave radiation (it wa~~i~~s held fixed for all RCMs), whereas physics settings for PBL, microphysics, cumulus, and LSM we~~a~~re varied. Of the 36 simulations, 18 used the Noah-Unified LSM, whilst the remainder used Community Land Model version 4.0 (CLM4). The physics options tested are listed in Table 3, where these were selected based on literature review. Each physics test simulation is denoted by a 12-digit identifier which comprises 6 pairs of digits, with each pair corresponding to the choice of a specific physics option as specified in the WRF namelist.input file. These pairs of digits follow the order: planetary boundary layer (pbl) ¦ cloud microphysics (mp) ¦ cumulus convection (cu) ¦ shortwave radiation (sw) ¦ longwave radiation (lw) ¦ LSM (sf) and correspond to the WRF namelist options shown in Table 3. For example, the simulation ~~‘~~050601040402~~’~~ is interpreted as: 05 ¦ 06 ¦ 01 ¦ 04 ¦ 04 ¦ 02 and denotes that this simulation uses the following physics settings:

| | |
|---|---|
| bl_pbl_physics | = 05 (MYNN2) |
| mp_physics | = 06 (WSM6) |
| cu_physics | = 01 (Kain-Fritsch) |
| ra_sw_physics | = 04 (RRTMG) |
| ra_lw_physics | = 04 (RRTMG) |
| sf_surface_physics | = 02 (Noah Unified) |

The complete set of WRF RCM configurations tested in Phase I is shown in Supporting Information Table S2.

**Table 3.** Physics options used in phase I (N=36) tests.

| Physics Option Description | WRF Namelist | Options Tested | Reference |
|---|---|---|---|
| Planetary boundary layer | bl_pbl_physics | 01 = YSU | Hong et al. (2006) |
| | | 05 = MYNN2 | Nakanishi & Niino (2009) |
| | | 07 = ACM2 | Pleim (2007) |
| Microphysics | mp_physcis | 06 = WSM6 | Hong and Lim (2006) |
| | | 08 = Thompson | Thompson et al. (2008) |
| Cumulus parameterisation | cu_physics | 01 = Kain-Fritsch | Kain (2004) |
| | | 02 = BMJ | Janjić (2000) |
| | | 06 = Tiedtke | Tiedtke (1989) |
| Shortwave radiation | ra_sw_physics | 04 = RRTMG | Iacono et al. (2008) |
| Longwave radiation | ra_lw_physics | 04 = RRTMG | |
| Land surface model | sf_surface_physics | 02 = Noah-Unified | Tewari et al. (2016) |
| | | 05 = Community Land Model V4 | Oleson et al. (2010) |

| ~~Physics Option Description~~ | ~~WRF Namelist~~ | ~~Options Tested~~ |
|---|---|---|
| ~~Planetary boundary layer~~ | ~~bl_pbl_physics~~ | ~~01 = YSU~~ |
| | | ~~05 = MYNN2~~ |
| | | ~~07 = ACM2~~ |
| ~~Microphysics~~ | ~~mp_physcis~~ | ~~06 = WSM6~~ |
| | | ~~08 = Thompson~~ |
| ~~Cumulus parameterisation~~ | ~~cu_physics~~ | ~~01 = Kain-Fritsch~~ |
| | | ~~02 = BMJ~~ |
| | | ~~06 = Tiedtke~~ |
| ~~Shortwave radiation~~ | ~~ra_sw_physics~~ | ~~04 = RRTMG~~ |
| ~~Longwave radiation~~ | ~~ra_lw_physics~~ | ~~04 = RRTMG~~ |
| ~~Land surface model~~ | ~~sf_surface_physics~~ | ~~02 = Noah-Unified~~ |
| | | ~~05 = Community Land Model V4~~ |

### *~~3~~4.3.2 Phase II (N=60): additional LSM and radiation scheme tests*

Phase I RCMs using CLM4.0 were omitted from further testing because they did not consistently improve performance in simulating the Australian climate relative to RCMs using Noah-Unified. In addition, RCMs using CLM4.0 had increased simulation times (by approximately twice when compared to Noah-Unified). Hence, Phase II focused~~s~~ exclusively on further testing of the RCM configurations that used the Noah-Unified LSM.

The physics settings tested in Phase II are an alternative LSM to Noah-Unified (Noah Multi-Parameterisation; ~~‘~~Noah-MP~~’~~, Niu et al., 2011) and New Goddard radiation (Chou et al., 2001). Owing to time/resource constraints, testing all eighteen Phase I RCMs using Noah-Unified was not feasible. To reduce the number of RCMs for further testing, the worst-performing Noah-Unified based RCM configurations identified in Phase I were excluded. The N=18 RCMs using Noah-Unified are listed along with their overall performance total scores in Table 4 where the lowest scores under ‘Rank totals’ indicate the RCMs that overall perform relatively well versus their peers (see ~~s~~Sect. 3 Evaluation Methods). Note that the ‘Overall rank’ denotes the RCMs’ relative ranking among all Phase I RCMs. There is a sharp reduction in rank totals for RCMs #13-18 inclusive, relative to RCMs #1-12. Therefore, RCMs #13-18 are excluded from further testing, and RCMs #1-12 are retained.

**Table 4.** RCM physics combination ranks of the Phase I, N=18 Noah Unified (NU) based RCMs. Scores/ranks are based on model bias and root mean square error for annual and seasonal precipitation, minimum temperature, maximum temperature, climate extremes (wettest and hottest days), and Perkins Skill Scores (see ~~s~~Sect. 3). RCMs #1-12 are selected for further testing.

| **RCM #** | **RCM ID** | **Physics combination** | | | | | **Rank total** | **Overall rank in N=36 Phase I** |
|---|---|---|---|---|---|---|---|---|
| | | **PBL** | **MP** | **Cumulus** | **SW/LW** | **LSM** | | |
| 1 | 070801040402 | ACM2 | Thom | KF | RRTMG | NU | 484 | 1 |
| 2 | 070601040402 | ACM3 | WSM6 | KF | RRTMG | NU | 495 | 2 |
| 3 | 070802040402 | ACM4 | Thom | BMJ | RRTMG | NU | 527 | 3 |
| 4 | 070602040402 | ACM5 | WSM6 | BMJ | RRTMG | NU | 559 | 4 |
| 5 | 010802040402 | YSU | Thom | BMJ | RRTMG | NU | 574 | 7 |
| 6 | 050801040402 | MYNN2 | Thom | KF | RRTMG | NU | 583 | 8 |
| 7 | 010801040402 | YSU | Thompson | KF | RRTMG | NU | 617 | 11 |
| 8 | 050802040402 | MYNN2 | Thompson | BMJ | RRTMG | NU | 630 | 12 |
| 9 | 070606040402 | ACM2 | WSM6 | Tiedtke | RRTMG | NU | 639 | 13 |
| 10 | 050601040402 | MYNN2 | WSM6 | KF | RRTMG | NU | 662 | 16 |
| 11 | 070806040402 | ACM2 | Thompson | Tiedtke | RRTMG | NU | 662 | 16 |
| 12 | 010602040402 | YSU | WSM6 | BMJ | RRTMG | NU | 674 | 19 |
| 13 | 010601040402 | YSU | WSM6 | KF | RRTMG | NU | 702 | 23 |
| 14 | 010606040402 | YSU | WSM6 | Tiedtke | RRTMG | NU | 759 | 25 |
| 15 | 050606040402 | MYNN2 | WSM6 | Tiedtke | RRTMG | NU | 766 | 27 |
| 16 | 050602040402 | MYNN2 | WSM6 | BMJ | RRTMG | NU | 811 | 31 |
| 17 | 010806040402 | YSU | Thompson | Tiedtke | RRTMG | NU | 830 | 34 |
| 18 | 050806040402 | MYNN2 | Thompson | Tiedtke | RRTMG | NU | 857 | 35 |

This gives two sets of physics combinations for additional testing: 1) one replaces only RRTMG (|04|04|) for short and longwave radiation with New Goddard (|05|05|) making no other changes; and 2) RRTMG radiation is retained, but Noah-MP (|04|) replaces Noah-Unified (|02|). This creates an additional 24 RCM configurations for assessment, bringing the total RCMs tested to 60. Although Noah-MP has several parameter options, Phase II uses its default settings.

### *~~3~~4.3.3 Phase III (N=78): parameterising Noah-MP*

Phase II shows that RCM performance using New Goddard radiation is generally inferior to the same RCMs using RRTMG (see ~~s~~Sect. 5. RCM Physics test results). Consequently, RRTMG radiation is re-adopted for Phase III. Conversely, a general performance improvement is conferred by using Noah-MP over Noah-Unified (~~s~~Sect. 5). Given this performance improvement using Noah-MP with default settings, Phase III assesses RCM performances using specific parameter settings for Noah-MP.

Noah-MP provides a ~~'~~dynamic vegetation cover~~'~~ model option (referred to as dynamic vegetation in the WRF users' guide) (Niu et al., 2011). When deactivated (the default), monthly leaf area index (LAI) is prescribed for various vegetation types and the greenness vegetation fraction (GVF) comes from monthly GVF climatological values. Conversely, when dynamic vegetation cover is activated, LAI and GVF are calculated using a dynamic leaf model. We clarify here that dominant plant-functional types do not change when using this option, but only the LAI and GVF, ~~i.e.~~i.e., only the amount of green cover changes.

Noah-MP also provides several options for modelling surface run-off and groundwater processes including a TOPMODEL (TOPography based hydrological MODEL)-based surface runoff scheme and a simple groundwater model (SIMGM; Niu et al., 2011). Some studies have shown that using this option improves the modelling of soil moisture (e.g. Zhuo et al., 2019). Thus, three new sets of physics configurations are tested using Noah-MP where default options for specific settings are changed as follows:

~~3.~~4. activate dynamic vegetation cover (dveg=2 in the WRF namelist); no other changes.

~~4.~~5. activate TOPMODEL runoff with simple groundwater (opt_run=1); no other changes.

~~5.~~6. activate both dynamic vegetation and TOPMODEL runoff with simple groundwater;~~,~~ no other changes.

As above, the worst performing RCMs in Phase II are excluded from Phase III testing. Based on the RCM configuration performance rankings (Table 5), there is a sharp reduction in performance starting from RCM #7 inclusive. Therefore, RCMs #7-12 are excluded from further testing. Phase III thus comprises 18 new test simulations (sets 1-3 each comprising 6 RCMs) bringing the total RCMs tested to N=78. Phase III physics tests are denoted using the same RCM identification schemes distinguished by appending ~~'~~set_1~~'~~, ~~'~~set_2~~'~~, ~~'~~set_3~~'~~ to identifiers.

**Table 5.** RCM physics combination ranks of the Phase II Noah-MP RCMs. Scores/ranks are based on model bias and root mean square error for annual and seasonal precipitation, minimum temperature, maximum temperature, climate extremes (wettest and hottest days), and Perkins Skill Scores (see ~~s~~Sect. 3).

| No. | Physics combination | Rank total |
|---|---|---|

| | | |
|---|---|---|
| 1 | 50801040404 | 721 |
| 2 | 70806040404 | 822 |
| 3 | 50802040404 | 848 |
| 4 | 70802040404 | 872 |
| 5 | 70601040404 | 880 |
| 6 | 50601040404 | 891 |
| 7 | 10802040404 | 988 |
| 8 | 70602040404 | 1005 |
| 9 | 70606040404 | 1028 |
| 10 | 10801040404 | 1042 |
| 11 | 70801040404 | 1056 |
| 12 | 10602040404 | 1264 |

### *4~~3~~.3.4 Shortlisting Physics Test RCMs for ERA5-~~NARCliM2.0~~NARCliM 2.0 evaluation simulations*

Considering the complete ~~NARCliM2.0~~NARCliM 2.0 N=78 physics test ensemble, to identify physics test RCMs that perform poorly overall, RCMs are eliminated if they are in the lowest 1/3 for RCM performance ranks for any of maximum temperature, minimum temperature, precipitation, or for the overall model performance rank across these variables (see ~~s~~Sect. 5. RCM Physics test results). Under this scheme, 20 RCMs remain. The independence measures are then applied to the remaining 20 RCMs to choose a final subset of 7 RCMs for ERA5-forced evaluation simulations (see ~~s~~Sect. 4.4). The ensemble size limit of N=7 is determined by available compute resources. These 7 candidate RCMs are assessed for potential use in the CMIP6 GCM-forced downscaling phase of ~~NARCliM2.0~~NARCliM 2.0 (~~s~~Sect. 4.4 and Di Virgilio et al. in review).

## ~~3~~4.4 CORDEX ERA5-~~NARCliM2.0~~NARCliM 2.0 evaluation simulations

NARCliM1.x performed production climate simulations using a two-phase process. Its RCM physics testing selected definitive ~~'~~production-grade~~'~~ RCMs which were then used to downscale both reanalysis data and CMIP3/5 GCMs. In contrast, for ~~NARCliM2.0~~NARCliM 2.0, as described above the N=78 RCM physics testing culminates in shortlisting 7 ~~'~~production-candidate~~'~~ RCMs which are used to downscale the ERA5 reanalysis for 42-years (1979-2020). This enables assessment of ~~shortlisted RCM~~ the performances of these 7 shortlisted RCMs over a climatological period rather than the single year (2016) of the physics testing, which helps ascertain that performance differences between shortlisted RCMs are robust across a multi-decadal timescale capturing climatologically diverse years. The aim is that two definitive production-grade RCMs can be selected for CMIP6-forced downscaling from these ERA5-forced CORDEX ~~'~~evaluation~~'~~ simulations. Thus, the seven ERA5-~~NARCliM2.0~~NARCliM 2.0 RCMs were driven by ERA5.0 boundary conditions for January 1979 to

December 2020 using the model and nested domain setups described above for ~~NARCliM2.0~~NARCliM 2.0. The skill of these RCMs in simulating the recent Australian climate was assessed as follows (see Di Virgilio et al. in review): annual and seasonal means were calculated for maximum and minimum temperature and precipitation using monthly means for temperature variables, and the monthly sum for precipitation. Extremes of maximum temperature and precipitation ($99^{th}$ percentiles) and extreme minimum temperature ($1^{st}$ percentile) were calculated using daily data. RCM performances in reproducing observations over these timescales were assessed by calculating model outputs minus observations (~~i.e.~~i.e., model bias), and the RMSE of modelled versus observed fields. RCM skill in simulating distributions of observed variables was assessed by comparing the PDFs for daily mean observations versus those of the RCMs. The ultimate outcome of these ERA5-forced simulations and their evaluation is the selection of two definitive RCM configurations, R3 and R5, to run the CMIP6-forced phase of ~~NARCliM2.0~~NARCliM 2.0, see Di Virgilio et al. (in review) for further details on the evaluation methods and results. Supporting Information Figure S1 shows the WRF namelist settings for the R3 and R5 RCMs (see also ~~s~~Sect. 9. Code Availability).

## 4~~3~~.5 CORDEX CMIP6-forced ~~NARCliM2.0~~NARCliM 2.0 simulations

The ideal CMIP6 GCM variables and their frequencies required to run the WRF RCM are listed in Table S1. A minority of variables in Table S1 are not available at sub-daily frequencies for every target GCM. This necessitates assumptions/data proxies to be made. For instance, soil moisture and soil temperature variables were unavailable for some selected GCMs; hence, surrogate data, such as surface temperature, were used for initialisation (noting that soil data are only used by the RCM at initialisation). In these cases, we investigated how long it took for uncertainty in the initial conditions to disappear from the WRF output by analysing the regionally averaged soil moisture time series. The data were regionalised according to the four Australian Natural Resource Management (NRM) regions / climate zones (Supporting Information Figure S2) which are broadly aligned with climatological boundaries (Fiddes et al., 2021) and with the IPCC reference regions (Iturbide et al., 2020). Time series plots (Figure S3) show that soil moisture equilibrates to be within a normal range following initialisation, indicating that the 12-month spin-up year (1950) is sufficient to account for the assumptions made at model initialisation.

Boundary and initial conditions were prepared using selected GCM data to run the 151-year GCM-driven simulations using WRF version 4.1.2. The GCM-driven simulations were run and completed using the pre-defined RCM settings for the two definitive RCM configurations using the WRF namelists in Supporting Information Figure S1 (see also ~~s~~Sect. 9. Code Availability). A cold restart was performed on the last Historical experiment year (2014), thus enabling the SSP1-2.6 and SSP3-7.0 experiments to be run for 2015-2100 concurrently with the Historical experiment. Testing the time duration required for soil moisture to equilibrate from the cold start showed that 1 year is sufficient. The 2014 cold start year is eventually overwritten by Historical runs initiated in 1950.

# ~~6.~~5. RCM Physics test results

## 5.1 Phase I RCM performance summary

The spatial variation and magnitudes for Phase I RCM biases and RMSEs for annual mean maximum and minimum temperature and precipitation are shown in Figures 4-5, respectively. Overall, RCMs are biased cold for maximum temperature (mean absolute bias for the ensemble mean = 1.18 K), and warm-biased for minimum temperature (mean absolute bias = 1.31 K; Figure 4a-b). Maximum temperature RMSE magnitudes are large over the elevated terrain of the southeast coast and over western regions (Figure 5a). The simulation of precipitation shows biases of varying sign, with wet biases that are strongest over eastern coastal regions (Figure 4c). Precipitation RMSEs are particularly large along the eastern coastline (>15 mm), and generally show an east-west gradient, ~~i.e.~~i.e., progressively decreasing further inland from the coast (Figure 5c).

## 5.2 Comparing Phase II Physics Test RCM performances versus Phase I

### *5.2.1 Climate Means*

Overall, the RCM ensemble using New Goddard (NG) radiation has inferior performance to the corresponding RCMs using RRTMG in terms of annual/seasonal mean maximum temperature biases, RMSEs, and PSS (Table 7). In contrast, NG confers superior performance for annual/seasonal mean minimum temperature for these statistics. RCMs using NG show reduced biases for annual mean and spring-time precipitation, but larger errors for DJF and JJA (Table 7). RMSEs for annual and seasonal precipitation are similarly variable.

**Table 7.** Climate means performance: phase II physics tests (~~i.e.~~i.e., N=12 set 1 changing only RRTMG to New Goddard (NG) and N=12 set 2 changing only land surface model (LSM) from Noah-Unified to Noah-MP (NMP) compared with the phase I physics test RCMs that were shortlisted for further testing (N=12).

| | | **Bias** | | | **RMSE** | | | **PSS** | | |
|---|---|---|---|---|---|---|---|---|---|---|
| **Variable** | **Timescale** | **Phase I (N=12) ensemble mean** | **Phase II (NG rad.) ensemble mean** | **Phase II (NMP LSM) ensemble mean** | **Phase I (N=12) ensemble mean** | **Phase II (NG rad.) ensemble mean** | **Phase II (NMP LSM) ensemble mean** | **Phase I (N=12) ensemble mean** | **Phase II (NG rad.) ensemble mean** | **Phase II (NMP LSM) ensemble mean** |
| **Temp. Max. (K)** | Annual | 0.87 | 1.27 | 0.58 | 3.56 | 3.73 | 3.50 | **0.950** | **0.936** | **0.955** |
| | DJF | 0.74 | 1.29 | 0.63 | 4.41 | 4.70 | 4.43 | - | - | - |
| | MAM | 1.40 | 2.06 | 0.83 | 3.68 | 3.92 | 3.55 | | | |

| | | | | | | | | | | |
|---|---|---|---|---|---|---|---|---|---|---|
| | JJA | 0.62 | 0.81 | 0.52 | 2.64 | 2.66 | 2.65 | | | |
| | SON | 0.87 | 1.04 | 0.66 | 3.25 | 3.32 | 3.20 | | | |
| | Annual | 1.35 | 0.95 | 1.2 | 3.53 | 3.41 | 3.42 | **0.927** | **0.941** | **0.931** |
| | DJF | 1.50 | 1.08 | 0.87 | 3.86 | 3.82 | 3.66 | | | |
| **Temp. Min. (K)** | MAM | 1.21 | 0.84 | 0.92 | 3.55 | 3.45 | 3.50 | - | - | - |
| | JJA | 0.82 | 0.51 | 0.91 | 3.00 | 2.92 | 3.00 | | | |
| | SON | 1.88 | 1.47 | 1.92 | 3.63 | 3.40 | 3.58 | | | |
| | Annual | 0.25 | 0.24 | 0.25 | 7.21 | 7.32 | 6.78 | **0.943** | **0.950** | **0.946** |
| | DJF | 0.41 | 0.53 | 0.49 | 8.28 | 8.83 | 8.85 | | | |
| **Prec. (mm)** | MAM | 0.32 | 0.32 | 0.25 | 5.91 | 6.47 | 5.53 | - | - | - |
| | JJA | 0.37 | 0.53 | 0.44 | 7.63 | 7.34 | 7.65 | | | |
| | SON | 0.34 | 0.22 | 0.39 | 6.68 | 6.18 | 6.92 | | | |

Phase II RCMs using Noah-MP with RRTMG retained show improved performance in simulating mean maximum and minimum temperature at annual timescales and most seasons relative to corresponding Phase I RCMs using Noah-Unified (Table 7; Figure 4-5). For instance, the mean absolute bias for annual mean maximum temperature is 0.58 K for the Noah-MP ensemble mean versus 1.18 K for the Noah-Unified ensemble. In particular, cold bias magnitudes for maximum temperature are considerably lower over eastern and southern regions for the RCMs using Noah-MP (Figure 4d). RMSE magnitudes for maximum temperature are substantially reduced over the topographically complex regions of the southeast, and southwest and central regions (Figure 5d).

Overall, the magnitude of warm biases for minimum temperature are broadly similar for Phase I and Phase II RCMs (Figure 4b,c). Conversely, while RCMs in both Phases show large RMSEs for minimum temperature over several eastern regions, RMSEs are smaller for the Noah-MP ensemble over some southern areas (Figure 5b,c).

In contrast to the above results for the simulation of maximum temperature, overall, Phase II RCMs using Noah-MP show smaller performance improvements for the simulation of precipitation relative to the Phase I RCMs (Table 7). However, precipitation bias magnitudes are smaller for the Noah-MP ensemble over specific regions, e.g., north-eastern coastal regions and the elevated terrain of the south-east (Figure 4c,f).

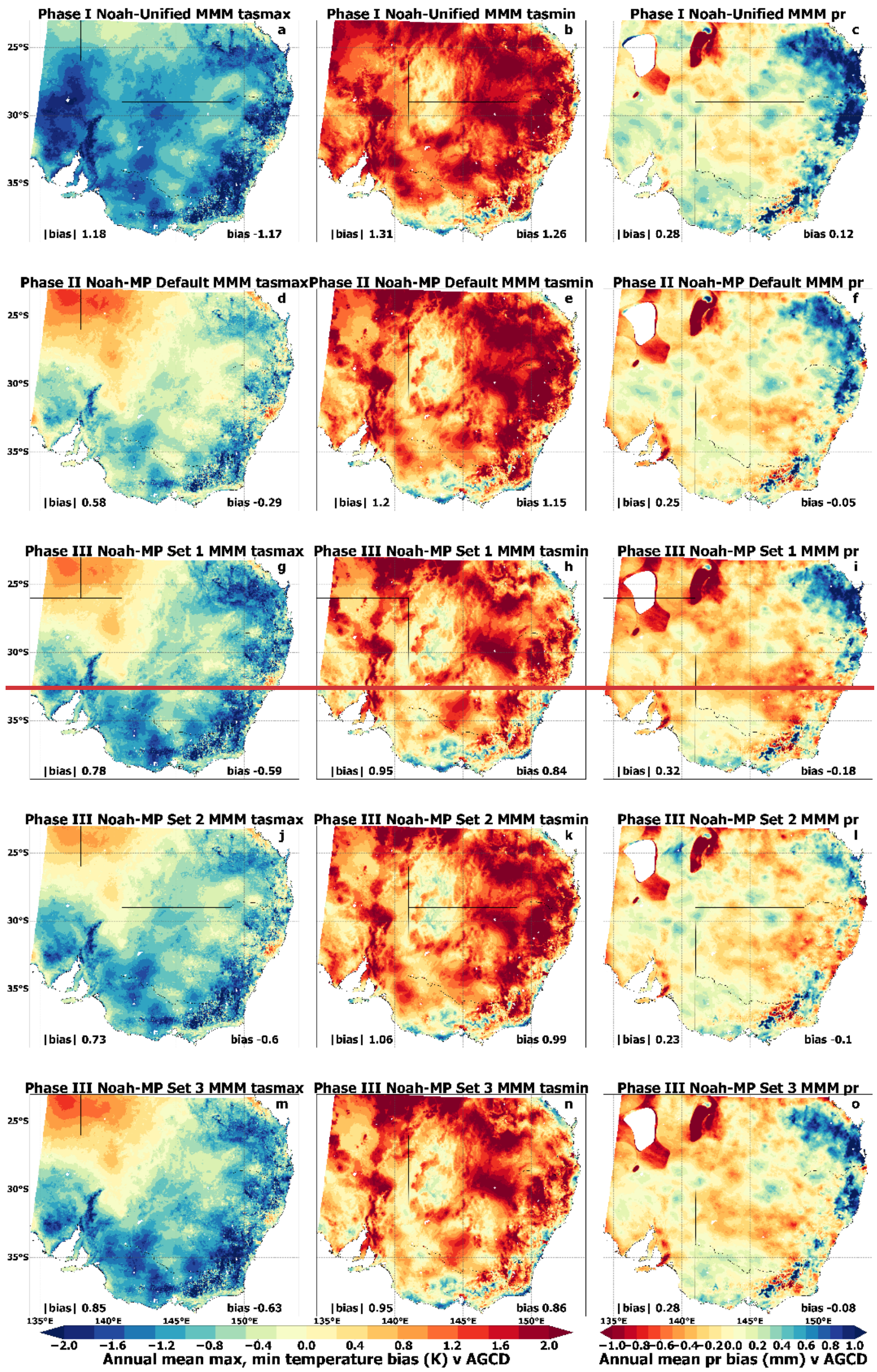
Phase I Noah-Unified MMM tasmax
a
|bias| 1.18
bias -1.17
Phase I Noah-Unified MMM tasmin
b
|bias| 1.31
bias 1.26
Phase I Noah-Unified MMM pr
c
|bias| 0.28
bias 0.12
Phase II Noah-MP Default MMM tasmax
d
|bias| 0.58
bias -0.29
Phase II Noah-MP Default MMM tasmin
e
|bias| 1.2
bias 1.15
Phase II Noah-MP Default MMM pr
f
|bias| 0.25
bias -0.05
Phase III Noah-MP Set 1 MMM tasmax
g
|bias| 0.78
bias -0.59
Phase III Noah-MP Set 1 MMM tasmin
h
|bias| 0.95
bias 0.84
Phase III Noah-MP Set 1 MMM pr
i
|bias| 0.32
bias -0.18
Phase III Noah-MP Set 2 MMM tasmax
j
|bias| 0.73
bias -0.6
Phase III Noah-MP Set 2 MMM tasmin
k
|bias| 1.06
bias 0.99
Phase III Noah-MP Set 2 MMM pr
l
|bias| 0.23
bias -0.1
Phase III Noah-MP Set 3 MMM tasmax
m
|bias| 0.85
bias -0.63
Phase III Noah-MP Set 3 MMM tasmin
n
|bias| 0.95
bias 0.86
Phase III Noah-MP Set 3 MMM pr
o
|bias| 0.28
bias -0.08
25°S
30°S
35°S
135°E
140°E
145°E
150°E
−2.0 −1.6 −1.2 −0.8 −0.4 0.0 0.4 0.8 1.2 1.6 2.0
Annual mean max, min temperature bias (K) v AGCD
−1.0 −0.8 −0.6 −0.4 −0.2 0.0 0.2 0.4 0.6 0.8 1.0
Annual mean pr bias (mm) v AGCD

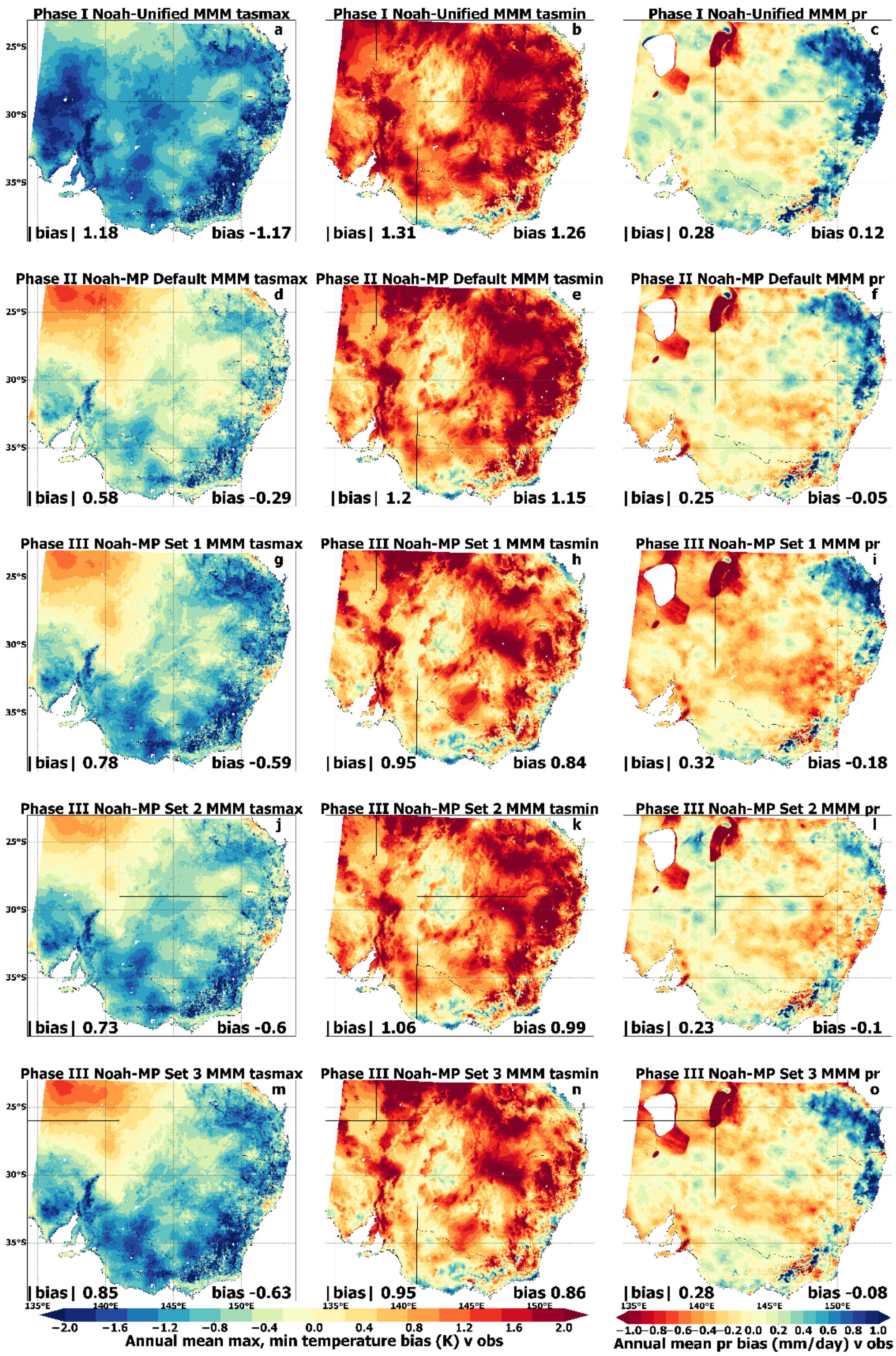


**Figure 4.** Phase I (N=36), Phase II (N=60) and Phase III (N=78) ensemble mean biases for annual mean maximum temperature, minimum temperature and precipitation with respect to Australian Gridded Climate Data (AGCD) observations for ~~NARClIM2.0~~NARCliM 2.0 Phase I physics test RCMs using Noah-Unified as the land surface model (LSM) (a-c); Phase II physics test RCMs using Noah-MP as the LSM and its default settings (d-f); Phase III ~~‘~~set 1~~’~~ physics test RCMs using Noah-MP with dynamic vegetation cover activated (g-i); Phase III ~~‘~~set 2~~’~~ physics test RCMs using Noah-MP with TOPMODEL surface runoff and simple groundwater activat-

ed (j-l); and Phase III ‘set 3’ physics test RCMs using Noah-MP with both dynamic vegetation cover and TOPMODEL runoff activated (m-o).

596

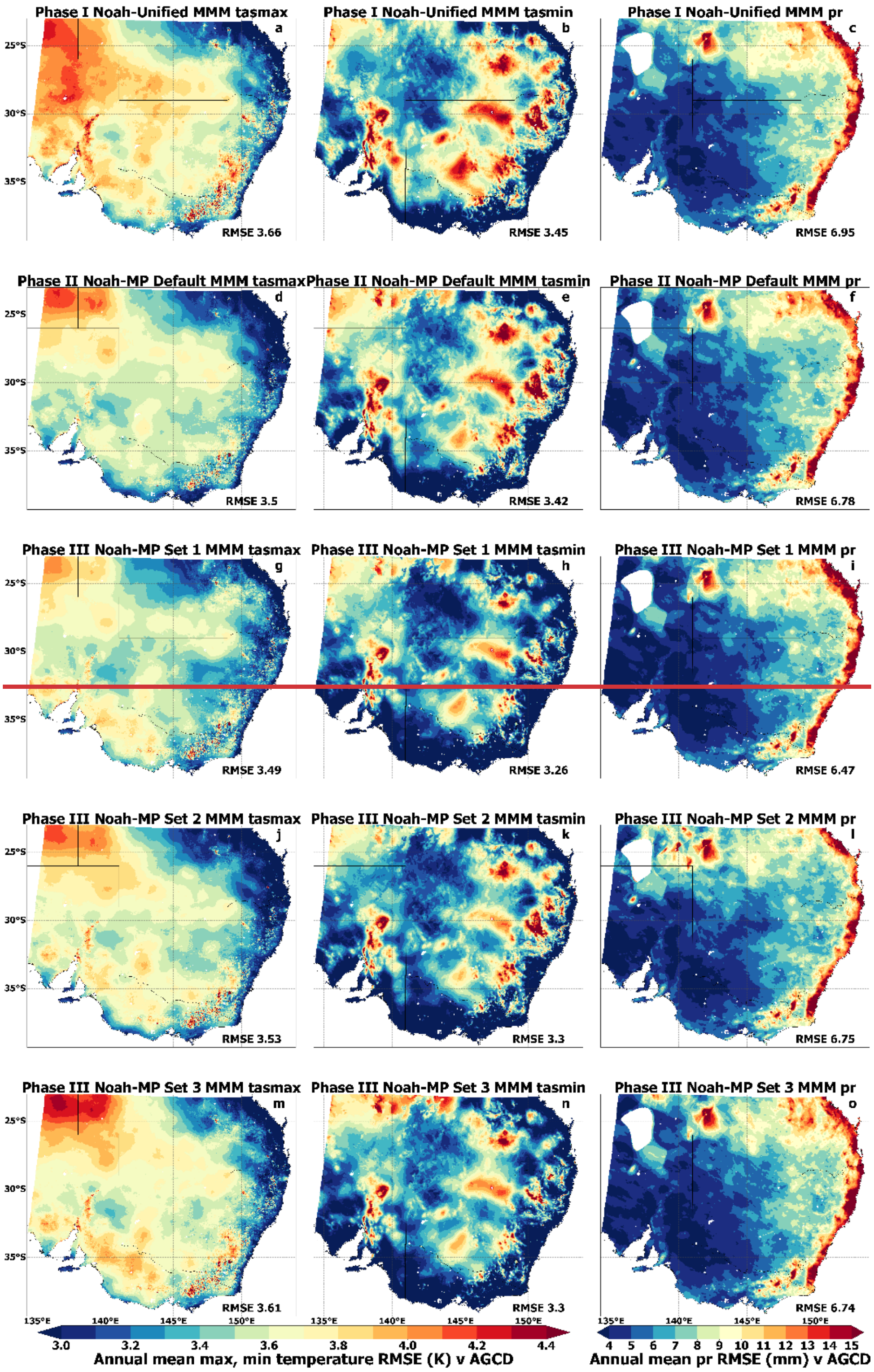

Phase I Noah-Unified MMM tasmax
a
RMSE 3.66
Phase I Noah-Unified MMM tasmin
b
RMSE 3.45
Phase I Noah-Unified MMM pr
c
RMSE 6.95
Phase II Noah-MP Default MMM tasmax
d
RMSE 3.5
Phase II Noah-MP Default MMM tasmin
e
RMSE 3.42
Phase II Noah-MP Default MMM pr
f
RMSE 6.78
Phase III Noah-MP Set 1 MMM tasmax
g
RMSE 3.49
Phase III Noah-MP Set 1 MMM tasmin
h
RMSE 3.26
Phase III Noah-MP Set 1 MMM pr
i
RMSE 6.47
Phase III Noah-MP Set 2 MMM tasmax
j
RMSE 3.53
Phase III Noah-MP Set 2 MMM tasmin
k
RMSE 3.3
Phase III Noah-MP Set 2 MMM pr
l
RMSE 6.75
Phase III Noah-MP Set 3 MMM tasmax
m
RMSE 3.61
Phase III Noah-MP Set 3 MMM tasmin
n
RMSE 3.3
Phase III Noah-MP Set 3 MMM pr
o
RMSE 6.74
25°S
30°S
35°S
135°E 140°E 145°E 150°E
3.0 3.2 3.4 3.6 3.8 4.0 4.2 4.4
Annual mean max, min temperature RMSE (K) v AGCD
4 5 6 7 8 9 10 11 12 13 14 15
Annual mean pr RMSE (mm) v AGCD

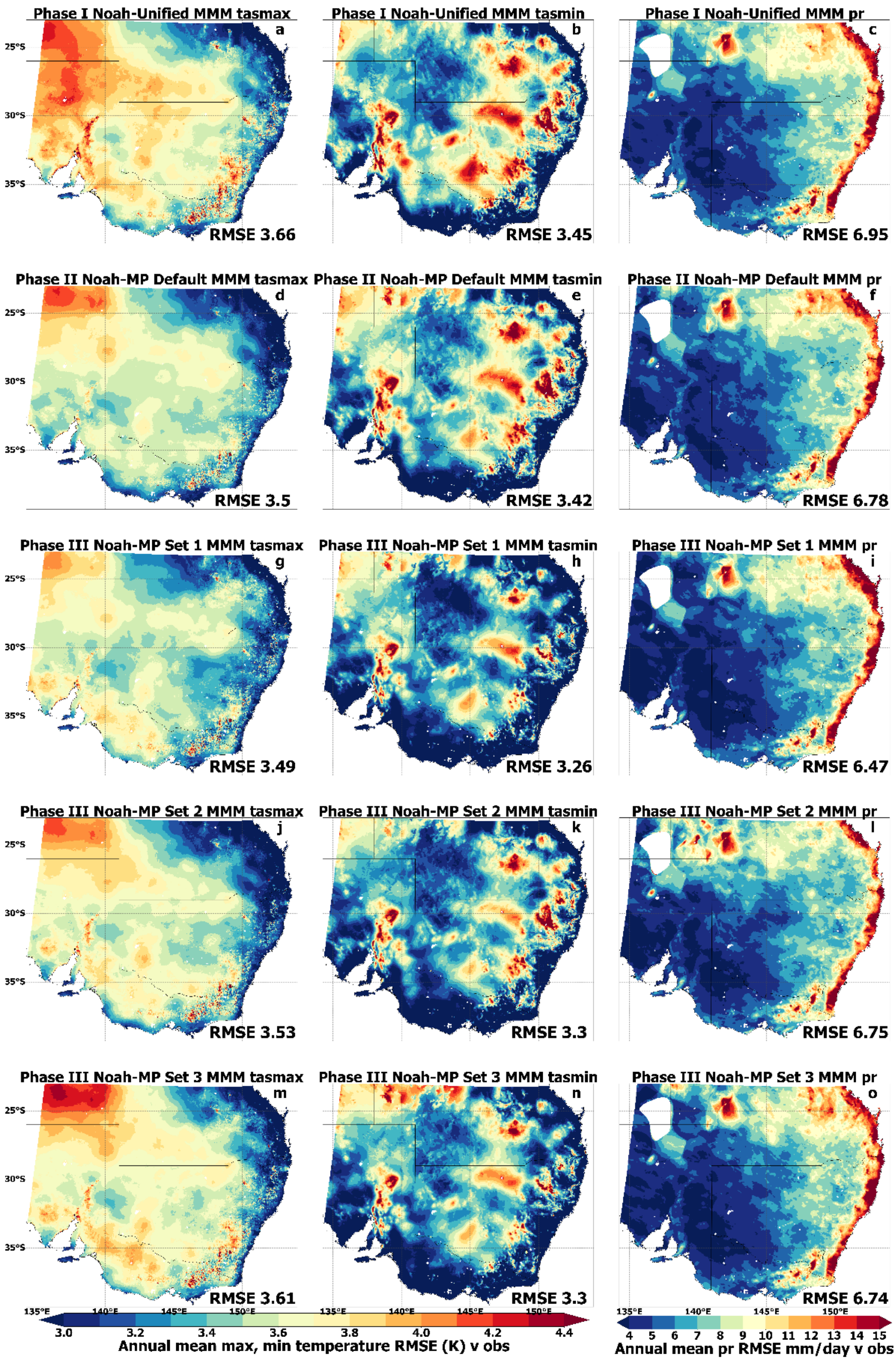


**Figure 5.** As per Figure 4 but showing RMSEs.

### *5.2.2. Climate Extremes*

Climate extreme analysis assesses RCM representations of the hottest and the wettest day versus AGCD. For both extremes and for RCM biases and RMSEs, Phase II RCMs using NG radiation showed inferior performance relative to phase I RCMs using RRTMG (Table 8). Conversely, Phase II RCMs using Noah-MP show substantial reductions in bias for both the hottest and wettest days (Table 8). Phase II Noah-MP RCMs show a small increase in RMSE for the hottest day (Phase I bias=3.59 K; Phase II bias=3.74 K); however, RMSEs are smaller for the wettest day (~~i.e.~~i.e., Phase I RMSE=19.20 mm; Phase II RMSE=18.47 mm) (Table 8).

**Table 8** Climate extremes performance: comparing phase I RCMs (N=12) with phase II RCMs (~~i.e.~~i.e., 12 RCMs changing radiation from RRTMG to New Goddard (NG) and 12 RCMs changing land surface model (LSM) from Noah-Unified to Noah-MP; NMP).

| | **Bias** | | | **RMSE** | | |
|---|---|---|---|---|---|---|
| **Variable** | **Phase I (N=12) ensemble mean** | **Phase II (NG rad.) ensemble mean** | **Phase II (NMP LSM) ensemble mean** | **Phase I (N=12) ensemble mean** | **Phase II (NG rad.) ensemble mean** | **Phase II (NMP LSM) ensemble mean** |
| **Temp. max: hottest (K)** | 1.11 | 1.93 | 0.81 | 3.59 | 3.97 | 3.74 |
| **Prec.: wettest (mm)** | 3.08 | 3.21 | 2.60 | 19.20 | 20.52 | 18.47 |

## 5.3 Phase III RCM performance summary and shortlisting N=7 RCMs for ERA5-~~NARCliM2.0~~NARCliM 2.0 evaluation simulations

Overall, RCM biases for mean maximum temperature do not show marked improvements once the dynamic vegetation cover and surface runoff options are activated for Noah-MP (Figure 4 g,j,m) relative to RCMs using Noah-MP with default settings (Figure 4d). However, specifically for the RCM ensemble with dynamic vegetation cover activated for Noah-MP, RMSE magnitudes for maximum temperature are lower over some eastern coastal regions (Figure 5g).

The simulation of mean minimum temperature shows clear performance improvements for Phase III RCMs using options activated for Noah-MP, relative to RCMs using Noah-MP defaults. Overall, both biases and RMSEs for minimum temperature are reduced in magnitude for RCMs using ~~the~~ either or both of dynamic vegetation cover and runoff/groundwater options activated for Noah-MP, relative to the default parameters (Figure 4-5). These performance improvements are largest over eastern and southern regions.

There are no substantial overall performance improvements in the simulation of precipitation for Phase III RCMs relative to Phase II RCMs (Figures 4-5 f,i,l,o). However, using Noah-MP with specific LSM options remains favourable to using RCMs with Noah-Unified, albeit the performance gains are generally small, except for some coastal regions and especially the north-east.

All 78 RCMs in the complete RCM physics test ensemble are ranked for performance as described in ~~s~~Sect. 3~~4~~.2. Once the poor-performing RCMs are excluded, there are 20 RCMs remaining (Table 9; Figures 6-8). In Table 9, we see that 16 Noah-MP-based RCMs from Phase II and Phase III comprise this set of 20 RCMs, with 3 of the 20 RCMs using Noah-Unified, and 1 using CLM4.0. For maximum temperature, some shortlisted RCMs show ~~large~~ substantial RMSEs over north-western and inland areas (e.g., Figure 6 d-f) that are of ~~similar~~ larger magnitude over these areas ~~to those of~~than the ensemble means of Phase I-III RCMs (Figure 5). Conversely, several shortlisted RCMs show very low RMSEs for maximum temperature across eastern and southern regions, especially along the eastern coast (Figure 6, e.g., RCMs in panels d,l,n,o,q). For minimum temperature, a subset of the twenty shortlisted RCMs show substantially reduced RMSEs over many regions relative to the Phase I-III ensemble means (Figure 7, e.g., RCMs in panels: b,h,i). Additionally, several shortlisted RCMs show reduced RMSEs for precipitation over the eastern coast and north-east (Figure 8, e.g., RCMs in panels: c, l, m, n, o) relative to the Phase I-III RCM ensemble means in Figure 5c,f,i,l,o.

These 20 RCMs are assessed for statistical independence and 7 RCMs from this RCM set are shortlisted for the ERA5-forced RCM simulations considering both their performance and independence scores (Table 9). These 7 shortlisted RCMs are listed in **bold** in Table 9 and are identified as R1-R7 in the ERA5-forced evaluation simulations (Table 9; final column). RCMs are shortlisted from the set of 20 if they rank highly for both performance and independence. For instance, RCM 050801040404_set_3 (top row, Table 9) is top-ranked for performance, however, its independence scores/ranks are low, hence it is not shortlisted. It is important to note that, while a general performance gain is observed in the physics testing when using Noah-MP, there are some specific RCM configurations using Noah-Unified that perform well in simulating the Australian climate. For instance, the RCM 010602050502 (row 7; Table 9; ~~'~~R1~~'~~) uses Noah-Unified and performs well overall (its overall performance rank=7), and especially for the simulation of maximum temperature (Figure 6a). It is also the only RCM in this set of 20 RCMs to use YSU for PBL. Importantly, this RCM is highly ranked for statistical independence, hence, this RCM is shortlisted for the N=7 set. We note here that R1-R7 are simply a chronological naming convention and do not imply any ranking for these 7 RCM configurations.

**Table 9**. The 20 ~~NARCliM2.0~~NARCliM 2.0 physics test RCMs shortlisted from the ensemble of 78 RCMs based on their performance in simulating the Australian climate and independence (Ind.). N=7 ~~'~~R1-R7~~'~~ RCMs shortlisted for ERA5-forced evaluation simulations shown in **bold**. R1-R7 are a naming convention and do not

imply a ranking for these 7 RCMs. NU=Noah Unified; NMP=Noah-MP; DV=dynamic vegetation cover; TOP=topmodel runoff.

| # | RCM Physics Combination | PBL | MP | Cumulus | SW/LW | LSM | Test Phase | Overall Performance Rank | Bishop Abramowitz Ind. Rank | Herger Ind. Set 1 | Herger Ind. Set 2 | ERA5-forced RCM Identifier |
|---|---|---|---|---|---|---|---|---|---|---|---|---|
| 1 | 050801040404_set_3 | MYNN2 | Thom | KF | RRTMG | NMP DV+TOP | III | 1 | 19 | 20 | 20 | |
| **2** | **070806040404_set_1** | **ACM2** | **Thom** | **Td** | **RRTMG** | **NMP DV** | **III** | **2** | **8** | **5** | **6** | **R6** |
| 3 | 50801040404 | MYNN2 | Thom | KF | RRTMG | NMP | II | 3 | 16 | 12 | 13 | |
| **4** | **070802040404_set_1** | **ACM2** | **Thom** | **BMJ** | **RRTMG** | **NMP DV** | **III** | **4** | **4** | **3** | **3** | **R5** |
| 5 | 070802040404_set_2 | ACM2 | Thom | BMJ | RRTMG | NMP TOP | III | 5 | 15 | 13 | 12 | |
| **6** | **050601040404_set_1** | **MYNN2** | **WSM6** | **KF** | **RRTMG** | **NMP DV** | **III** | **6** | **7** | **10** | **10** | **R2** |
| **7** | **10602050502** | **YSU** | **WSM6** | **BMJ** | **NG** | **NU** | **II** | **7** | **1** | **3** | **3** | **R1** |
| **8** | **070806040404_set_2** | **ACM2** | **Thom** | **Td** | **RRTMG** | **NMP TOP** | **III** | **8** | **9** | **9** | **5** | **R7** |
| 9 | 70806040404 | ACM2 | Thom | Td | RRTMG | NMP | II | 9 | 11 | 14 | 14 | |
| # | 50802040404 | MYNN2 | Thom | BMJ | RRTMG | NMP | II | 10 | 20 | 19 | 19 | |
| **#** | **050802040404_set_1** | **MYNN2** | **Thom** | **BMJ** | **RRTMG** | **NMP DV** | **III** | **11** | **5** | **2** | **2** | **R3** |
| # | 070806040404_set_3 | ACM2 | Thom | Td | RRTMG | NMP DV+TOP | III | 14 | 12 | 10 | 10 | |
| # | 70802040404 | ACM2 | Thom | BMJ | RRTMG | NMP | II | 17 | 13 | 15 | 15 | |
| # | 070601040404_set_3 | ACM2 | WSM6 | KF | RRTMG | NMP DV+TOP | III | 22 | 14 | 16 | 16 | |
| **#** | **050802040404_set_2** | **MYNN2** | **Thom** | **BMJ** | **RRTMG** | **NMP TOP** | **III** | **23** | **2** | **4** | **4** | **R4** |
| # | 70802050502 | ACM2 | Thom | BMJ | NG | NU | II | 24 | 18 | 18 | 18 | |
| # | 50801040405 | MYNN2 | Thom | KF | RRTMG | CLM4 | I | 28 | 17 | 17 | 17 | |
| # | 070601040404_set_1 | ACM2 | WSM6 | KF | RRTMG | NMP DV | III | 29 | 6 | 7 | 8 | |
| # | 70801040404 | ACM2 | Thom | KF | RRTMG | NMP | II | 30 | 3 | 1 | 1 | |
| # | 50801040402 | MYNN2 | Thom | KF | RRTMG | NU | I | 31 | 10 | 6 | 7 | |

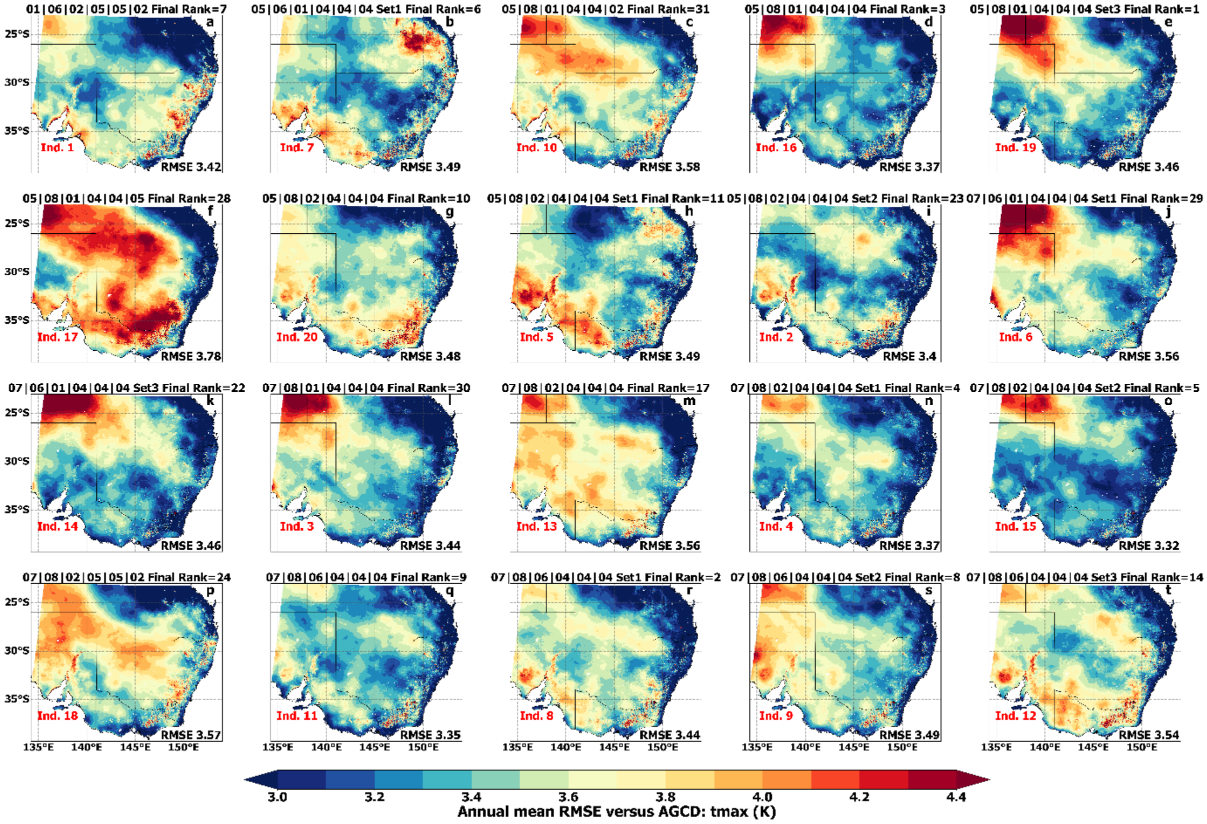


**Figure 6.** RMSEs for modelled mean maximum temperature (tmax) versus observations for the twenty ~~NARCliM2.0~~NARCliM 2.0 physics test RCMs shortlisted from the full ensemble of seventy-eight RCMs based on their performance in simulating the recent south-east Australian climate. Overall (final) performance ranks and Bishop and Abramowitz (2013) method independence (Ind.) scores are shown.

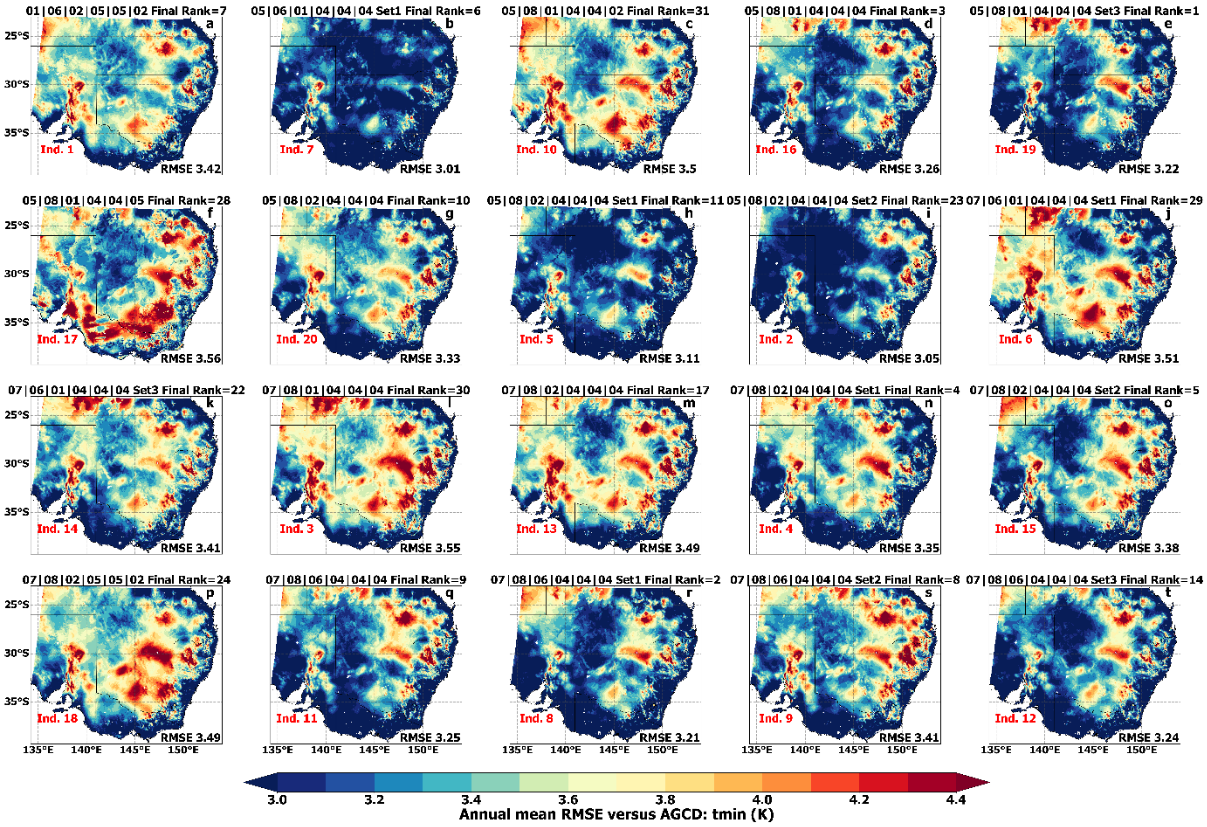


**Figure 7.** As per Figure 6 but for mean minimum temperature (tmin).

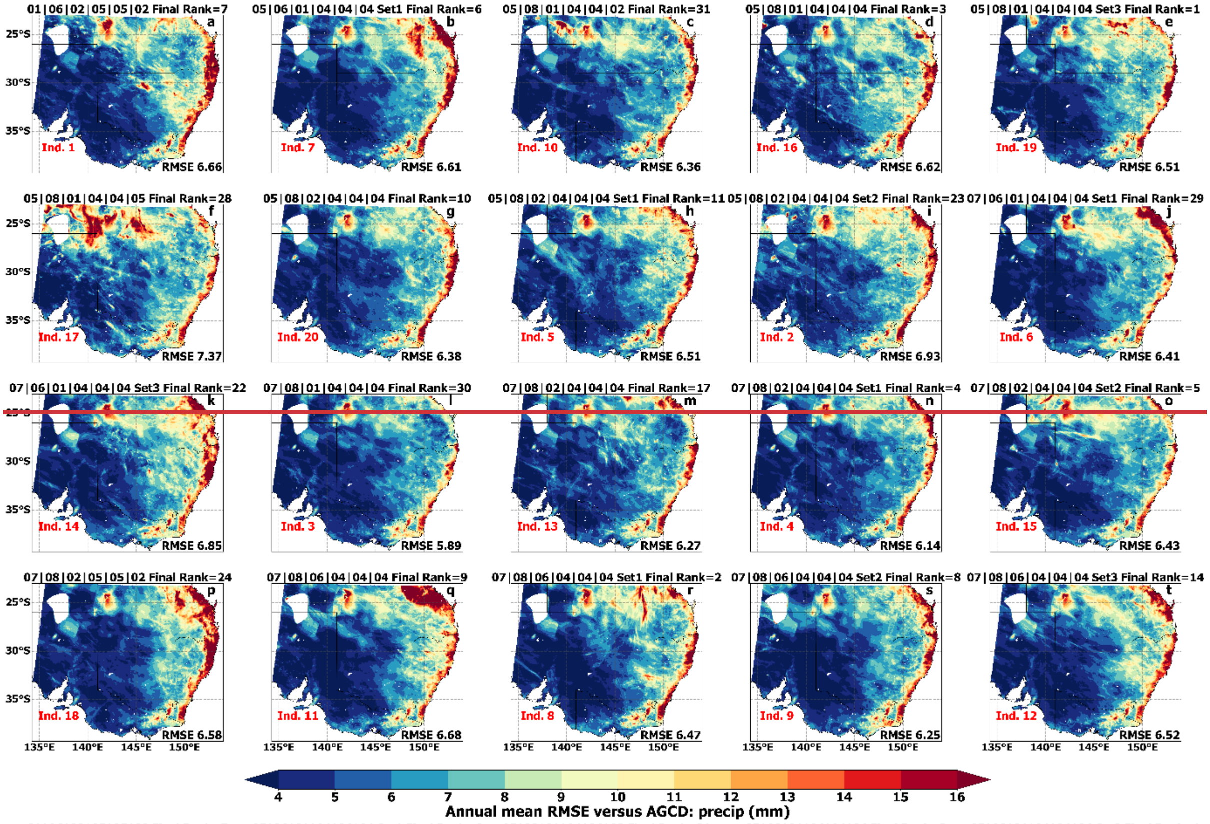


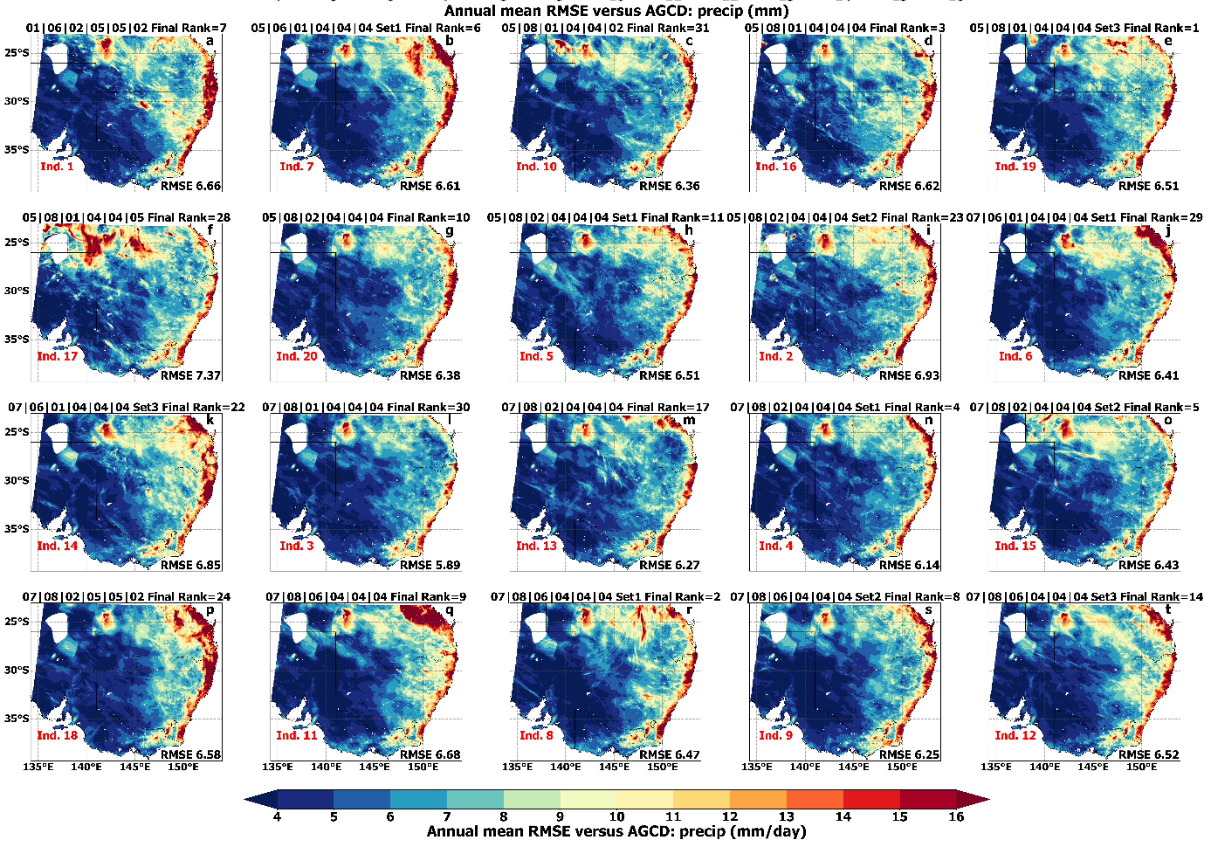


**Figure 8.** As per Figure 6 but for mean precipitation (precip.).

# ~~7.~~6. CORDEX-CMIP6 ~~NARCliM2.0~~NARCliM 2.0 historical evaluation

## 6.1 Maximum temperature

~~NARCliM2.0~~Overall, NARCliM 2.0 RCMs simulate maximum temperature more accurately than NARCliM1.x, with widespread, statistically significant reductions in cold biases in the ensemble mean (Figure 9), as well as for many individual RCMs (Supporting Information Figure S4-S6). These reductions in bias apply for all timescales but are largest for the annual mean, ~~i.e.~~i.e., the area-averaged mean absolute bias for the NARCliM 2.0 ensemble is 0.75 K~~°C~~ (range: 0.61 to 2.03 K) ~~for the NARCliM2.0 ensemble~~, 1.73 K~~°C~~ (range: 1.1 to  2.37 K) for ~~NARCliM1.5~~NARCliM 1.5, and 1.89~~°C~~ K (range: 0.55 to 4.12 K) for ~~NARCliM1.0~~NARCliM 1.0 (Figure 9d,g,j and Figure S4). Notably, the NARCliM2.0 ensemble mean annual mean maximum temperature bias magnitudes are ~~very~~ small, ~~i.e.~~i.e., around <0.5 K~~°C~~, over south-west WA, southern coastal regions, and several eastern regions. This may be important from a climate change adaptation and mitigation perspective as these regions are heavily populated and economically significant. ~~NARCliM2.0~~NARCliM 2.0 retains warm biases of similar magnitude to ~~NARCliM1.5~~NARCliM 1.5 along the north-west coast of Australia (Figure 9d,g). Moreover, these warm biases cover additional areas for ~~NARCliM2.0~~NARCliM 2.0, especially during DJF (Figure 9e,h). A~~A~~ wide range of bias signs are evident for the individual ~~NARCliM2.0~~NARCliM 2.0 ensemble members (Figures S4-S6) and a minority of NARCliM 2.0 RCMs retain strong cold biases, e.g., at an annual timescale NARCliM 2.0-NorESM2-MM R3 (mean absolute bias = 2.03 K) and UKESM-1-0-LL R3 (1.77 K). Additionally, ~~T~~the R5 RCM is generally warmer than R3~~,~~ (e.g., ~~(~~Figure S4c,d). Considering the forcing GCM data, overall, ensemble means for the CMIP6 and CMIP5 GCMs generally show similar patterns and magnitudes of cold bias for maximum temperature (Supporting Information S7).

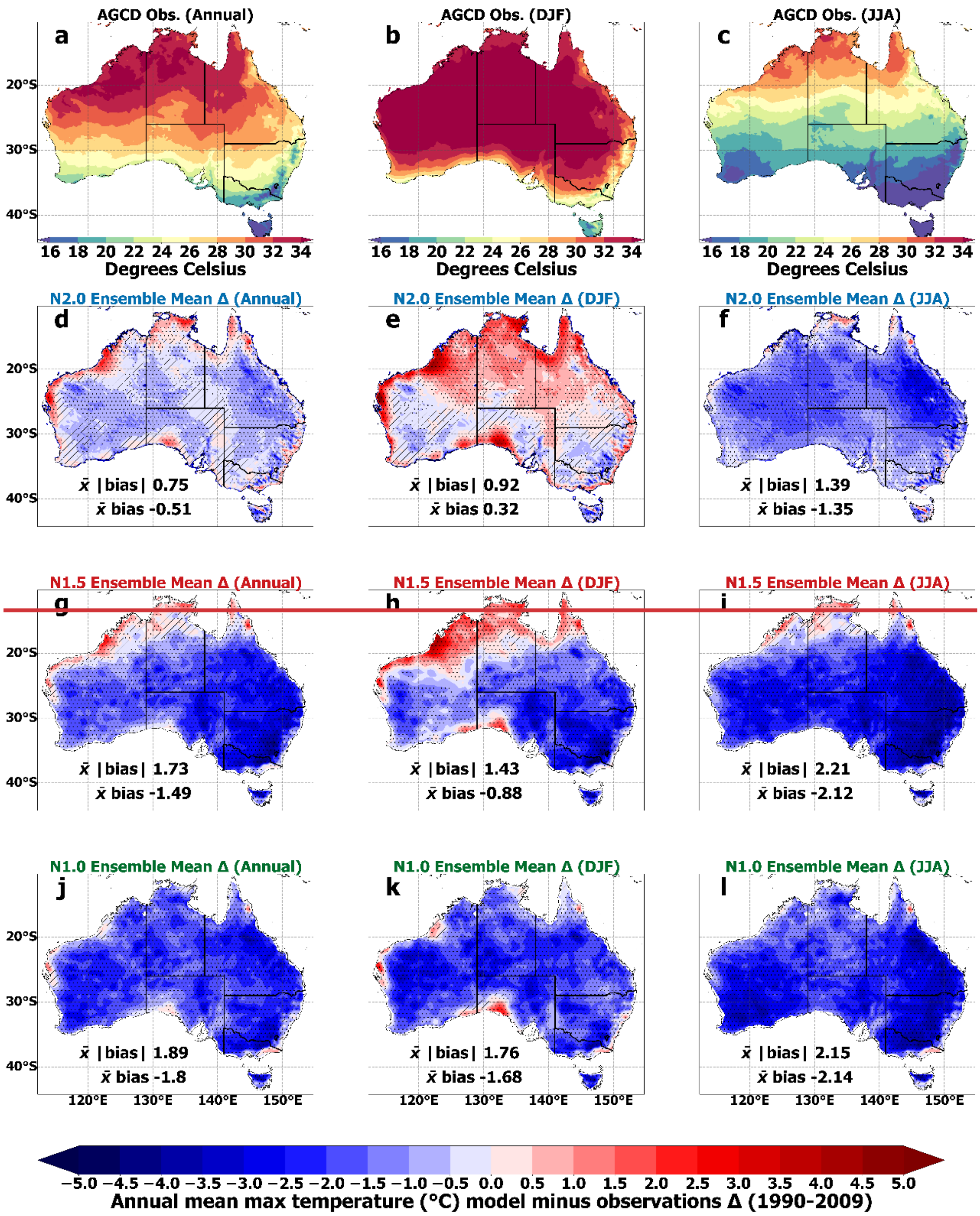
AGCD Obs. (Annual)
AGCD Obs. (DJF)
AGCD Obs. (JJA)
a
b
c
20°S
30°S
40°S
16 18 20 22 24 26 28 30 32 34
Degrees Celsius
N2.0 Ensemble Mean Δ (Annual)
N2.0 Ensemble Mean Δ (DJF)
N2.0 Ensemble Mean Δ (JJA)
d
e
f
x̄ |bias| 0.75
x̄ bias -0.51
x̄ |bias| 0.92
x̄ bias 0.32
x̄ |bias| 1.39
x̄ bias -1.35
N1.5 Ensemble Mean Δ (Annual)
N1.5 Ensemble Mean Δ (DJF)
N1.5 Ensemble Mean Δ (JJA)
g
h
i
x̄ |bias| 1.73
x̄ bias -1.49
x̄ |bias| 1.43
x̄ bias -0.88
x̄ |bias| 2.21
x̄ bias -2.12
N1.0 Ensemble Mean Δ (Annual)
N1.0 Ensemble Mean Δ (DJF)
N1.0 Ensemble Mean Δ (JJA)
j
k
l
x̄ |bias| 1.89
x̄ bias -1.8
x̄ |bias| 1.76
x̄ bias -1.68
x̄ |bias| 2.15
x̄ bias -2.14
120°E 130°E 140°E 150°E
−5.0 −4.5 −4.0 −3.5 −3.0 −2.5 −2.0 −1.5 −1.0 −0.5 0.0 0.5 1.0 1.5 2.0 2.5 3.0 3.5 4.0 4.5 5.0
Annual mean max temperature (°C) model minus observations Δ (1990-2009)

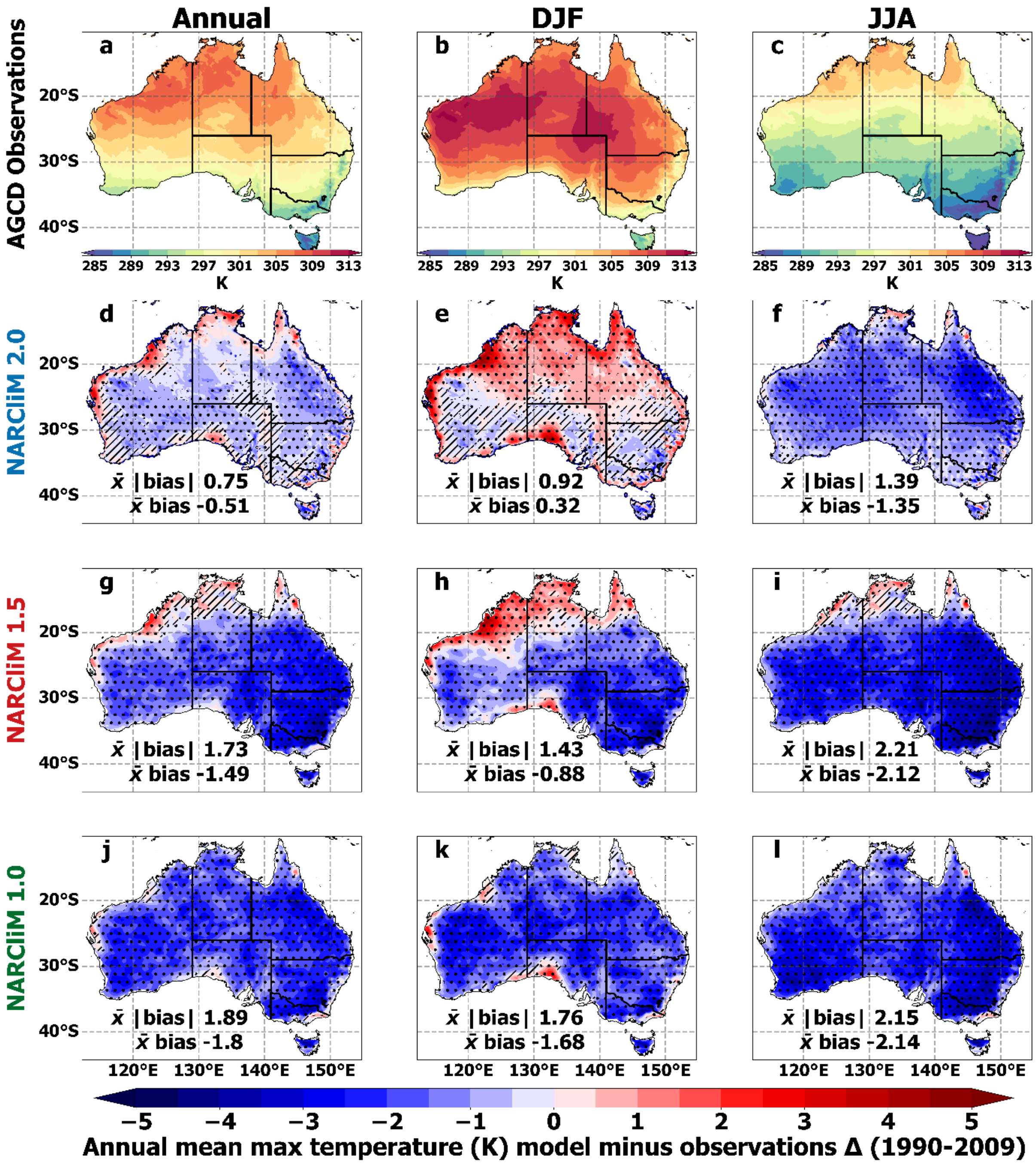


**Figure 9.** Annual, DJF and JJA mean near-surface atmospheric maximum temperature biases for ~~NARCliM2.0~~NARCliM 2.0, 1.5 and 1.0 historical ensemble means with respect to Australian Gridded Climate Data (AGCD) observations for 1990-2009. Stippled areas indicate locations where an RCM shows statistically significant bias. Significance stippling for the ensemble mean bias follows Tebaldi et al. (2011) and is applied separately to each RCM ensemble. Statistically insignificant areas are shown in colour, denoting that less than half of the models are significantly biased. In significant agreeing areas (stippled), at least half of RCMs are significantly biased, and at least 70% of significant RCMs in each ensemble agree on the direction of the bias. Significant disagreeing areas are shown in hatching, which are where at least half of the models are significantly biased and less than 70% of significant models in each ensemble agree on the bias direction - see main text for additional detail on the stippling regime.

## 6.2 Minimum temperature

The simulation of mean minimum temperature by ~~NARCliM2.0~~NARCliM 2.0 is generally warm biased at all timescales (Figure 10). Its bias magnitudes over many regions are larger versus ~~NARCliM1.5~~NARCliM 1.5, e.g.~~.~~, annual mean area-averaged absolute biases are 0.98 ~~°C~~K and 0.79 ~~°C~~K for ~~NARCliM2.0~~NARCliM 2.0 and ~~NARCliM1.5~~NARCliM 1.5, respectively (Figure 10 d,g). However, there are exceptions to this result over specific regions, for example, parts of south-west western Australia show annual mean bias magnitudes of <1 ~~°C~~K for ~~NARCliM2.0~~NARCliM 2.0, but these areas show biases below -2 ~~°C~~K for NARCliM1.x (Figure 10d,g,j). Most individual RCMs comprising the ~~NARCliM2.0~~NARCliM 2.0 ensemble show stronger warm biases than their ~~NARCliM1.5~~NARCliM 1.5 peers at both annual and seasonal timescales (Figures S8-S10). The ACCESS-ESM-1-5-forced ~~NARCliM2.0~~NARCliM 2.0 RCMs are considerably more warm-biased than the other ~~NARCliM2.0~~NARCliM 2.0 RCMs, with average absolute biases of 1.74 ~~°C~~K and 1.9 ~~°C~~K; Fig. S8c-d).

Many of the CMIP6 GCMs used to force the ~~NARCliM2.0~~NARCliM 2.0 RCMs are warmer than the CMIP5 GCMs used to force ~~NARCliM1.5~~NARCliM 1.5, such that the ensemble mean bias of the former is 1.9 ~~°C~~K versus 1.11 ~~°C~~K (Figure S11). In particular, ACCESS-ESM-1-5 and MPI-ESM1-2-HR are substantially more warm-biased relative to all other selected GCMs, with mean absolute biases of 2.2~~°C~~K and 3.47~~°C~~K, respectively (Figure S11). This suggests that ~~NARCliM2.0~~NARCliM 2.0's warm biases for mean minimum temperature are at least partially inherited from the driving data. However, whilst the ACCESS-ESM-1-5-forced ~~NARCliM2.0~~NARCliM 2.0 RCMs are much warmer than their counterparts (~~i.e.~~i.e., 1.74 ~~°C~~K and 1.9 ~~°C~~K), this does not apply to the MPI-ESM1-2-HR-forced RCMs, which have biases of only 1.01 ~~°C~~K and 1.09 ~~°C~~K. Hence, factors additional to the driving data, such as changes in RCM parameterisations between NARCliM generations and other model design changes likely contribute to the warmer biases observed for ~~NARCliM2.0~~NARCliM 2.0.

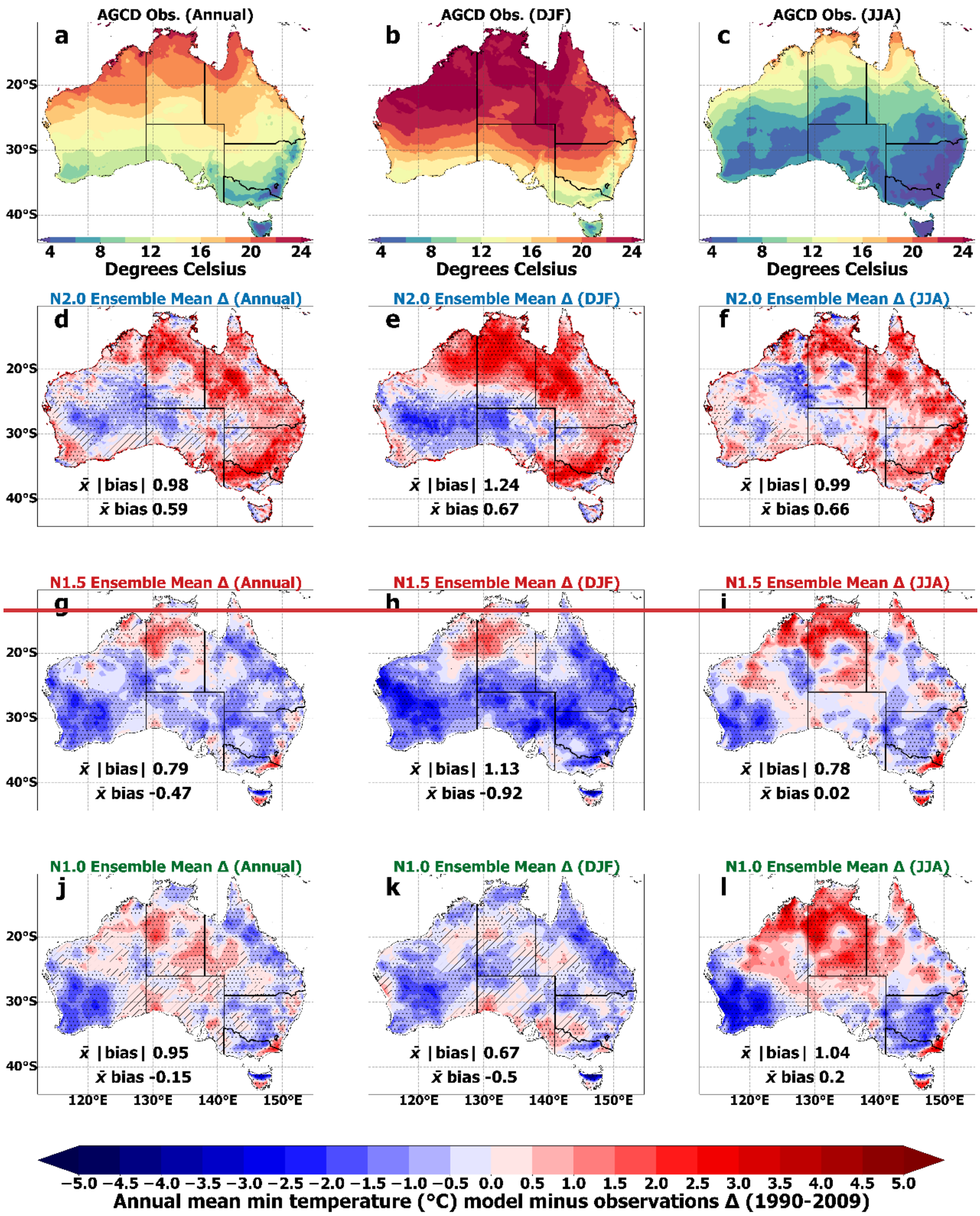
AGCD Obs. (Annual)
a
AGCD Obs. (DJF)
b
AGCD Obs. (JJA)
c
20°S
30°S
40°S
4 8 12 16 20 24
Degrees Celsius
N2.0 Ensemble Mean Δ (Annual)
d
x̄ |bias| 0.98
x̄ bias 0.59
N2.0 Ensemble Mean Δ (DJF)
e
x̄ |bias| 1.24
x̄ bias 0.67
N2.0 Ensemble Mean Δ (JJA)
f
x̄ |bias| 0.99
x̄ bias 0.66
N1.5 Ensemble Mean Δ (Annual)
g
x̄ |bias| 0.79
x̄ bias -0.47
N1.5 Ensemble Mean Δ (DJF)
h
x̄ |bias| 1.13
x̄ bias -0.92
N1.5 Ensemble Mean Δ (JJA)
i
x̄ |bias| 0.78
x̄ bias 0.02
N1.0 Ensemble Mean Δ (Annual)
j
x̄ |bias| 0.95
x̄ bias -0.15
N1.0 Ensemble Mean Δ (DJF)
k
x̄ |bias| 0.67
x̄ bias -0.5
N1.0 Ensemble Mean Δ (JJA)
l
x̄ |bias| 1.04
x̄ bias 0.2
120°E 130°E 140°E 150°E
−5.0 −4.5 −4.0 −3.5 −3.0 −2.5 −2.0 −1.5 −1.0 −0.5 0.0 0.5 1.0 1.5 2.0 2.5 3.0 3.5 4.0 4.5 5.0
Annual mean min temperature (°C) model minus observations Δ (1990-2009)

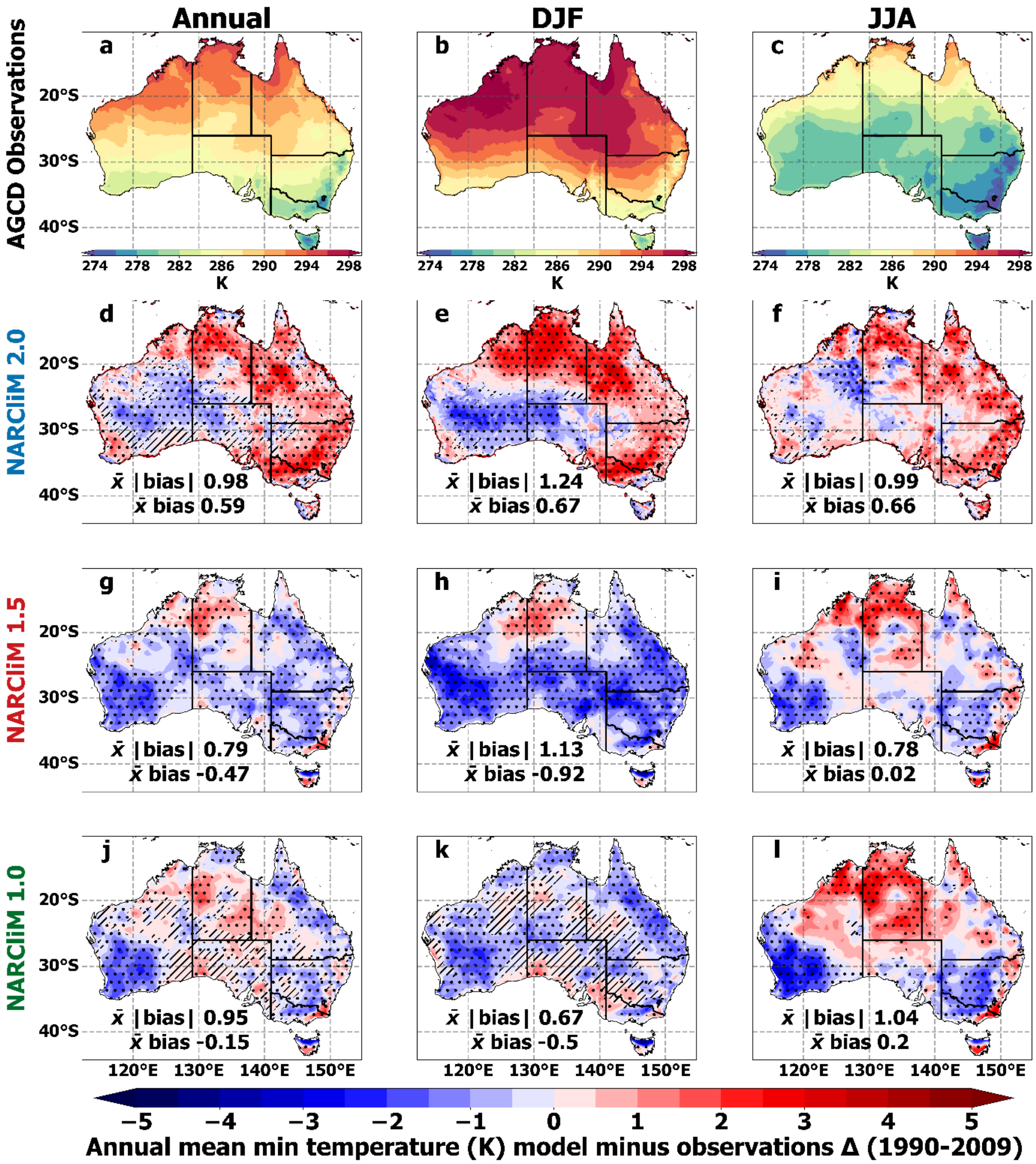


**Figure 10.** As per Figure 9 but for mean minimum temperature.

## 6.3 Precipitation

The ~~NARCliM2.0~~NARCliM 2.0 ensemble shows small dry biases for mean precipitation over most regions, except for some areas mainly in the east of the country which show slight wet biases (Figure 11d-f). This contrasts with stronger~~, statistically significant~~ wet biases of ~~NARCliM1.5~~NARCliM 1.5 that are statistically significant over many regions (Figure 11g-i) and the even stronger wet biases of ~~NARCliM1.0~~NARCliM 1.0 (Figure 11j-l). Area-averaged bias magnitudes are considerably smaller for ~~NARCliM2.0~~NARCliM 2.0 relative to NARCliM1.x, especially for the annual mean, ~~i.e.~~i.e., 8.03

mm versus 16.69 mm and 33.25 mm, respectively. Annual mean precipitation biases are particularly small over eastern regions, often being <5 mm. ~~NARCliM2.0~~NARCliM 2.0 retains the strong summertime dry biases for precipitation over northern Australia that are also evident for ~~NARCliM1.5~~NARCliM 1.5 (Figure 11e,h), noting that this region also shows strong warm biases for maximum temperature (Figure 9).

The individual RCMs comprising ~~NARCliM2.0~~NARCliM 2.0 show a range of results for annual and seasonal mean precipitation biases (Fig S12-S14). Notably, three of the ten ~~NARCliM2.0~~NARCliM 2.0 RCMs have substantially larger bias magnitudes than their peers at annual and summer timescales, ~~i.e.~~i.e., both MPI-ESM1-2-HR-R3 and R5 (absolute biases are 15.53 mm and 22.45 mm for annual mean precipitation, Figure S12g-h) and EC-Earth3-Veg-R5 (Figure S12f; 18.59 mm). Despite EC-Earth3-Veg-R5 being strongly dry-biased, EC-Earth3-Veg-R3 simulates precipitation more accurately ~~i.e.~~i.e., its mean absolute bias=9.53 mm (Figure S12e). Analogously to ~~NARCliM2.0~~NARCliM 2.0's performance~~s~~ for temperature, R5 is drier than R3. Comparing the ensemble means of the driving GCMs, the ~~CMPI6~~CMIP6 GCMs are marginally more accurate in simulating annual mean precipitation than the CMIP5 GCMs (Figure S15). Whilst the CMIP6 ensemble produces small biases over inland ~~regions~~areas, its biases are larger along the east coast.

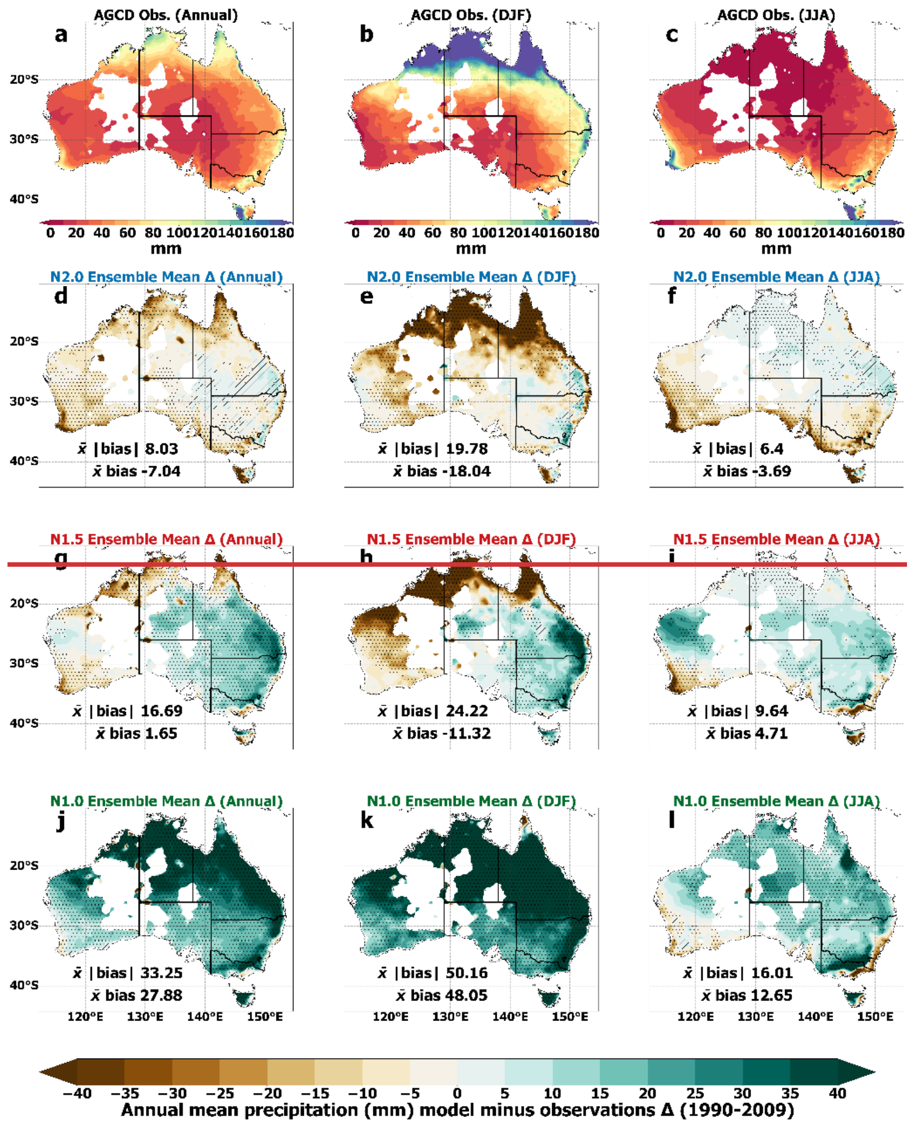
AGCD Obs. (Annual)
AGCD Obs. (DJF)
AGCD Obs. (JJA)
a
b
c
20°S
30°S
40°S
0 20 40 60 80 100120140160180
mm
N2.0 Ensemble Mean Δ (Annual)
N2.0 Ensemble Mean Δ (DJF)
N2.0 Ensemble Mean Δ (JJA)
d
e
f
x̄ |bias| 8.03
x̄ bias -7.04
x̄ |bias| 19.78
x̄ bias -18.04
x̄ |bias| 6.4
x̄ bias -3.69
N1.5 Ensemble Mean Δ (Annual)
N1.5 Ensemble Mean Δ (DJF)
N1.5 Ensemble Mean Δ (JJA)
g
h
i
x̄ |bias| 16.69
x̄ bias 1.65
x̄ |bias| 24.22
x̄ bias -11.32
x̄ |bias| 9.64
x̄ bias 4.71
N1.0 Ensemble Mean Δ (Annual)
N1.0 Ensemble Mean Δ (DJF)
N1.0 Ensemble Mean Δ (JJA)
j
k
l
x̄ |bias| 33.25
x̄ bias 27.88
x̄ |bias| 50.16
x̄ bias 48.05
x̄ |bias| 16.01
x̄ bias 12.65
120°E 130°E 140°E 150°E
−40 −35 −30 −25 −20 −15 −10 −5 0 5 10 15 20 25 30 35 40
Annual mean precipitation (mm) model minus observations Δ (1990-2009)

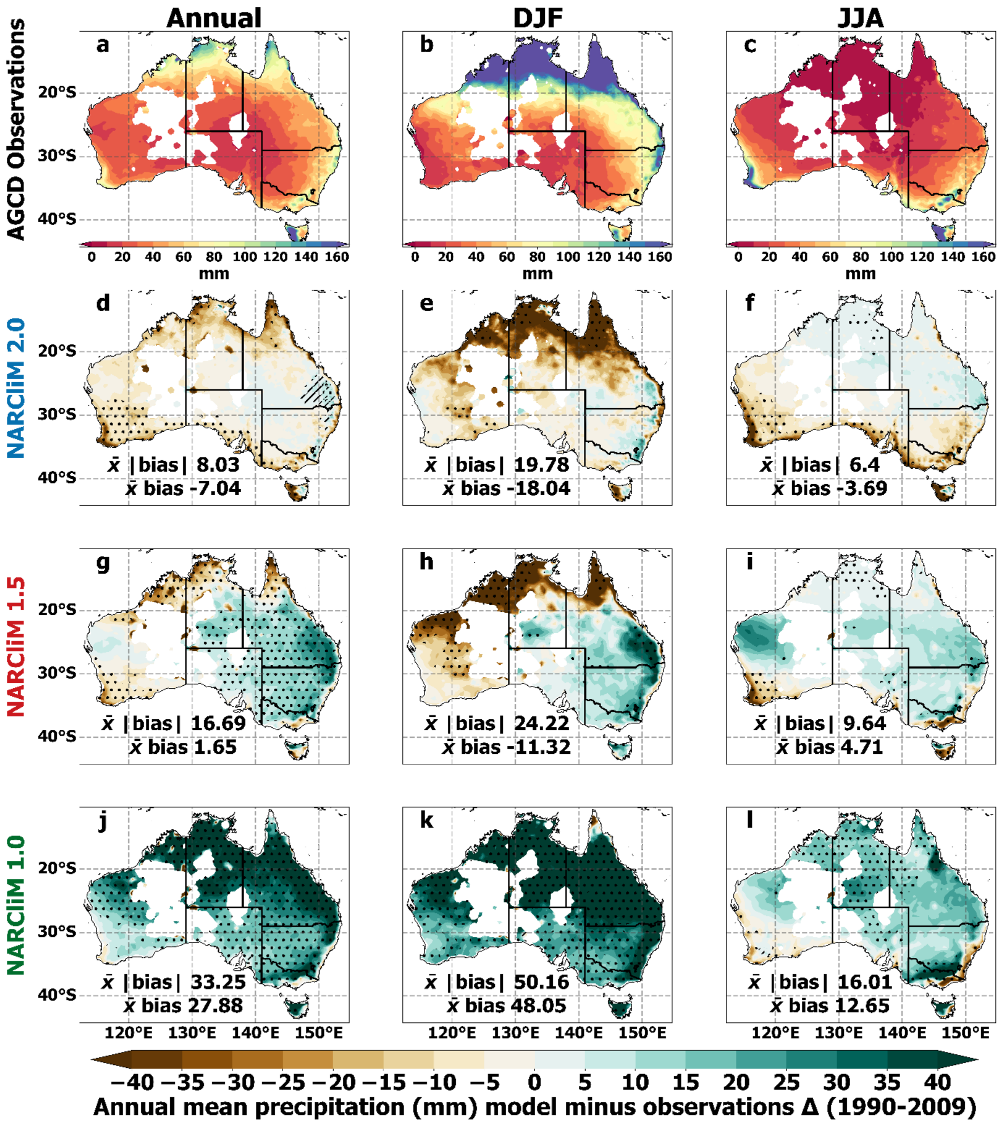


**Figure 11.** As per Figure 9 but for mean precipitation (precip.).

# ~~8.~~7. CORDEX-CMIP6 ~~NARCliM2.0~~NARCliM 2.0 climate change projections

Dependent on location, the largest maximum temperature projected increases for ~~NAR-CliM2.0~~NARCliM 2.0 under SSP3-7.0 are over ~3 ~~°C~~K, and over ~1.5 ~~°C~~K under SSP1-2.6 (Figure 12a,d). SSP3-7.0-~~NARCliM2.0~~NARCliM 2.0 shows faster warming over inland than coastal regions, with greater warming across a horizontal band of the continent during annual and summer timescales (Figure 12a-b). This contrasts with ~~NARCliM1.5~~NARCliM 1.5 which shows a north-south warming gradient at annual and seasonal timescales, with its fastest warming rate over northern regions, and ~~NARCliM1.0~~NARCliM 1.0 which projects fastest warming over the west (Figure 12). For ~~NAR-CliM2.0~~NARCliM 2.0, the tropical north warms faster during the winter dry season than during the summer wet season under SSP3-7.0, but this is not the case for SSP1-2.6 (Figure 12b-c; e-f). ~~NAR-CliM2.0~~NARCliM 2.0 simulations under SSP3-7.0 show less warming than ~~NARCliM1.5~~NARCliM

1.5-RCP8.5, but warmer futures than for ~~NARCliM1.0~~NARCliM 1.0-SRES A2, with differences in the underlying driving GCMs and GHG scenarios likely contributing to these variations in warming. As per NARCliM1.x, all ~~NARCliM2.0~~NARCliM 2.0 maximum temperature projections are significant-agreeing with all RCMs projecting statistically significant temperature increases.

775

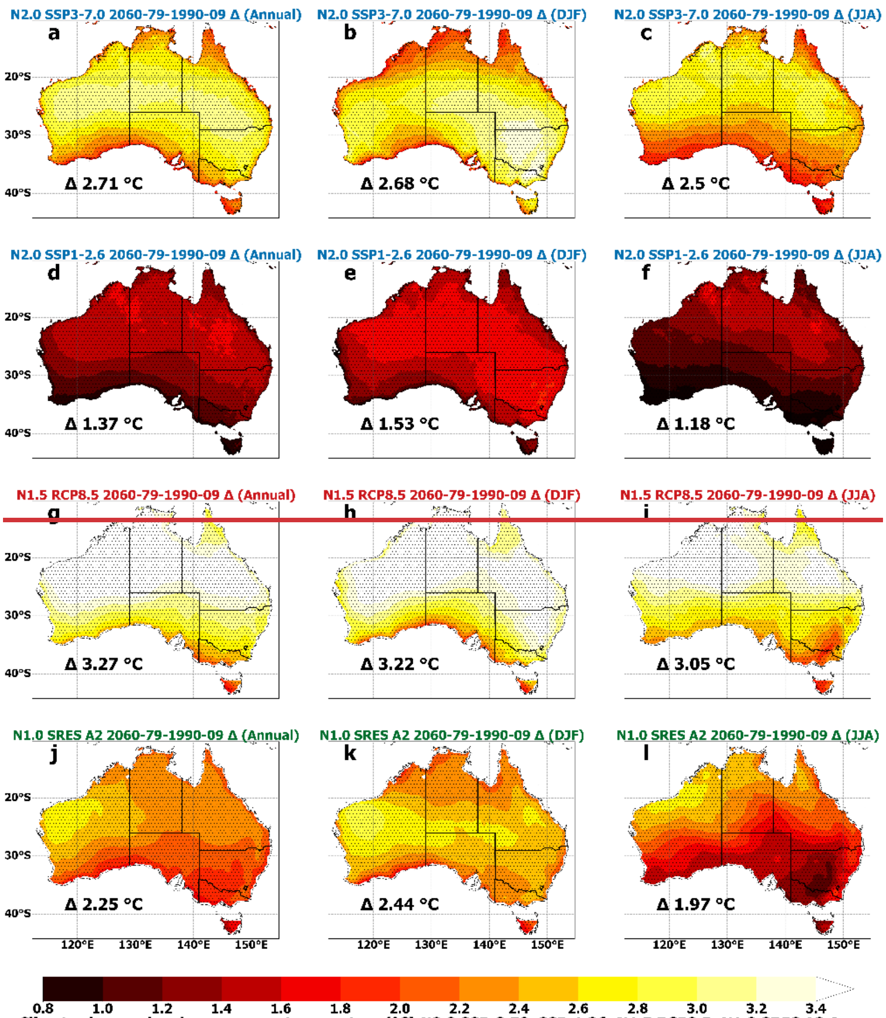

Climate change signals: mean max temperature (°C) N2.0 SSP-3.70, SSP-1.26; N1.5 RCP8.5; N1.0 SRES A2 Δ

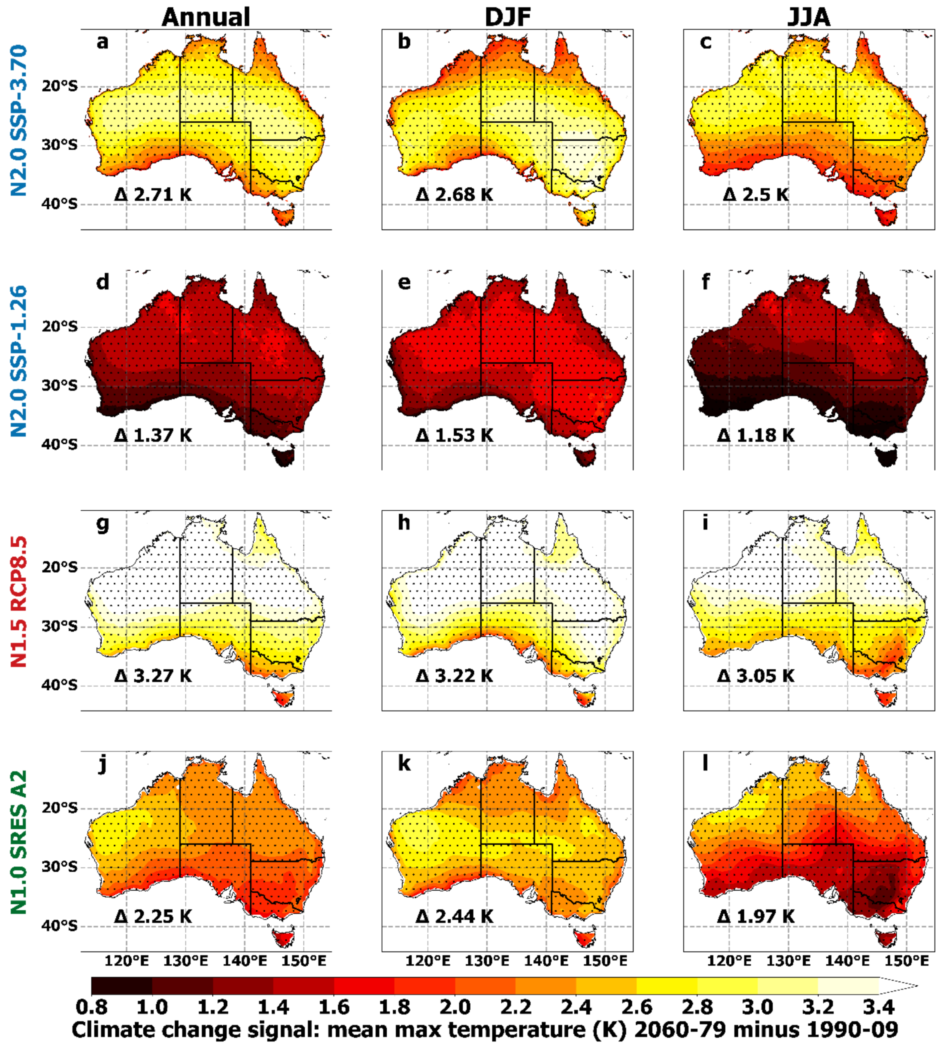


**Figure 12.** Ensemble mean climate change projections (far future minus present-day) for annual, DJF and JJA mean maximum temperatures with significance stippling as per Figure 9.

Projected increases in annual mean minimum temperature for ~~NARCliM2.0~~NARCliM 2.0 exceed 3 ~~°C~~K over some regions for SSP3-7.0, and 1.6 ~~°C~~K for SSP1-2.6 (Figure 13). Under both GHG scenarios, at annual and winter timescales warming is fastest over north-east Australia. Conversely, NARCliM1.x minimum temperature future increases are generally largest over northwest or northern Australia, though the summertime projection for ~~NARCliM1.0~~NARCliM 1.0 is an exception (Figure 13k). As for maximum temperature projections, all RCMs for all NARCliM generations project statistically significant increases.

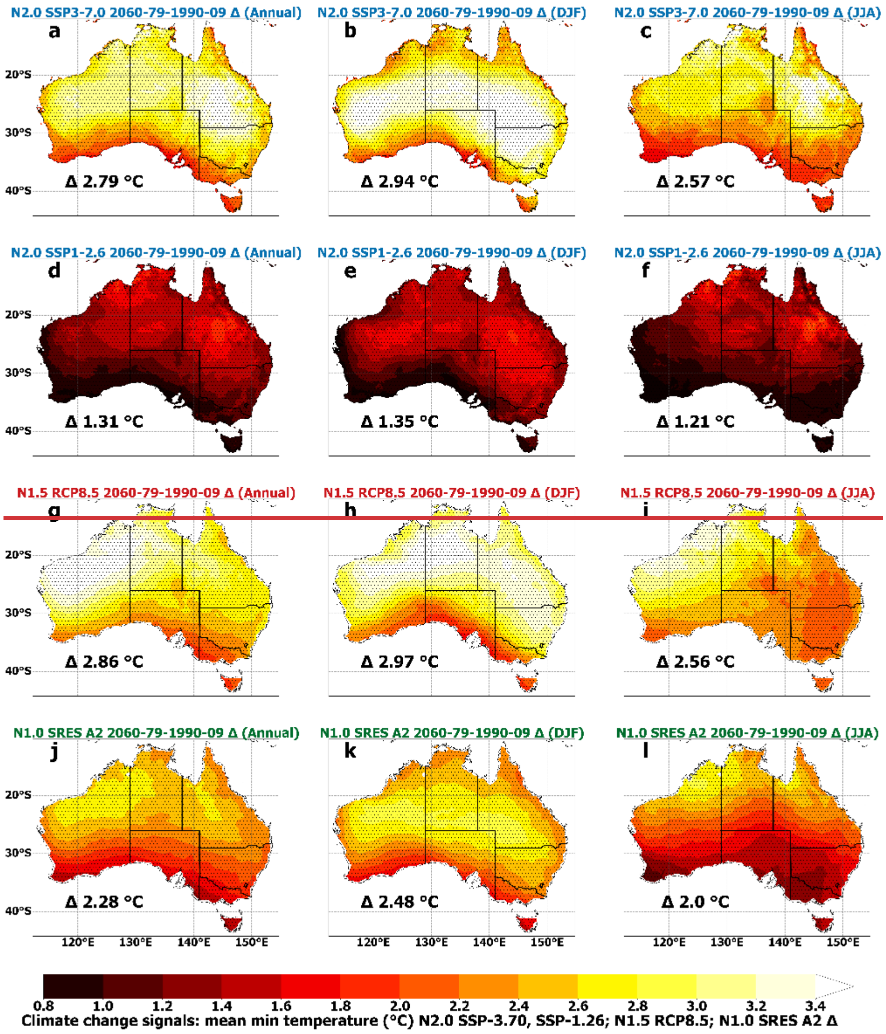

N2.0 SSP3-7.0 2060-79-1990-09 Δ (Annual)
a
Δ 2.79 °C
N2.0 SSP3-7.0 2060-79-1990-09 Δ (DJF)
b
Δ 2.94 °C
N2.0 SSP3-7.0 2060-79-1990-09 Δ (JJA)
c
Δ 2.57 °C
N2.0 SSP1-2.6 2060-79-1990-09 Δ (Annual)
d
Δ 1.31 °C
N2.0 SSP1-2.6 2060-79-1990-09 Δ (DJF)
e
Δ 1.35 °C
N2.0 SSP1-2.6 2060-79-1990-09 Δ (JJA)
f
Δ 1.21 °C
N1.5 RCP8.5 2060-79-1990-09 Δ (Annual)
g
Δ 2.86 °C
N1.5 RCP8.5 2060-79-1990-09 Δ (DJF)
h
Δ 2.97 °C
N1.5 RCP8.5 2060-79-1990-09 Δ (JJA)
i
Δ 2.56 °C
N1.0 SRES A2 2060-79-1990-09 Δ (Annual)
j
Δ 2.28 °C
N1.0 SRES A2 2060-79-1990-09 Δ (DJF)
k
Δ 2.48 °C
N1.0 SRES A2 2060-79-1990-09 Δ (JJA)
l
Δ 2.0 °C
20°S
30°S
40°S
120°E
130°E
140°E
150°E
0.8 1.0 1.2 1.4 1.6 1.8 2.0 2.2 2.4 2.6 2.8 3.0 3.2 3.4
Climate change signals: mean min temperature (°C) N2.0 SSP-3.70, SSP-1.26; N1.5 RCP8.5; N1.0 SRES A2 Δ

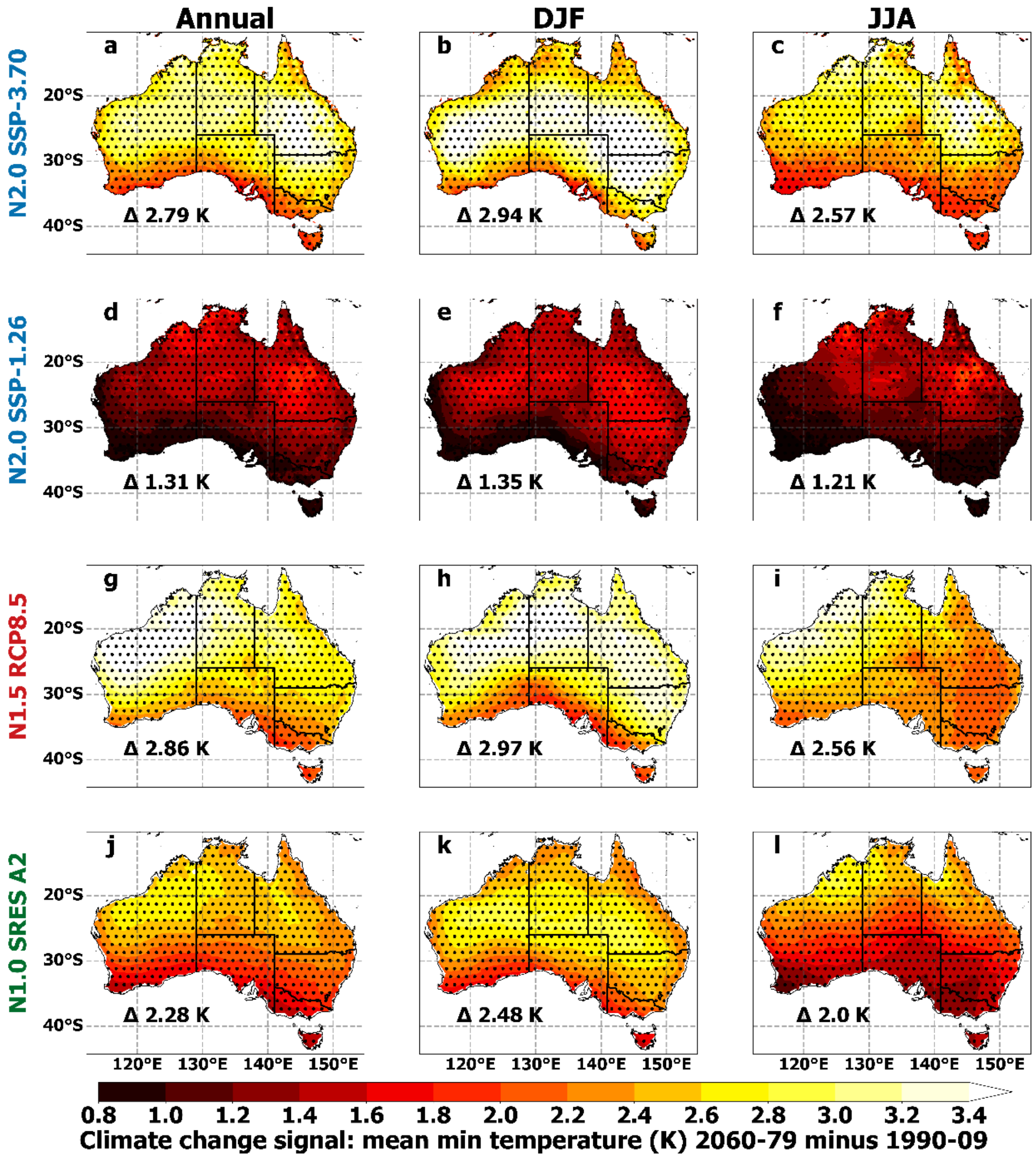


**Figure 13.** Ensemble mean climate change projections (far future minus present-day) for annual, DJF and JJA mean minimum temperatures with significance stippling as per Figure 9.

~~NARCliM2.0~~NARCliM 2.0 SSP3-7.0 projects a dry future over most of Australia, except for wetter futures over northern and western regions, which are largest in magnitude in summer (Figure 14a-b). In contrast, overall, ~~NARCliM2.0~~NARCliM 2.0 SSP1-2.6 projects dry changes across most of Australia, with the strongest drying over northern Australia during summer (Figure 14e). Similarities between ~~NARCliM2.0~~NARCliM 2.0 projections for the low and high GHG SSPs include faster drying over the eastern coastline at all timescales, especially during summer. The wetter futures projected by RCMs downscaling SSP3-7.0-GCMs relative to SSP1-2.6 may be partially inherited from the driving CMIP6 GCMs, because overall, SSP3-7.0 GCMs show wetter futures than corresponding SSP1-2.6 GCMs (Fig. S16).

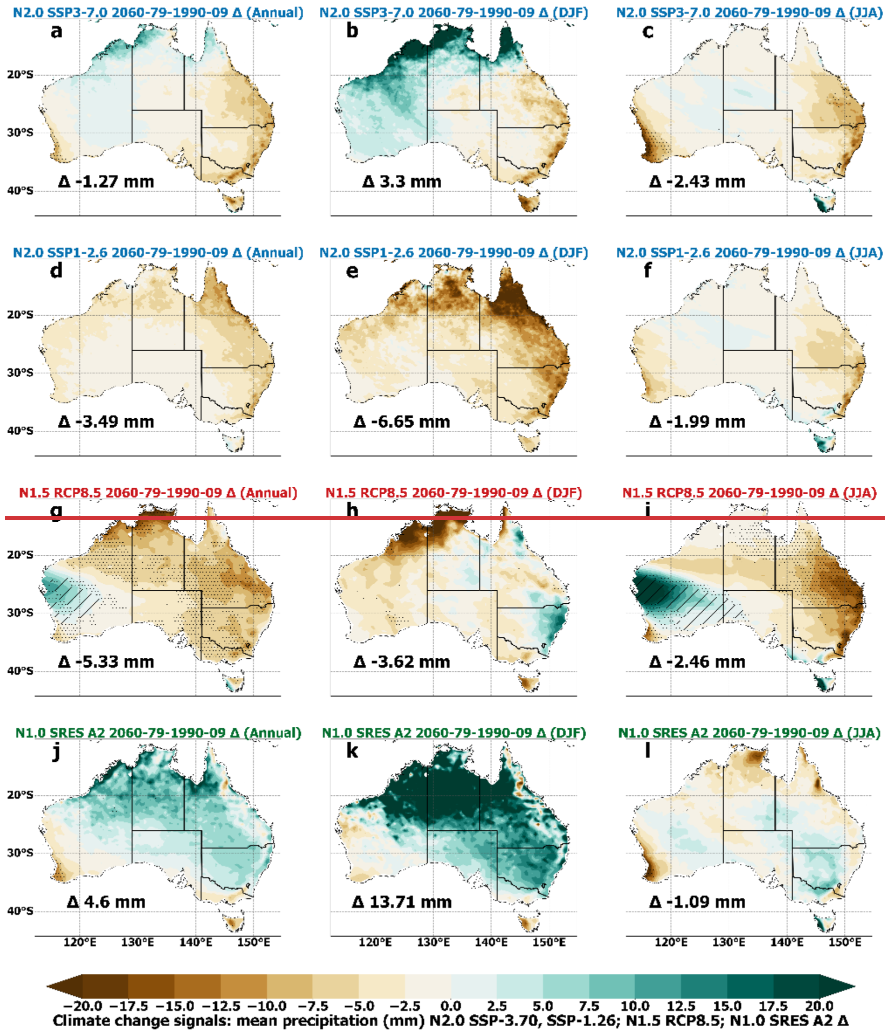
N2.0 SSP3-7.0 2060-79-1990-09 Δ (Annual)
a
Δ -1.27 mm
N2.0 SSP3-7.0 2060-79-1990-09 Δ (DJF)
b
Δ 3.3 mm
N2.0 SSP3-7.0 2060-79-1990-09 Δ (JJA)
c
Δ -2.43 mm
N2.0 SSP1-2.6 2060-79-1990-09 Δ (Annual)
d
Δ -3.49 mm
N2.0 SSP1-2.6 2060-79-1990-09 Δ (DJF)
e
Δ -6.65 mm
N2.0 SSP1-2.6 2060-79-1990-09 Δ (JJA)
f
Δ -1.99 mm
N1.5 RCP8.5 2060-79-1990-09 Δ (Annual)
g
Δ -5.33 mm
N1.5 RCP8.5 2060-79-1990-09 Δ (DJF)
h
Δ -3.62 mm
N1.5 RCP8.5 2060-79-1990-09 Δ (JJA)
i
Δ -2.46 mm
N1.0 SRES A2 2060-79-1990-09 Δ (Annual)
j
Δ 4.6 mm
N1.0 SRES A2 2060-79-1990-09 Δ (DJF)
k
Δ 13.71 mm
N1.0 SRES A2 2060-79-1990-09 Δ (JJA)
l
Δ -1.09 mm
20°S
30°S
40°S
120°E
130°E
140°E
150°E
−20.0 −17.5 −15.0 −12.5 −10.0 −7.5 −5.0 −2.5 0.0 2.5 5.0 7.5 10.0 12.5 15.0 17.5 20.0
Climate change signals: mean precipitation (mm) N2.0 SSP-3.70, SSP-1.26; N1.5 RCP8.5; N1.0 SRES A2 Δ

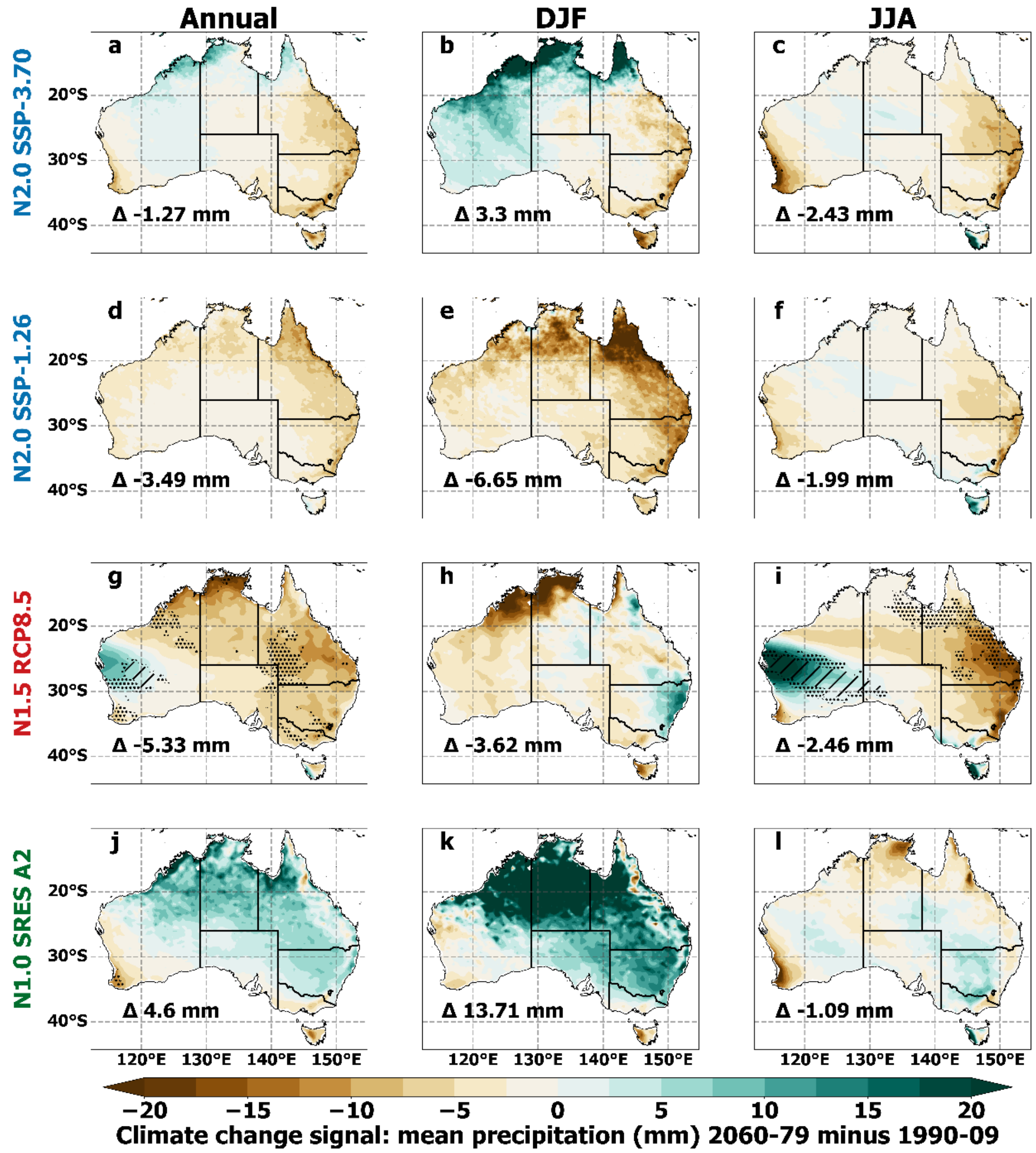


**Figure 14.** Ensemble mean climate change projections (far future minus present-day) for annual, DJF and JJA mean precipitation with significance stippling as per Figure 9.

Considering mean precipitation projections for individual ~~NARCliM2.0~~NARCliM 2.0 RCMs, in some cases, R3 and R5 RCMs produce similar results when downscaling the same GCM. For instance, ACCESS-ESM-1-5 forced R3 and R5 both show strong projected decreases in annual mean precipitation across Australia (Figure 15b-c). In contrast, while UK-ESM1-0-LL R3-R5 both show projected decreases in annual mean precipitation over eastern Australia, R3 shows precipitation increases that are substantially more widespread over western and northern regions relative to R5 (Figure 15j-k). Overall, the ~~NARCliM2.0~~NARCliM 2.0 ensemble members show a variety of climate change signals for precipitation (Figure 15) and temperature (not shown), reflecting the range within the larger CMIP6 ensemble (Di Virgilio et al. 2022).

There are some key differences between the mean precipitation projections of ~~NARCliM2.0~~NARCliM 2.0 relative to those of previous NARCliM generations. For instance, ~~NARCliM1.5~~NARCliM 1.5 shows stronger reductions in future precipitation over northern and eastern regions at annual and winter timescales (Figure 14), and these changes are statistically significant over a few regions, whereas projected changes for ~~NARCliM2.0~~NARCliM 2.0 are largely non-significant. Additionally, ~~NARCliM2.0~~NARCliM 2.0 projects marked precipitation decreases along the south-east coast during summer, while ~~NARCliM1.5~~NARCliM 1.5 shows the opposite result (Figure 14). ~~NARCliM1.0~~NARCliM 1.0 generally projects wet futures across larger portions of Australia, especially at annual and summer timescales.

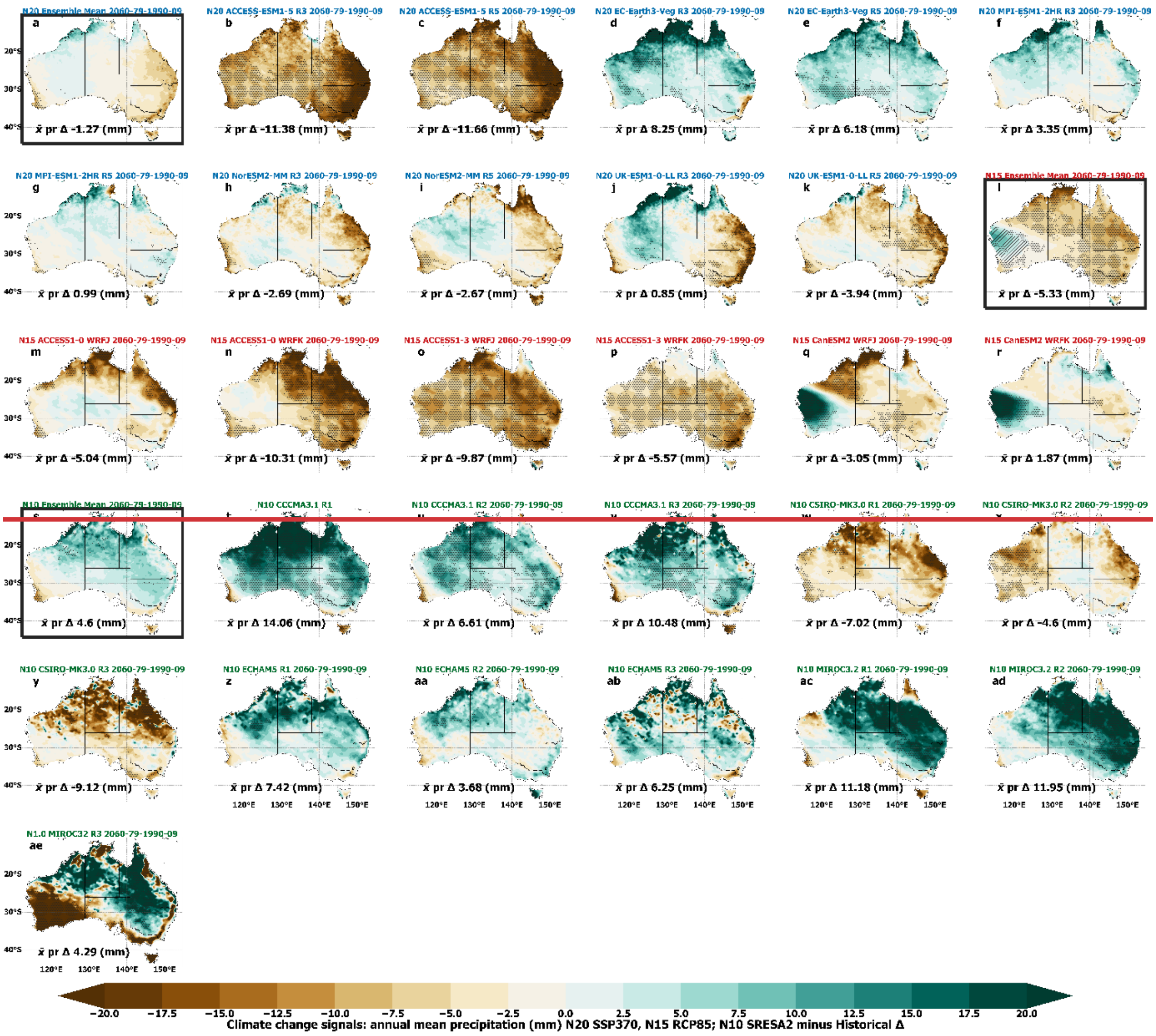
N20 Ensemble Mean 2060-79-1990-09
a
x̄ pr Δ -1.27 (mm)
N20 ACCESS-ESM1-5 R3 2060-79-1990-09
b
x̄ pr Δ -11.38 (mm)
N20 ACCESS-ESM1-5 R5 2060-79-1990-09
c
x̄ pr Δ -11.66 (mm)
N20 EC-Earth3-Veg R3 2060-79-1990-09
d
x̄ pr Δ 8.25 (mm)
N20 EC-Earth3-Veg R5 2060-79-1990-09
e
x̄ pr Δ 6.18 (mm)
N20 MPI-ESM1-2HR R3 2060-79-1990-09
f
x̄ pr Δ 3.35 (mm)
N20 MPI-ESM1-2HR R5 2060-79-1990-09
g
x̄ pr Δ 0.99 (mm)
N20 NorESM2-MM R3 2060-79-1990-09
h
x̄ pr Δ -2.69 (mm)
N20 NorESM2-MM R5 2060-79-1990-09
i
x̄ pr Δ -2.67 (mm)
N20 UK-ESM1-0-LL R3 2060-79-1990-09
j
x̄ pr Δ 0.85 (mm)
N20 UK-ESM1-0-LL R5 2060-79-1990-09
k
x̄ pr Δ -3.94 (mm)
N15 Ensemble Mean 2060-79-1990-09
l
x̄ pr Δ -5.33 (mm)
N15 ACCESS1-0 WRFJ 2060-79-1990-09
m
x̄ pr Δ -5.04 (mm)
N15 ACCESS1-0 WRFK 2060-79-1990-09
n
x̄ pr Δ -10.31 (mm)
N15 ACCESS1-3 WRFJ 2060-79-1990-09
o
x̄ pr Δ -9.87 (mm)
N15 ACCESS1-3 WRFK 2060-79-1990-09
p
x̄ pr Δ -5.57 (mm)
N15 CanESM2 WRFJ 2060-79-1990-09
q
x̄ pr Δ -3.05 (mm)
N15 CanESM2 WRFK 2060-79-1990-09
r
x̄ pr Δ 1.87 (mm)
N10 Ensemble Mean 2060-79-1990-09
x̄ pr Δ 4.6 (mm)
N10 CCCMA3.1 R1
x̄ pr Δ 14.06 (mm)
N10 CCCMA3.1 R2 2060-79-1990-09
x̄ pr Δ 6.61 (mm)
N10 CCCMA3.1 R3 2060-79-1990-09
x̄ pr Δ 10.48 (mm)
N10 CSIRO-MK3.0 R1 2060-79-1990-09
x̄ pr Δ -7.02 (mm)
N10 CSIRO-MK3.0 R2 2060-79-1990-09
x̄ pr Δ -4.6 (mm)
N10 CSIRO-MK3.0 R3 2060-79-1990-09
y
x̄ pr Δ -9.12 (mm)
N10 ECHAM5 R1 2060-79-1990-09
z
x̄ pr Δ 7.42 (mm)
N10 ECHAM5 R2 2060-79-1990-09
aa
x̄ pr Δ 3.68 (mm)
N10 ECHAM5 R3 2060-79-1990-09
ab
x̄ pr Δ 6.25 (mm)
N10 MIROC3.2 R1 2060-79-1990-09
ac
x̄ pr Δ 11.18 (mm)
N10 MIROC3.2 R2 2060-79-1990-09
ad
x̄ pr Δ 11.95 (mm)
N1.0 MIROC32 R3 2060-79-1990-09
ae
x̄ pr Δ 4.29 (mm)
20°S
30°S
40°S
120°E 130°E 140°E 150°E
−20.0 −17.5 −15.0 −12.5 −10.0 −7.5 −5.0 −2.5 0.0 2.5 5.0 7.5 10.0 12.5 15.0 17.5 20.0
Climate change signals: annual mean precipitation (mm) N20 SSP370, N15 RCP85; N10 SRESA2 minus Historical Δ

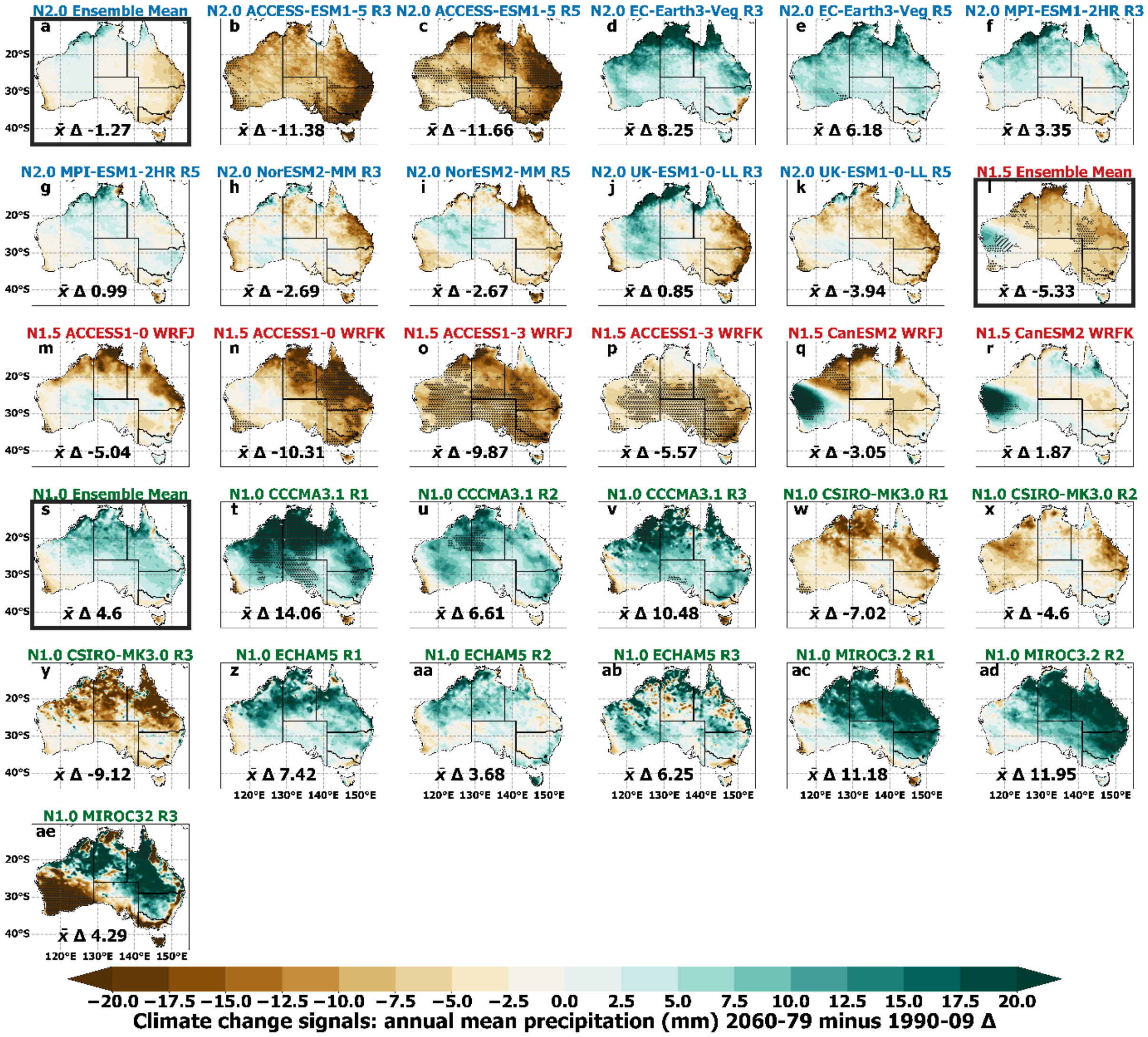


**Figure 15.** Climate change projections (1990-2009 versus 2060-2079) for annual mean precipitation for NARCliM ensemble mean climate change signals (a,l,s) and for individual ensemble members for each generation of NARCliM simulation (NARCliM 2.0 under SSP3-7.0, NARCliM 1.5 under RCP8.5 and NARCliM 1.0 under SRES A2). Significance stippling as per Figure 9.

# ~~9.~~8. Discussion and Summary

NARCliM regional climate models produce robust climate projections at spatial scales suitable for local-scale climate change analysis and impact decision-making. The third and latest generation of these regional climate models, ~~NARCliM2.0~~NARCliM 2.0, encompasses several model design advancements over its predecessors. A key aim of this paper is to describe how NARCliM 2.0 differs from its predecessors and explain the rationale for these design decisions. We also~~Here, our aims were to describe the new CORDEX-CMIP6 NARCliM2.0 RCM ensemble and its design process, including the model test and evaluation approaches used, and~~ characterise the improvements in model skill in simulating the Australian climate relative to previous NARCliM generations, as well as ~~differences~~

~~in~~compare climate projections across NARCliM generations. The next section discusses aspects of NARCliM2.0 RCM design and parameterisation in relation to previous studies before reviewing differences in the model biases and the climate projections of the NARCliM 2.0 versus NARCliM 1.x RCMs.

## 8.1 ~~NARCliM2.0~~NARCliM 2.0 RCM physics testing

~~A key aim of this paper is to describe how NARCliM2.0 differs from its predecessors and explain the rationale for these design decisions.~~ In addition to RCM design choices including increased resolution, and incorporation of convection-permitting modelling and urban physics, a major change for ~~NARCliM2.0~~NARCliM 2.0 relative to its predecessors is to use new WRF RCM configurations which are selected via a large suite of physics tests. RCM performance evaluations for the ~~NARCliM2.0~~NARCliM 2.0 RCM physics testing focused on the 4 km resolution convection-permitting domain which does not use a cumulus physics parameterisation. Notably, the 7 candidate shortlisted RCMs from the N=78 physics test ensemble used three different cumulus parameterisations for their outer domains, with 4 RCMs using BMJ, 2 RCMs using Tiedtke, and 1 using Kain-Fritsch. This indicates that differences in the outer domain boundary conditions have key influences on the RCM performances in the convection-permitting domain.~~Notably, the 7 ‘candidate’ shortlisted RCMs from the N=78 physics test ensemble used three different cumulus parameterisations for their outer domains, with 4 RCMs using BMJ, 2 RCMs using Tiedtke, and 1 using Kain-Fritsch. This indicates that differences in the outer domain boundary conditions have key influences on the RCM performances in the convection-permitting domain.~~

~~The u~~Us~~ing~~e ~~of~~ the Noah-MP LSM in the ~~NARCliM2.0~~NARCliM 2.0 RCM physics tests conferred overall RCM skill improvements relative to ~~the test Phase I~~ RCMs using the Noah-Unified LSM, especially in terms of the simulation of temperature. Although using Noah-MP also improved the simulation of precipitation in some respects, these improvements were smaller relative to the gains for temperature, and improvements were mainly located over coastal regions. The developers of Noah-MP suggest that some limitations in the Noah-Unified LSM have been modified to better represent several parameters. These include surface layer radiation balances, snow depth, soil moisture and heat fluxes, leaf area-rainfall interaction, vegetation and canopy temperature distinction, drainage of soil, and runoff.

~~The developers of Noah-MP suggest that some limitations in the Noah-Unified LSM have been modified to better represent several parameters. These include surface layer radiation balances, snow depth, soil moisture and heat fluxes, leaf area-rainfall interaction, vegetation and canopy temperature distinction, drainage of soil, and runoff.~~

In the NARCliM2.0 physics testing, improvements in RCM skill were evident for Noah-MP with default settings. Activating specific parameterisations for this LSM (i.e. dynamic vegetation cover and surface runoff-simple groundwater) delivered comparatively smaller gains in RCM performances. Some previous studies have found no overall benefit of using Noah-MP with default settings. For instance, ~~In the NARCliM2.0 physics testing, improvements in RCM skill were evident for Noah-MP with default settings. Activating specific parameterisations for this LSM (i.e. dynamic vegetation cover and surface runoff-simple groundwater) delivered comparatively smaller gains in RCM performances. Some previous studies have found no overall benefit of using Noah-MP with default settings. For instance,~~ Imran et al. (2018) conducted an evaluation of WRF coupled with a variety of LSMs including Noah-MP using its default settings. The~~ir focus was on~~y simulated~~ing~~ short-duration (~3-day) heatwaves in Melbourne, Australia~~. They~~ and observed larger temperature biases using Noah-MP relative to RCMs using Noah-Unified and CLM4.0. However, their focus on specific short duration heatwave events ~~of short duration~~ over one urban area was not intended as a comprehensive evaluation of Noah-MP's performance~~ over longer timescales~~. ~~It is also important to consider that~~Additionally, several physics schemes used by these authors differed to those used in the ~~NARCliM2.0~~NARCliM 2.0 physics testing, ~~i.e.~~i.e., they used: PBL=MYJ; microphysics=Thompson; cumulus=Grell3D; radiation=RRTMG/RRTMG. ~~The o~~Only ~~similarities between these settings and those of the NARCliM2.0 physics testing are the use of~~ Thompson microphysics and RRTMG radiation are used in the NARCliM 2.0 physics testing. WRF and Noah-MP versions also differed, ~~i.e.~~i.e., Imran et al. used WRF3.6.1 and a Noah-MP version prior to 3.7, whereas ~~NARCliM2.0~~NARCliM 2.0 uses WRF4.1.2 and Noah-MP version 4.1. Additionally, there are also several studies that have reported benefits of using Noah-MP with default parameters relative to other LSMs for other regions globally e.g. Chen et al. (2014b), Chen et al. (2014a) and Salamanca et al. (2018).

~~In an assessment of the performances of several WRF-LSMs for Sub-Saharan Africa, Glotfelty et al. (2021) noted deficiencies in the simulation of land use and land cover change (LULCC) parameters such as surface albedo by Noah-MP. Despite these deficiencies, the spatial patterns and magnitudes of temperature and precipitation were well-represented by Noah-MP. However, the land surface parameter errors impacted the magnitude and sign of LULCC-induced changes in temperature and precipitation. These deficiencies were linked to substantial underestimations of surface albedo in arid areas due to inaccurate soil albedo treatments by Noah-MP. Moreover, errors in Noah-MP's LAI profiles may occur because it was developed principally for application in Northern Hemisphere mid-latitudes. It is possible that modifying/tuning Noah-MP to specific aspects of the Australian context would yield performance benefits for follow-up dynamical downscaling. Overall, these authors concluded that "Noah-MP is least flawed of the [WRF] default LSMs". Additionally, there are also several studies that have reported benefits of using Noah-MP with default parameters relative to other LSMs e.g. Chen et al. (2014b), Chen et al. (2014a) and Salamanca et al. (2018).~~

The ~~NARCliM2.0~~NARCliM 2.0 physics testing found that the optimal LSM configuration for simulation of minimum temperature used Noah-MP with dynamic vegetation cover activated, even though the performance gain relative to Noah-MP with default settings was small. Constantinidou et al. (2020) ran WRF coupled with four LSMs (Noah-Unified, Noah-MP, CLM and, Rapid Update Cycle) over the Middle East North Africa CORDEX domain. The~~yir study~~ compared the performance of Noah-MP with dynamic vegetation cover turned on and off~~. They~~ and ~~showed~~ found that air and land temperatures were best simulated using Noah-MP with dynamic vegetation cover activated.

~~Overall, Noah-MP performed well in the NARCliM2.0 physics tests, conferring some clear advantages over RCMs using Noah-Unified. However, given the nature of its development and performance characteristics, it may be more suited to application over the temperate regions of Australia rather than the semi-arid interior.~~

In terms of ~~PBL~~ other NARCliM2.0 RCM parameterisations, focusing on PBL, by the completion of Phase I physics testing, only 3 of 12 RCMs shortlisted for further testing use the YSU scheme. By the completion of Phase II testing, all remaining RCMs using YSU are discarded, with only RCMs using PBL schemes other than YSU remaining (~~i.e.~~i.e., ACM2 and MYNN2). YSU PBL is a first-order closure scheme that expresses turbulent mixing via mean variables rather than prognostic variables (Hong et al., 2006). It is classed as a 'non-local' scheme because it estimates turbulent mixing by small-scale eddies as well as representing transport caused by convective large eddies. Two previous studies evaluating convection permitting WRF simulations using different parameterisations that included YSU for the PBL scheme found that, relative to other PBL schemes, YSU produced the highest bias for simulated precipitation (Huang et al., 2023; Nuryanto et al., 2019). However, these studies focused on different regions globally and used various experimental setups that are not directly comparable to those used here. Hence, a separate study investigating sensitivities of the ~~NARCliM2.0~~NARCliM 2.0 RCMs to the different PBL schemes is currently underway.

## 8.2 CORDEX-CMIP6 ~~NARCliM2.0~~NARCliM 2.0~~:~~ historical evaluation ~~and climate change projections~~

We characterised the improvements conferred by ~~NARCliM2.0~~NARCliM 2.0 over its predecessors in simulating the present-day Australian climate. ~~NARCliM2.0~~NARCliM 2.0 simulates mean maximum temperature and precipitation more accurately than NARCliM1.x. Specifically, NARCliM1.x has strong maximum temperature cold biases which are in keeping with other downscaling projects of the CMIP3-CMIP5 eras, e.g., (Andrys et al., 2016; Evans et al., 2020b), but these are substantially reduced in ~~NARCliM2.0~~NARCliM 2.0. A contributing cause of CMIP5-forced RCM cold biases of maximum temperature is their overestimation of precipitation (Evans et al., 2020). This relationship was also noted in ERA-Interim forced RCMs of this same modelling era (Di Virgilio et al. 2019). In ~~NARCliM2.0~~NARCliM 2.0, the widespread wet biases that characterise the NARCliM1.x RCMs are ~~greatly~~ reduced in magnitude. ~~NARCliM2.0~~NARCliM 2.0 produces smaller wet biases over eastern Australia, and smaller dry biases elsewhere, except for Australia's tropical north. This marked reduction in wet bias magnitudes is ~~a~~one plausible contributing factor for the reduction in maximum temperature cold bias for the ~~NARCliM2.0~~NARCliM 2.0 RCMs. The CMIP6 and CMIP5 GCMs used to drive ~~NARCliM2.0~~NARCliM 2.0 and 1.5 RCMs generally show similar magnitudes of maximum temperature cold bias. This suggests that the underlying nature of the CMIP6 driving data is not a principal factor underlying the observed improvements for ~~NARCliM2.0~~NARCliM 2.0's simulation of maximum temperature. In fact, the RCMs appear to have a substantial influence on the reduced maximum temperature biases.

That ~~NARCliM2.0~~NARCliM 2.0 underestimates precipitation over tropical northern Australia during the wet season (summer) to a similar degree of magnitude to the ~~NARCliM1.5~~NARCliM 1.5 RCMs indicates that the newer models still struggle to accurately capture the strength of the Australian monsoon. That NARCliM1.x strongly overestimates precipitation over south-eastern Australia~~,~~ whereas wet biases over this region are reduced for ~~NARCliM2.0~~NARCliM 2.0 indicates that the newer models may confer an improved simulation of broad-scale processes associated with synoptic-scale systems interacting with the extratropical storm track over Australia (Grose et al., 2019).

~~In terms of whether~~The extent to which NARCliM2.0's improved simulation of precipitation ~~is~~ might be attributable to ~~the~~its driving data warrants consideration.~~,~~ O~~o~~verall, the CMIP6 GCMs used to drive NARCliM 2.0 show marginally reduced wet biases versus the CMIP5 GCMs used for NARCliM1.5 (e.g. area-averaged ensemble mean absolute biases are 7.13 mm and 8.89 mm, respectively; Supporting Information Figure S15). This suggests that the underlying nature of the CMIP6 driving data ~~is~~ might not be the principal factor underlying the observed improvements for NARCliM 2.0's simulation of mean precipitation. Conversely, in terms of RCM design features, the use of the Noah-MP LSM in the NARCliM 2.0 RCM physics tests conferred overall RCM skill improvements relative to RCMs using the Noah-Unified LSM for both mean precipitation and mean maximum temperature. As noted above, ~~T~~the developers of Noah-MP suggest that some features of the Noah-Unified LSM have been modified to better represent several parameters~~ such as soil moisture and heat fluxes, leaf area-rainfall interaction, vegetation and canopy temperature distinction, drainage of soil, and runoff~~. The production NARCliM2.0 RCMs ~~forced with CMIP6 GCMs~~ used Noah-MP, whereas NARCliM1.x RCMs used Noah-Unified. Given these performance improvements observed for RCMs using Noah-MP versus ~~RCMs~~ using Noah-Unified, it is plausible that the ~~different~~ newer ~~land surface scheme~~LSM~~s~~ ~~(i.e. Noah-MP for NARCliM 2.0 versus Noah-Unified for NARCliM 1.x) play a role in~~contributes to the improved NARCliM2.0 ~~RCM~~ skill in simulating ~~mean~~ precipitation and maximum temperature, for instance, via changing the land surface feedback (via soil moisture) to the simulation of precipitation. ~~However, t~~This possibility requires more extensive investigation via future studies.

More generally, ~~in~~ th~~is~~e scope of the present study~~, the scope~~ was to focus on an initial "first-order" evaluation of mean precipitation rather than extremes of precipitation. However, clearly valuable research can now be undertaken into evaluating the skill of NARCliM 2.0 in simulating extreme precipitation, subdaily precipitation, etc, using NARCliM 2.0 20 km and 4 km data, noting these data are now publicly available. A good avenue for further research is to assess the potential added value in simulating extreme and subdaily precipitation at convection permitting scale versus the convection-parameterised 20 km data. Several previous studies have confirmed that convection-permitting resolution models can improve the simulation of~~ng~~ daily and sub-daily rainfall extremes (Xie et al., 2024; Cannon and Innocenti, 2019; Kendon et al., 2017).

~~NARCliM2.0~~NARCliM 2.0 RCMs overestimate minimum temperatures across Australia, and these biases are larger relative to ~~NARCliM1.5~~NARCliM 1.5 but comparable to those of ~~NARCliM1.0~~NARCliM 1.0. The CMIP6 GCMs used to force ~~NARCliM2.0~~NARCliM 2.0 show substantially stronger warm biases for minimum temperature than the CMIP5 GCMs used for ~~NARCliM1.5~~NARCliM 1.5. This suggests that the increased warm bias for minimum temperature in ~~NARCliM2.0~~NARCliM 2.0-RCMs ~~is~~could be partially inherited from the driving GCMs. However, ~~as noted above, the~~ Noah-MP's ~~LSM~~ simulation of factors such as LAI and other aspects of vegetation as well as surface albedo in semi-arid and arid areas has been shown to have deficiencies (Glotfelty et al., 2021). These issues may contribute to some of the biases shown by the ~~NARCliM2.0~~NARCliM 2.0 RCMs. Moreover, the ~~NARCliM2.0~~NARCliM 2.0 ensemble mean reduces the overall minimum temperature bias of the CMIP6 GCM ensemble by almost half, attesting to the added value conferred by the ~~NARCliM2.0~~NARCliM 2.0 RCMs with respect to near-surface temperature variables.

Consideration of observational uncertainty is warranted. We have evaluated NARCliM RCM skill via comparison with AGCD observations. Whilst AGCD are a high quality gridded observational data set, like any set of observations, they contain errors and uncertainties. Consequently, the outcomes of our evaluations depend on both the models being evaluated and the AGCD observational dataset. This is clearly a broader issue that applies to any model evaluation versus observations. Uncertainties in AGCD for temperature and precipitation arise from sparse station coverage in some locations, especially in remote areas, and interpolation errors in generating gridded data. More specifically, temperature uncertainties include urban heat island effects, inhomogeneities in observation records, and elevation differences. Precipitation uncertainties involve underestimation of extremes, rain gauge measurement errors, and challenges in representing complex terrain. For our purposes, the question of how much of a model bias of ~0.5 K is due to the model errors versus the observational uncertainty cannot be currently quantified, because the models are evaluated against this single observational dataset. This leaves the observational uncertainty as implicitly included in our results. In the future observational uncertainty could be explicitly considered using a method like the Observation Range Adjusted (ORA) statistics (Evans and Imran, 2024).

## 8.3 CORDEX-CMIP6 NARCliM 2.0 climate change projections

In terms of ~~NARCliM2.0~~NARCliM 2.0 future climate projections, major changes between NARCliM generations such as differences in GHG scenarios mean that ~~NARCliM2.0~~NARCliM 2.0 projected temperature changes differ in some respects to those of its predecessors. Overall, as is expected, projected warming is less intense in ~~NARCliM2.0~~NARCliM 2.0 under SSP3-7.0 than for ~~NARCliM1.5~~NARCliM 1.5 under RCP8.5. Other differences in the projections between NARCliM generations require further investigation in order to explain, such as ~~NARCliM1.5~~NARCliM 1.5's latitudinal warming gradient for maximum temperature that contrasts with ~~NARCliM2.0~~NARCliM 2.0's band of faster warming over central Australia relative to northern and southern regions. Irrespective of these differences, all three NARCliM ensembles show widespread statistically significant-agreeing results for warming projections.

Precipitation projections for the different NARCliM generations show some key similarities, such as reductions in mean annual precipitation over eastern Australia for ~~NARCliM2.0~~NARCliM 2.0 and ~~NARCliM1.5~~NARCliM 1.5, though a difference is that these are statistically significant over some areas only for ~~NARCliM1.5~~NARCliM 1.5. The ~~NARCliM2.0~~NARCliM 2.0-SSP3-7.0 and SSP1-2.6 ensembles differ in that the former generally projects wet changes over northern and western Australia, whereas the latter is generally dry, results that appear partially traceable to the underlying driving CMIP6-SSP data (Supporting Information Figure S16). ~~Other notable differences are that some NARCliM2.0 RCMs produce very similar precipitation projections for certain GCM-RCM combinations, such as for~~

Some ~~NARCliM2.0~~NARCliM 2.0 RCMs produce very similar precipitation projections for certain GCM-RCM combinations. Notably, -ACCESS-ESM-1-5~~forced~~ -R3 ~~versus~~ and R5 under SSP3-7.0 both produce ~~(i.e.~~ widespread dry projections that are substantially drier than other NARCliM 2.0 models~~for both RCMs)~~. This GCM projects very dry futures across Australia (Di Virgilio et al., 2022), so this result in the R3 and R5 RCMs could be largely inherited from the driving data. There are 40 realisations for ACCESS-ESM1-5, but only realisation 6 provides sub-daily outputs that can be used in dynamical downscaling using WRF. This realisation simulates a particularly dry projection over Australia, especially for eastern Australia, making it a useful "stress test" case. In terms of GCM skill versus observations, globally, this GCM is dry biased over a few regions owing to a location bias with the Inter-tropical Convergence Zone (Rashid et al., 2022; Ziehn et al., 2020).

~~Conversely, i~~In other instances, there are marked divergences between the NARCliM 2.0 R3 versus R5 precipitation projections when forced with the same GCM~~,~~. An example is ~~for instance,~~ UK-ESM-1-0-LL under SSP3-7.0 where R3 projects stronger precipitation increases that are more geographically widespread relative to R5. This raises the question of varying sources of uncertainty in the climate projections, ~~i.e.~~i.e., to what extent these are attributable to GCMs versus RCMs, as well as other factors.

## 8.4 Summary

In summary, the CORDEX-CMIP6 ~~NARCliM2.0~~NARCliM 2.0 regional climate projections are a 10-member ensemble comprising two configurations of the WRF RCM dynamically downscaling five GCMs under three SSPs at 20 km resolution over CORDEX-Australasia and at 4 km convection-permitting resolution over south-east Australia. In addition to several high-level model design changes, e.g., increased spatial resolution, a large (N=78) RCM-physics test suite is evaluated to select two new WRF RCM configurations for CMIP6-forced ~~NARCliM2.0~~NARCliM 2.0 climate projections. ~~Due to resource constraints and the aim to test a large number of RCM physics parameterisations, the NARCliM2.0 physics tests are performed for a single year. This is one reason why the final selection of two production-grade RCMs for the CMIP6-NARCliM2.0 runs is based on the CORDEX ERA5-forced 42-year evaluation simulations.~~ The ~~NARCliM2.0~~NARCliM 2.0 physics tests identified RCM configurations that generally performed well in simulating the recent Australian climate over south-east Australia. A key finding was that WRF RCMs using the Noah-MP LSM generally out-performed RCMs using other ~~WRF~~ LSMs in representing regional climate. Despite the overall performance gains evident for RCMs using Noah-MP, ~~RCM~~ these improvements~~skill~~ w~~as~~ere superior over ~~the~~ temperate/coastal regions of southeast Australia~~,~~ relative to the semi-arid interior. These performance characteristics might be linked to Noah-MP's development being focused on Northern Hemisphere mid-latitudes, including assumptions such as accounting for differences in seasonality in the Northern versus Southern Hemispheres by shifting the Northern Hemisphere LAI profiles by 6 months. For the southeast Australian context, noting its distinctive coastal dry-sclerophyll and expansive inland grassland biomes, such assumptions might lead to discontinuities in quantities such as LAI. ~~Hence, future investigation into processes such as land-surface coupling in NARCliM2.0 RCMs is warranted.~~Given the geographic focus of Noah-MP's development, as well as its performance characteristics, it may be more suited to application over the temperate regions of Australia rather than the semi-arid interior. It is also possible that modifying/tuning Noah-MP to specific aspects of the Australian context would yield performance benefits for follow-up dynamical downscaling.

Overall, the CMIP6-~~NARCliM2.0~~NARCliM 2.0 ensemble produces a good representation of recent mean climate that in several key respects improves upon the model skill of earlier NARCliM generations. This study provides a foundation for more detailed investigations of the model biases and future climate changes described here, including process-focused studies exploring their mechanisms. CORDEX-CMIP6 ~~NARCliM2.0~~NARCliM 2.0 RCM data provide valuable resources to investigate projected climate changes, their impacts on societies and natural systems, and potential climate change mitigation and adaptation actions for the CORDEX-Australasia region.

## 9. Code Availability

A frozen version of the source code for the Weather Research and Forecasting (WRF) version 4.1.2 used in this study, as well as the configuration files for the simulations, is available on Zenodo at: https://doi.org/10.5281/zenodo.11184830~~The Weather Research and Forecasting (WRF) version 4.1.2 used in this study is freely available from: https://github.com/coecms/WRF/tree/V4.1.2. A static copy of all scripts used for this study can be found at: https://bitbucket.org/oehcas/narclim2-0_design_and_evaluation_2024_support_materials/src/main/~~

## 10. Data Availability

Data for the ~~NARCliM2.0~~NARCliM 2.0 CMIP6-forced R3 and R5 RCMs are being made available via National Computing Infrastructure (NCI). WRF namelist settings for the ~~NARCliM2.0~~NARCliM 2.0 CMIP6-forced R3 and R5 RCMs are shown in Supplementary Material Figure S1 and are also available at: https://doi.org/10.5281/zenodo.11184830. Data ~~NARCliM1.5~~NARCliM 1.5 RCMs are available via the New South Wales Climate Data Portal and CORDEX-DKRZ. Data for ~~NARCliM1.0~~NARCliM 1.0 RCMs are available via the New South Wales Climate Data Portal. CMIP6 GCM data are available via the Earth System Grid Federation.

## 11. Author Contribution

GDV and JPE designed the models and the simulations. FJ, ET, and CT setup the models and conducted the model simulations with contributions from JPE, JK, JA, DC, CR, SW, YL, MER, RG and JL. GDV prepared the manuscript with contributions from all co-authors.

## 12. Competing Interests

The authors declare that they have no conflict of interest, noting that JK is a Topic Editor of Geoscientific Model Development.

## 13. Funding

This research was supported by the New South Wales Department of Climate Change, Energy, the Environment and Water as part of the ~~NARCliM2.0~~NARCliM 2.0 dynamical downscaling project contributing to CORDEX Australasia. Funding was provided by the NSW Climate Change Fund for NSW and Australia Regional Climate Modelling (NARCliM) Project. This research was undertaken with the assistance of resources and services from the National Computational Infrastructure (NCI), which is supported by the Australian Government.

# 14. References


Andrys, J., Lyons, T. J., and Kala, J.: Evaluation of a WRF ensemble using GCM boundary conditions to quantify mean and extreme climate for the southwest of Western Australia (1970–1999), International Journal of Climatology, 36, 4406-4424, https://doi.org/10.1002/joc.4641, 2016.

Australian Bureau of Statistics.: Regional population, Online at: https://www.abs.gov.au/statistics/people/population/regional-population/latest-release, 2024.

Bjordal, J., Storelvmo, T., Alterskjaer, K., and Carlsen, T.: Equilibrium climate sensitivity above 5 degrees C plausible due to state-dependent cloud feedback, Nat. Geosci., 13, 718-+, 10.1038/s41561-020-00649-1, 2020.

Bureau of Meteorology.: Annual climate statement 2016, 2017.

Cannon, A. J. and Innocenti, S.: Projected intensification of sub-daily and daily rainfall extremes in convection-permitting climate model simulations over North America: implications for future intensity–duration–frequency curves, Nat. Hazards Earth Syst. Sci., 19, 421-440, 10.5194/nhess-19-421-2019, 2019.

Chen, F., Liu, C. H., Dudhia, J., and Chen, M.: A sensitivity study of high-resolution regional climate simulations to three land surface models over the western United States, Journal of Geophysical Research-Atmospheres, 119, 7271-7291, 10.1002/2014jd021827, 2014a.

Chen, F., Barlage, M., Tewari, M., Rasmussen, R., Jin, J. M., Lettenmaier, D., Livneh, B., Lin, C. Y., Miguez-Macho, G., Niu, G. Y., Wen, L. J., and Yang, Z. L.: Modeling seasonal snowpack evolution in the complex terrain and forested Colorado Headwaters region: A model intercomparison study, Journal of Geophysical Research-Atmospheres, 119, 13795-13819, 10.1002/2014jd022167, 2014b.

Chou, M. D., Suarez, M. J., Liang, X. Z., and Yan, M. M. H.: A thermal infrared radiation parameterization for atmospheric studies, NASA Tech. Memo. NASA/TM-2001-104606, 19, 68 pp. https://ntrs.nasa.gov/citations/20010072848, 2001.

Constantinidou, K., Hadjinicolaou, P., Zittis, G., and Lelieveld, J.: Performance of Land Surface Schemes in the WRF Model for Climate Simulations over the MENA-CORDEX Domain, Earth Systems and Environment, 19, 10.1007/s41748-020-00187-1, 2020.

Dee, D. P., Uppala, S. M., Simmons, A. J., Berrisford, P., Poli, P., Kobayashi, S., Andrae, U., Balmaseda, M. A., Balsamo, G., Bauer, P., Bechtold, P., Beljaars, A. C. M., van de Berg, L., Bidlot, J., Bormann, N., Delsol, C., Dragani, R., Fuentes, M., Geer, A. J., Haimberger, L., Healy, S. B., Hersbach, H., Hólm, E. V., Isaksen, L., Kållberg, P., Köhler, M., Matricardi, M., McNally, A. P., Monge-Sanz, B. M., Morcrette, J. J., Park, B. K., Peubey, C., de Rosnay, P., Tavolato, C., Thépaut, J. N., and Vitart, F.: The ERA-Interim reanalysis: configuration and performance of the data assimilation system, Quarterly Journal of the Royal Meteorological Society, 137, 553-597, 10.1002/qj.828, 2011.

Di Virgilio, G., Evans, J. P., Di Luca, A., Olson, R., Argüeso, D., Kala, J., Andrys, J., Hoffmann, P., Katzfey, J. J., and Rockel, B.: Evaluating reanalysis-driven CORDEX regional climate models over Australia: model performance and errors, Clim. Dyn., 53, 2985-3005, 10.1007/s00382-019-04672-w, 2019.

Di Virgilio, G., Ji, F., Tam, E., Nishant, N., Evans, J. P., Thomas, C., Riley, M. L., Beyer, K., Grose, M. R., Narsey, S., and Delage, F.: Selecting CMIP6 GCMs for CORDEX Dynamical Downscaling: Model Performance, Independence, and Climate Change Signals, Earth's Future, 10, e2021EF002625, https://doi.org/10.1029/2021EF002625, 2022.

Di Virgilio, G., Ji, F., Tam, E., Evans, J. P., Kala, J., Andrys, J., Thomas, C., Choudhury, D., Rocha, C., Li, Y., Riley, M.: Evaluation of CORDEX ERA5-forced 'NARCliM2. 0' regional climate models over Australia using the Weather Research and Forecasting (WRF) model version 4.1.2, Geoscientific Model Development, https://doi.org/10.5194/gmd-2024-41, In review.

DWER.: Climate Adaptation Strategy - Building WA's Climate Resilient Future, Government of Western Australia, 25 pages. Online at: https://www.wa.gov.au/system/files/2023-07/climate_adaption_strategy_220623.pdf, 2023.

Evans, A., Jones, D., Lellyett, S., and Smalley, R.: An Enhanced Gridded Rainfall Analysis Scheme for Australia, Australian Bureau of Meteorology2020a.

Evans, J. P. and Imran, H. M.: The observation range adjusted method: a novel approach to accounting for observation uncertainty in model evaluation, Environmental Research Communications, 6, 071001, 10.1088/2515-7620/ad5ad8, 2024.

Evans, J. P., Ji, F., Lee, C., Smith, P., Argüeso, D., and Fita, L.: Design of a regional climate modelling projection ensemble experiment - NARCliM, Geosci. Model Dev., 7, 621-629, 10.5194/gmd-7-621-2014, 2014.

Evans, J. P., Di Virgilio, G., Hirsch, A. L., Hoffmann, P., Remedio, A. R., Ji, F., Rockel, B., and Coppola, E.: The CORDEX-Australasia ensemble: evaluation and future projections, Clim. Dyn., 10.1007/s00382-020-05459-0, 2020b.

Fiddes, S., Pepler, A., Saunders, K., and Hope, P.: Redefining southern Australia's climatic regions and seasons, J. South Hemisph. Earth Syst. Sci., 71, 92-109, https://doi.org/10.1071/ES20003, 2021.

Giorgi, F.: Thirty Years of Regional Climate Modeling: Where Are We and Where Are We Going next?, Journal of Geophysical Research: Atmospheres, 124, 5696-5723, 10.1029/2018jd030094, 2019.

Glotfelty, T., Ramírez-Mejía, D., Bowden, J., Ghilardi, A., and West, J. J.: Limitations of WRF land surface models for simulating land use and land cover change in Sub-Saharan Africa and development of an improved model (CLM-AF v. 1.0), Geosci. Model Dev., 14, 3215-3249, 10.5194/gmd-14-3215-2021, 2021.

Grose, M., Narsey, S., Trancoso, R., Mackallah, C., Delage, F., Dowdy, A., Di Virgilio, G., Watterson, I., Dobrohotoff, P., Rashid, H. A., Rauniyar, S., Henley, B., Thatcher, M., Syktus, J., Abramowitz, G., Evans, J. P., Su, C.-H., and Takbash, A.: A CMIP6-based multi-model downscaling ensemble to underpin climate change services in Australia, Climate Services, 30, 100368, https://doi.org/10.1016/j.cliser.2023.100368, 2023.

Grose, M. R., Foster, S., Risbey, J. S., Osbrough, S., and Wilson, L.: Using indices of atmospheric circulation to refine southern Australian winter rainfall climate projections, Clim. Dyn., 10.1007/s00382-019-04880-4, 2019.

Grose, M. R., Narsey, S., Delage, F., Dowdy, A. J., Bador, M., Boschat, G., Chung, C., Kajtar, J., Rauniyar, S., Freund, M., Lyu, K., Rashid, H. A., Zhang, X., Wales, S., Trenham, C., Holbrook, N. J., Cowan, T., Alexander, L. V., Arblaster, J. M., and Power, S. B.: Insights from CMIP6 for Australia's future climate, Earth's Future, 8, e2019EF001469, https://doi.org/10.1029/2019EF001469, 2020.

Herger, N., Abramowitz, G., Knutti, R., Angélil, O., Lehmann, K., and Sanderson, B. M.: Selecting a climate model subset to optimise key ensemble properties, Earth Syst. Dynam., 9, 135-151, 10.5194/esd-9-135-2018, 2018.

Hong, S.-Y., Noh, Y., and Dudhia, J.: A New Vertical Diffusion Package with an Explicit Treatment of Entrainment Processes, Monthly Weather Review, 134, 2318-2341, https://doi.org/10.1175/MWR3199.1, 2006.

Hong, S. Y. and Lim, J.-O. J.: The WRF Single-Moment 6-Class Microphysics Scheme (WSM6), Asia-Pac. J. Atmos. Sci., 42, 129-151, 2006.

Hsiang, S., Kopp, R., Jina, A., Rising, J., Delgado, M., Mohan, S., Rasmussen, D. J., Muir-Wood, R., Wilson, P., Oppenheimer, M., Larsen, K., and Houser, T.: Estimating economic damage from climate change in the United States, Science, 356, 1362-1368, 10.1126/science.aal4369, 2017.

Huang, Y., Xue, M., Hu, X.-M., Martin, E., Novoa, H. M., McPherson, R. A., Perez, A., and Morales, I. Y.: Convection-Permitting Simulations of Precipitation over the Peruvian Central Andes: Strong Sensitivity to Planetary Boundary Layer Parameterization, J. Hydrometeorol., 24, 1969-1990, https://doi.org/10.1175/JHM-D-22-0173.1, 2023.

Iacono, M. J., Delamere, J. S., Mlawer, E. J., Shephard, M. W., Clough, S. A., and Collins, W. D.: Radiative forcing by long-lived greenhouse gases: Calculations with the AER radiative transfer models, Journal of Geophysical Research: Atmospheres, 113, https://doi.org/10.1029/2008JD009944, 2008.

Imran, H. M., Kala, J., Ng, A. W. M., and Muthukumaran, S.: An evaluation of the performance of a WRF multi-physics ensemble for heatwave events over the city of Melbourne in southeast Australia, Clim. Dyn., 50, 2553-2586, 10.1007/s00382-017-3758-y, 2018.

IPCC: Climate Change 2021: The Physical Science Basis. Contribution of Working Group I to the Sixth Assessment Report of the Intergovernmental Panel on Climate Change, Cambridge University Press, 2021.

Iturbide, M., Gutiérrez, J. M., Alves, L. M., Bedia, J., Cerezo-Mota, R., Cimadevilla, E., Cofiño, A. S., Di Luca, A., Faria, S. H., Gorodetskaya, I. V., Hauser, M., Herrera, S., Hennessy, K., Hewitt, H. T., Jones, R. G., Krakovska, S., Manzanas, R., Martínez-Castro, D., Narisma, G. T., Nurhati, I. S., Pinto, I., Seneviratne, S. I., van den Hurk, B., and Vera, C. S.: An update of IPCC climate reference regions for subcontinental analysis of climate model data: definition and aggregated datasets, Earth Syst. Sci. Data, 12, 2959-2970, 10.5194/essd-12-2959-2020, 2020.

Janjić, Z. I.: Comments on “Development and Evaluation of a Convection Scheme for Use in Climate Models”, Journal of the Atmospheric Sciences, 57, 3686-3686, https://doi.org/10.1175/1520-0469(2000)057<3686:CODAEO>2.0.CO;2, 2000.

Kain, J. S.: The Kain-Fritsch convective parameterization: An update, Journal of Applied Meteorology, 43, 170-181, 10.1175/1520-0450(2004)043<0170:tkcpau>2.0.co;2, 2004.

Kendon, E. J., Prein, A. F., Senior, C. A., and Stirling, A.: Challenges and outlook for convection-permitting climate modelling, Philosophical transactions. Series A, Mathematical, physical, and engineering sciences, 379, 20190547, 10.1098/rsta.2019.0547, 2021.

Kendon, E. J., Ban, N., Roberts, N. M., Fowler, H. J., Roberts, M. J., Chan, S. C., Evans, J. P., Fosser, G., and Wilkinson, J. M.: Do convection-permitting regional climate models improve projections of future precipitation change?, Bulletin of the American Meteorological Society, 98, 79-+, 10.1175/bams-d-15-0004.1, 2017.

King, A. D., Alexander, L. V., and Donat, M. G.: The efficacy of using gridded data to examine extreme rainfall characteristics: a case study for Australia, International Journal of Climatology, 33, 2376-2387, 10.1002/joc.3588, 2013.

Kusaka, H. and Kimura, F.: Coupling a Single-Layer Urban Canopy Model with a Simple Atmospheric Model: Impact on Urban Heat Island Simulation for an Idealized Case, Journal of the Meteorological Society of Japan. Ser. II, 82, 67-80, 10.2151/jmsj.82.67, 2004.

Lee, D., Min, S.-K., Ahn, J.-B., Cha, D.-H., Shin, S.-W., Chang, E.-C., Suh, M.-S., Byun, Y.-H., and Kim, J.-U.: Uncertainty analysis of future summer monsoon duration and area over East Asia using a multi-GCM/multi-RCM ensemble, Environ. Res. Lett., 18, 064026, 10.1088/1748-9326/acd208, 2023.

Lucas-Picher, P., Argüeso, D., Brisson, E., Tramblay, Y., Berg, P., Lemonsu, A., Kotlarski, S., and Caillaud, C.: Convection-permitting modeling with regional climate models: Latest developments and next steps, WIREs Climate Change, 12, e731, https://doi.org/10.1002/wcc.731, 2021.

Meehl, G. A., Senior, C. A., Eyring, V., Flato, G., Lamarque, J.-F., Stouffer, R. J., Taylor, K. E., and Schlund, M.: Context for interpreting equilibrium climate sensitivity and transient climate response from the CMIP6 Earth system models, Science Advances, 6, eaba1981, 10.1126/sciadv.aba1981, 2020.

Murphy, B. F. and Timbal, B.: A review of recent climate variability and climate change in southeastern Australia, International Journal of Climatology, 28, 859-879, https://doi.org/10.1002/joc.1627, 2008.

Nakanishi, M. and Niino, H.: Development of an Improved Turbulence Closure Model for the Atmospheric Boundary Layer, Journal of the Meteorological Society of Japan. Ser. II, 87, 895-912, 10.2151/jmsj.87.895, 2009.

Nishant, N., Evans, J. P., Di Virgilio, G., Downes, S. M., Ji, F., Cheung, K. K. W., Tam, E., Miller, J., Beyer, K., and Riley, M. L.: Introducing NARCliM1.5: Evaluating the Performance of Regional Climate Projections for Southeast Australia for 1950–2100, Earth's Future, 9, e2020EF001833, https://doi.org/10.1029/2020EF001833, 2021.

Niu, G.-Y., Yang, Z.-L., Mitchell, K. E., Chen, F., Ek, M. B., Barlage, M., Kumar, A., Manning, K., Niyogi, D., Rosero, E., Tewari, M., and Xia, Y.: The community Noah land surface model with multiparameterization options (Noah-MP): 1. Model description and evaluation with local-scale measurements, Journal of Geophysical Research: Atmospheres, 116, 10.1029/2010jd015139, 2011.

NSW Government.: NSW Climate Change Fund Annual Report 2021-22, 2022.

NSW Government.: NSW Climate Change Fund Annual Report 2022-23, 2023.

Nuryanto, D. E., Satyaningsih, R., Nuraini, T. A., Rizal, J., Heriyanto, E., Linarka, U. A., and Sopaheluwakan, A.: Evaluation of Planetary Boundary Layer (PBL) schemes in simulating heavy rainfall events over Central Java using high resolution WRF model, Sixth International Symposium on LAPAN-IPB Satellite, SPIE, 2019.

Oleson, K., Lawrence, D., Bonan, G. B., Flanner, M., Kluzek, E., Lawrence, P., Levis, S., Swenson, S. C., Thornton, P. E., Dai, A., Decker, M., Dickinson, R., Feddema, J., Heald, C., Hoffman, F., Lamarque, J.-F., Mahowald, N., Niu, G.-Y., Qian, T., and Zeng, X.: Technical Description of version 4.0 of the Community Land Model (CLM), 2010.

Pepler, A. and Dowdy, A.: Intense east coast lows and associated rainfall in eastern Australia, J. South Hemisph. Earth Syst. Sci., 71, 110-122, 10.1071/es20013, 2021.

Perkins, S. E., Pitman, A. J., Holbrook, N. J., and McAneney, J.: Evaluation of the AR4 climate models' simulated daily maximum temperature, minimum temperature, and precipitation over Australia using probability density functions, J. Clim., 20, 4356-4376, 10.1175/jcli4253.1, 2007.

Pleim, J. E.: A Combined Local and Nonlocal Closure Model for the Atmospheric Boundary Layer. Part I: Model Description and Testing, J. Appl. Meteorol. Climatol., 46, 1383-1395, https://doi.org/10.1175/JAM2539.1, 2007.

Rashid, H. A., Sullivan, A., Dix, M., Bi, D., Mackallah, C., Ziehn, T., Dobrohotoff, P., O'Farrell, S., Harman, I. N., Bodman, R., and Marsland, S.: Evaluation of climate variability and change in ACCESS historical simulations for CMIP6, J. South Hemisph. Earth Syst. Sci., 72, 73-92, https://doi.org/10.1071/ES21028, 2022.

Salamanca, F., Zhang, Y. Z., Barlage, M., Chen, F., Mahalov, A., and Miao, S. G.: Evaluation of the WRF-Urban Modeling System Coupled to Noah and Noah-MP Land Surface Models Over a Semiarid Urban Environment, Journal of Geophysical Research-Atmospheres, 123, 2387-2408, 10.1002/2018jd028377, 2018.

Sherwood, S. C., Webb, M. J., Annan, J. D., Armour, K. C., Forster, P. M., Hargreaves, J. C., Hegerl, G., Klein, S. A., Marvel, K. D., Rohling, E. J., Watanabe, M., Andrews, T., Braconnot, P., Bretherton, C. S., Foster, G. L., Hausfather, Z., von der Heydt, A. S., Knutti, R., Mauritsen, T., Norris, J. R., Proistosescu, C., Rugenstein, M., Schmidt, G. A., Tokarska, K. B., and Zelinka, M. D.: An Assessment of Earth's Climate Sensitivity Using Multiple Lines of Evidence, Rev. Geophys., 58, e2019RG000678, https://doi.org/10.1029/2019RG000678, 2020.

Skamarock, W. C., Klemp, J. B., Dudhia, J., Gill, D. O., Barker, D. M., Wang, W., and Powers, J. G.: A description of the Advanced Research WRF Version 3. NCAR Tech Note NCAR/TN-475+STR. NCAR, Boulder, CO, 2008.

Tegen, I., Hollrig, P., Chin, M., Fung, I., Jacob, D., and Penner, J.: Contribution of different aerosol species to the global aerosol extinction optical thickness: Estimates from model results, Journal of Geophysical Research: Atmospheres, 102, 23895-23915, https://doi.org/10.1029/97JD01864, 1997.

Tewari, M., Wang, W., Dudhia, J., LeMone, M. A., Mitchell, K., Ek, M., Gayno, G., Wegiel, J., and Cuenca, R.: Implementation and verification of the united NOAH land surface model in the WRF model, 11-15 pp.2016.

Thompson, G., Field, P. R., Rasmussen, R. M., and Hall, W. D.: Explicit Forecasts of Winter Precipitation Using an Improved Bulk Microphysics Scheme. Part II: Implementation of a New Snow Parameterization, Monthly Weather Review, 136, 5095-5115, https://doi.org/10.1175/2008MWR2387.1, 2008.

Tiedtke, M.: A Comprehensive Mass Flux Scheme for Cumulus Parameterization in Large-Scale Models, Monthly Weather Review, 117, 1779-1800, 10.1175/1520-0493(1989)117<1779:acmfsf>2.0.co;2, 1989.

Torma, C., Giorgi, F., and Coppola, E.: Added value of regional climate modeling over areas characterized by complex terrain—Precipitation over the Alps, Journal of Geophysical Research: Atmospheres, 120, 3957-3972, 10.1002/2014JD022781, 2015.

WCRP: CORDEX experiment design for dynamical downscaling of CMIP6 (DRAFT), https://cordex.org/wp-content/uploads/2020/06/CORDEX-CMIP6_exp_design_draft_20200610.pdf, 2020.

WCRP: CORDEX-CMIP6 Data Request, Coordinated Regional Downscaling Experiment (CORDEX), https://cordex.org/wp-content/uploads/2022/03/CORDEX-CMIP6_Data_Request_tutorial.pdf, 2022.

Whetton, P. and Hennessy, K.: Potential benefits of a "storyline" approach to the provision of regional climate projection information, International Climate Change Adaptation Conference, NCARF, Gold Coast, Australia, 2010.

Wilks, D. S.: "The Stippling Shows Statistically Significant Grid Points": How Research Results are Routinely Overstated and Overinterpreted, and What to Do about It, Bulletin of the American Meteorological Society, 97, 2263-2273, https://doi.org/10.1175/BAMS-D-15-00267.1, 2016.

Xie, K., Li, L., Chen, H., Mayer, S., Dobler, A., Xu, C. Y., and Gokturk, O. M.: Enhanced Evaluation of Sub-daily and Daily Extreme Precipitation in Norway from Convection-Permitting Models at Regional and Local Scales, Hydrol. Earth Syst. Sci. Discuss., 2024, 1-38, 10.5194/hess-2024-68, 2024.

Zhuo, L., Dai, Q., Han, D., Chen, N., and Zhao, B.: Assessment of simulated soil moisture from WRF Noah, Noah-MP, and CLM land surface schemes for landslide hazard application, Hydrol. Earth Syst. Sci., 23, 4199-4218, 10.5194/hess-23-4199-2019, 2019.

Ziehn, T., Chamberlain, M. A., Law, R. M., Lenton, A., Bodman, R. W., Dix, M., Stevens, L., Wang, Y.-P., and Srbinovsky, J.: The Australian Earth System Model: ACCESS-ESM1.5, J. South Hemisph. Earth Syst. Sci., 70, 193-214, https://doi.org/10.1071/ES19035, 2020.